



Title	An Integrated Building Performance Evaluation Method with Building Information Modeling and Environmental Simulations
Author(s)	Worawan, Natephra
Citation	大阪大学, 2018, 博士論文
Version Type	VoR
URL	https://doi.org/10.18910/70765
rights	
Note	

The University of Osaka Institutional Knowledge Archive : OUKA

<https://ir.library.osaka-u.ac.jp/>

The University of Osaka

Doctoral Dissertation

**An Integrated Building Performance Evaluation
Method with Building Information Modeling and
Environmental Simulations**

(ビムと環境シミュレーションを統合した建築性能評価方法)

Worawan Natephra

July 2018

Division of Sustainable Energy and Environmental
Engineering, Graduate School of Engineering,
Osaka University

Abstract

Building simulation engines have become an integral part of predicting the energy performance of buildings at the early stage of design. A major barrier of using a conventional energy model has been the required manual inputs data to define a building, its geometries information, material properties, its heating, ventilation, and air conditioning (HVAC), and other systems related to building operation. On the other hand, most of the building element information required in energy simulation is available in the Building Information Modeling (BIM). Utilizing BIM technology as data repository of building information and interoperability as format exchange for building energy efficiency analysis has become an effective tool for design decision-making methods and supporting building energy simulation. However, using BIM alone is not effective in supporting advanced analysis/simulation for improving the building design in terms of energy efficiency. In addition, the lack of integration between BIM with the respect to several standards for measuring energy efficiency design prevents BIM from being efficiently used for achieving ambitious energy efficiency requirements.

Although some BIM and energy simulation tools have been combined to provide the users with an opportunity to explore different energy saving solutions, some limitations exist in those tools. First, due to the lack of interoperability between BIM and environmental sensor data, it is difficult to evaluate the building performance in the actual locations efficiently. Furthermore, practicing architects and engineers are not familiar with programming to integrate various systems. Second, as the BIM database and the requirement of building regulations in different nations are not integrated for measuring thermal performance of building envelopes, it is hard to efficiently identify appropriate thermal characteristics for the building being designed. Third, it takes much time for deriving analysis outputs from the BIM model with lighting simulation tools. Additionally, to achieve the requirement of lighting design standards and design satisfaction, perceiving lighting phenomena and atmosphere through human visual perception is impossible in traditional lighting simulation tools.

Energy consumption of buildings is influenced by different factors. Based on previous studies, significant proportion of the total energy demand for buildings corresponds to the electricity required to maintain indoor environmental conditions and lighting system. The success of indoor thermal control can be achieved through understanding of the thermal performance of building envelope and to achieve a higher degree of satisfaction in terms of lighting design a better perceive and optimize lighting conditions through an immersive environment is required.

This thesis emphasizes on proposing novel methods to extend the capability of using BIM to evaluate three factors that has a profound effect on building energy consumption, i.e, indoor thermal comfort, thermal performance of building envelope and lighting design. The first part of this research presents a method for integrating environmental sensing data and thermographic images with BIM using visual programming. To map and extract spatio-temporal thermal data and to connect air temperature data with a 3D BIM model, the user develops visual scripts. This proposed method enables calculating thermal variables, e.g., mean radiant temperature (MRT) and assessing the thermal comfort level of

inside the building. Second, this thesis investigates a method to provide interoperability among BIM, visual programming interfaces, and BIM's application programming interface (API) for supporting the assessment of the thermal performance of building envelope based on Overall Thermal Transfer Value (OTTV) standards. The BIM-based Overall Thermal Transfer Value calculation (BOTTVC) system was developed to automatically extract thermal and physical properties from the BIM database for supporting OTTV calculation. Thirdly, this thesis develops a BIM-based lighting design feedback (BLDF) system for realistic visualization of lighting condition and the calculation of energy consumption. The developed system utilizes an interactive and immersive virtual reality (VR) environment to simulate daylighting and the illumination of artificial lights in buildings and visualizes realistic VR scenes using head mounted displays (HMD). The developed BLDF system allows its users to interact with design objects, to change them, and to compare multiple design scenarios, and can provide real-time illumination level and energy consumption feedback.

The applicability of the proposed systems was validated by case studies. The results of the case studies revealed that the developed prototype systems could provide valuable information and statistic data for analyzing building performance and assessing the proposed design solutions.

Acknowledgments

This Ph.D. dissertation would not have been possible without the assistance, support, patience, and guidance of the following people.

First of all, I would like to acknowledge Mahasarakham University and the Royal Thai Government Scholarship (Ministry of Science and Technology), which fully sponsored my Ph.D. study. Thanks are also due to all the staff of the Office of Educational Affairs, the Royal Thai Embassy, Tokyo, for their administrative assistance.

I would like to express my sincere gratitude to my supervisor, Professor Nobuyoshi Yabuki for his patience, motivation, intellectual and immense knowledge, and personal support. Without his precious support, it would not have been possible for me to have the opportunity to pursue my Ph.D. degree at Osaka University. I would also like to thank him for giving me the freedom to carry out various research projects and allowing me to participate in international conferences, which were my most valuable experience during my Ph.D. life. I am also very grateful to my co-supervisor, Associate Professor Tomohiro Fukuda for his kind support, encouragement, guidance, advice, and criticism on my research. I really appreciate his recommendations and valuable comments related to the development of the BIM-based lighting design feedback (BLDF) system, which made me gain so much through my Ph.D. journey. I would also like to express my appreciation to Dr. Ali Motamedi for providing me with great support, advice, and guidance in the research direction. I was very fortunate to know him and to have the opportunity to work with him. Dr. Motamedi has also spent a lot of his precious time to read and comment on my research. Dr. Motamedi is the one who taught me how to carry out a research and how to write research papers. Without his help, I would not have been able to imagine how this research should be. Thanks a lot for your assistance in language editing. I will forever be thankful to the Yoneyama Foundation for partially supporting my first year in Japan.

I was very lucky to be part of Professor Yabuki's laboratory. Thanks are also due to my friend in the lab refers to Mr. Kazuki Yokoi, whose help was indispensable to me during my stay in Japan. My stay in Japan was great with my all friends in the lab. I will never forget the many wonderful parties and fun activities in the lab. I would like to thank every one of you for your friendship and moral support.

I wish to express my deepest gratitude to my family. I am greatly indebted to my parents, Chanya and Wara Natephra, and my sister for their unconditional love and great support. Thanks for being there when I needed someone to talk to. Thanks also go to Mahasarakham University, my colleagues at the Faculty of Architecture Urban Design and Creative Arts, my faculty dean, and all the staff at my faculty office. Finally, I would like to thank the thesis committees for spending their precious time reading this thesis and for providing me with constructive feedback and suggestions. I also would like to thank Professor Masanori Sawaki for vice referee of my Ph.D. examination.

Table of Contents

Abstract.....	i
Acknowledgments	iii
Table of Contents	v
List of Figures.....	ix
List of Tables	xi
Chapter 1 Introduction.....	1
1.1 General background	1
1.2 Problem statement and research gaps	3
1.3 Research objectives.....	4
1.4 Thesis organization	5
Chapter 2 Literature review	8
2.1 Building Information Modeling (BIM)	8
2.1.1 A definition of BIM	8
2.1.2 BIM interoperability and data exchange.....	9
2.1.3 BIM-based building performance simulation	10
2.2 Extending BIM capabilities	11
2.2.1 Graphical visual programming.....	11
2.2.2 BIM's API.....	11
2.2.3 Environmental sensing data with BIM.....	12
2.2.4 Game engine and virtual reality technology with BIM.....	12
2.3 Indoor thermal comfort analysis	13
2.3.1 Thermal comfort determinants.....	13
2.3.2 3D mean radiant temperature calculation	14
2.3.3 Infrared thermography	15
2.4 Thermographic 3D modeling and RGB thermal textures	16
2.5 Visual analytics for root-cause detection	17
2.6 Evaluating thermal performance of building envelopes	18
2.6.1 Building envelopes.....	18
2.6.2 Building regulations worldwide for energy-efficient building envelope design.....	19
2.6.3 Measurement of the thermal performance of a building envelope.....	21
2.7 Lighting design analysis using BIM and VR technology	26
2.7.1 Integrating building information modeling (BIM) with a game engine.....	26
2.7.2 Lighting design metrics in the game environment	26
2.7.3 Human visual perception through VR technology	28
2.7.4 Discomfort glare indices	29
Chapter 3 Overview of the research.....	31
3.1 Introduction.....	31
3.2 Overview of the proposed methodology	32

3.3 Integrating thermal data with BIM for evaluating thermal performance of building envelope and indoor thermal comfort in the operational stage	33
3.4 Extracting BIM database for overall thermal transfer value calculation	34
3.5 Integrating BIM and VR for lighting design feedback	36
3.6 Conclusions.....	37
Chapter 4 Integrating 4D thermal information with BIM for building envelope thermal performance analysis and thermal comfort evaluation.....	38
4.1 Introduction.....	38
4.2 Proposed system.....	38
4.2.1 3D BIM modeling and environmental data acquisition	39
4.2.2 Mapping thermal data on a BIM model and preparing environmental data	41
4.2.3 Creating 4D thermal information	42
4.2.4 Data extraction and data processing.....	43
4.2.5 Calculating thermal comfort variables using visual scripting.....	45
4.2.6 Data integration for assessing thermal comfort level.....	45
4.2.7 Information output	46
4.2.8 Visual analysis	46
4.3 Case study	47
4.3.1 Experimental room.....	47
4.3.2 BIM modeling and environmental data collection.....	48
4.3.3 Integrating thermographic images and temperature data with BIM	48
4.3.4 4D thermal model visualization output.....	49
4.3.5 Calculating thermal comfort variables	50
4.3.6 Thermal performance and thermal comfort analysis	53
4.4 Discussion	54
4.5 Chapter conclusions	55
Chapter 5 Optimizing the evaluation of building envelope design for thermal performance using a BIM-based OTTV calculation	57
5.1 Introduction.....	57
5.2 Development of the BOTTVC system.....	57
5.2.1 3D BIM modeling	58
5.2.2 Acquisition of required thermal properties and physical assets from the BIM database	58
5.2.3 Text-scripting in <i>Code Block</i> node.....	58
5.2.4 Python scripting	59
5.3 Calculating OTTV coefficients using visual scripting	59
5.3.1 Acquisition of WWR and SSR or SKR values	60
5.3.2 Acquisition of SC or ESM coefficients.....	60
5.3.3 Acquisition of TDeq and SF coefficients.....	61
5.3.4 Accommodating OTTV coefficients for assessing the thermal performance of a building envelope	63
5.3.5 Information output	63
5.4 Usage process flow for BOTTVC.....	63
5.5 Case study	64
5.5.1 Baseline building.....	64

5.5.2 Acquisition of OTTV coefficients using BOTTVC	65
5.5.3 Calculating WWR and SSR or SKR coefficients	66
5.5.4 Integrating extracted BIM information with constant coefficients	67
5.6 Calculating OTTV for assessing the performance of a building envelope	70
5.7 Optimization scenarios.....	74
5.8 Discussion	83
5.9 Chapter conclusions	84
Chapter 6 Integrating BIM and VR development engines for building indoor lighting design .	86
6.1 Introduction.....	86
6.2 Development of the BLDF system.....	87
6.2.1 BLDF system user interface components and supported interactions	87
6.2.2 BLDF's usage process flow	91
6.2.3 Updating BIM with new design parameters.....	92
6.3 System accuracy verification	93
6.4 Case study	96
6.4.1 BIM modeling and game engine integration.....	96
6.4.2 Immersive VR for BLDF	98
6.5 Results and discussion	103
6.6 Chapter conclusions	105
Chapter 7 Conclusions and future works	107
7.1 Introduction.....	107
7.2 Research contribution	107
7.3 Summary of research	109
7.4 Limitations and future works	110
References.....	113

List of Figures

Figure 1 Thesis organization diagram.....	7
Figure 2 Content relationship.....	31
Figure 3 Overview of the proposed methodology.....	32
Figure 4 Overview of the system for integrating infrared thermography and sensing data with BIM model	34
Figure 5 Overview the proposed method of BOTTVC.....	35
Figure 6 Overview of the proposed method for integrating BIM and VR for lighting design feedback	36
Figure 7 Capturing thermographic images.....	40
Figure 8 Adjusting the perspective distortion and stitching multiple thermographic images	41
Figure 9 Workflow for integrating sensor data and thermographic data with BIM	42
Figure 10 Process flow for creating 4D thermal information	43
Figure 11 Workflow for data extraction and data interpretation.....	44
Figure 12 Data extraction and data interpretation.....	44
Figure 13 Dividing surfaces for calculating MRT and corresponding Grasshopper setup	45
Figure 14 Reading the recorded data by the data processing module	46
Figure 15 Experiment room and placement of air temperature and humidity sensors.....	47
Figure 16 Process of BIM model transfer	48
Figure 17 Visualization of thermal information.....	49
Figure 18 Example of 4D thermographic visualization	50
Figure 19 Locations of assessment points.....	50
Figure 20 Indoor/outdoor air temperature and calculated value of MRT and operative temperature considering angle factors of six occupant locations in summer and autumn	51
Figure 21 Results of MRT and the operative temperature calculations at six locations in the room in summer (August), Osaka, Japan	52
Figure 22 Results of MRT and operative temperature calculations at six locations in the room in autumn (October), Osaka, Japan	52
Figure 23 Thermal comfort conditions in the adaptive comfort standard.....	54
Figure 24 Process flow for acquiring OTTV coefficients from the BIM database	58
Figure 25 Example of extracting coefficients from the BIM thermal properties database	59
Figure 26 Example of extracting some coefficients from the BIM thermal properties database.....	59
Figure 27 Workflow for extracting the total area of target surfaces of walls/roofs and calculating WWR and SSR or SKR values	60

Figure 28 The proposed visual scripting to obtain variables for finding an SC or ESM value for external shading devices	61
Figure 29 Workflow for calculating TDeq on the basis of OTTV standards in different countries	62
Figure 30 Usage process flow for BOTTVC	64
Figure 31 A 3D view of the model building in Revit (a) and in Dynamo (b).....	65
Figure 32 Comparing OTTV results of different optimization scenarios	76
Figure 33 Screenshot of the main interface of the prototype BLDF system with all widgets visible..	88
Figure 34 Sample visualizations using BLDF's GUI	90
Figure 35 BLDF's usage process flow.....	91
Figure 36 Updating the design parameters in BIM.....	92
Figure 37 Actual room condition	93
Figure 38 Conditions for the accuracy test	94
Figure 39 BLDF lighting simulations and the comparison of the results	96
Figure 40 3D BIM model and 2D plan of existing fixtures position of the case study room	97
Figure 41 BIM model transfers to the game environment 3ds.....	98
Figure 42 Lighting illumination level at daytime (left) and nighttime (right)	99
Figure 43 Examples of the illumination visualization outputs.....	99
Figure 44 Lighting energy consumption for two scenarios.....	100
Figure 45 Illuminance levels using different bulbs.....	101
Figure 46 Lighting atmospheres.....	101
Figure 47 Illuminance levels of different furniture layouts	102
Figure 48 Adding occupancy sensors for ambient light and task light in the virtual environment Task	103

List of Tables

Table 1 Example of the minimum requirement for the U-value of building envelopes in cold-climate countries (i.e., Europe).....	20
Table 2 OTTV standards in various countries.....	22
Table 3 Comparison of the forms of OTTV equations of different countries in Southeast Asia	25
Table 4 Extracting thermal properties from the BIM database of the baseline building.....	66
Table 5 Calculating 1-WWR, WWR, 1-SSR, and SSR values using BOTTVC.....	67
Table 6 TDeq values under the OTTV codes of Thailand and Hong Kong	68
Table 7 Results of SC, ESM, ESR, SF, and CF values for the baseline building	69
Table 8 Summary of all input coefficients and OTTV outputs of the baseline building.....	71
Table 9 OTTV outputs of different optimization scenarios	77
Table 10 BLDF lighting simulations and results.....	95

Chapter 1 Introduction

1.1 Background

The World Energy Council estimated that buildings account for nearly 40% of the total global energy consumption (WEC, 2013). A major proportion of the total energy demand for buildings is electricity for maintaining indoor comfort levels and lighting. For example, 37% and 28% of the total energy in the building sector are used for maintaining indoor comfort levels (e.g., space heating, cooling, and ventilation) in the U.S. and Japan, respectively (U.S. Department of Energy, 2012; The Energy Conservation Center Japan, 2010). Lighting consumes approximately 16.7% of the commercial building energy in the U.S. (U.S. Department of Energy, 2012), 20 to 40% in large office buildings in China (Zhou et al., 2015) and 40% in commercial buildings. A reduction in energy use for heating, cooling, and lighting can make a substantial contribution toward minimizing the energy demand for buildings.

To achieve the goals of reducing energy consumption, the improvement of the energy efficiency performance of buildings must begin at the architectural building design stage of a project. Building performance evaluation is a process of measuring and monitoring building in diverse purposes for achieving high performance goals. A number of previous studies have shown that cooling and lighting systems are considered as the key roles in achieving the goals of energy efficiency. In response to this issue, there is growing consensus in the building and design communities about reducing energy demand by quantifying the performance of building components.

The evaluation of building performance can be divided into five aspects: (1) the building envelope, (2) the air conditioning and ventilation, (3) the water heating system, (4) the dynamic equipment, and (5) the illumination (Egwunatum et al., 2016). Building envelopes have a significant impact on the proportion of heat loss and gain, which are important factors affecting the energy demand of buildings during their operational phase. For example, Utama et al. (2009) found that building envelopes contribute approximately 20-30% of the total heat gain in buildings. Almujahid et al. (2013) stated that one-third of energy loss occurs through walls in the case of uninsulated brick veneer dwelling. Additionally, previous studies have shown that the thermal performance of the building envelope exerts a significant impact on the energy performance and energy consumption of a building. For example, Fang et al. (2014) investigated the effect of external wall insulation on the energy consumption and indoor thermal environment. They found that rooms with well-insulated walls consumed 23.5% less energy than rooms with normal-constructed walls. Thormark et al. (2006) stated that making

improvements to the insulation of the building envelope can reduce the amount of operating energy of buildings. To effectively reduce the energy consumption of buildings, selecting the envelope construction materials requires careful attention to determine the appropriate thermal properties of materials (Noori et al., 2015).

In the meantime, Benya et al. (2001) stated that the lighting design primarily affects the energy efficiency and lighting quality. Lighting design is the combination of artificial light and daylight for creating a proper illuminance level, mood, atmosphere, and environment for different indoor activities. Lighting requires careful design in order to preserve the effect of daylight and minimize energy use for artificial lighting systems. Lighting has been considered a crucial factor in workers' performance. Appropriate indoor lighting conditions can enhance the effectiveness and well-being of office workers.

Building simulation engines have become an integral tool for predicting the performance of the design building to help the designers make informed decisions during the design stage. Although the simulation results generally cannot be reflected with buildings' actual energy use since there are many other factors that need to be considered (e.g., climate, equipment energy use, occupancy schedule, and internal load), energy modeling can influence decisions among the chaos of early design (Anderson, 2014).

The use of Building Information Modeling (BIM)-based computer simulation tools is growing rapidly and such tools assist designers in making better decisions to reduce energy consumption and create better indoor thermal comfort and lighting conditions for occupants. BIM-based simulations are increasingly being used to assess the success and failure of thermal performance of building envelope, indoor thermal comfort, and indoor lighting design. Due to the ability to share multidisciplinary information, BIM has numerous potential benefits to support and increase efficiency in analyzing the thermal performance of buildings and examining indoor lighting performance. However, there are several limitations in using the existing BIM (e.g., difficulty integrating BIM models with environmental sensor data to assess/analyze the performance of a building). Although BIM can create 3D virtual models that contain all of the building information needed to support the design, using BIM alone is inefficient to support advanced analyses/simulations for improving the design of buildings for energy efficiency. Integrating BIM with various technologies (e.g., visual programming, coding, virtual and augmented reality, energy analysis tools, Radio Frequency Identification (RFID), and laser scanning, has great potential to change the traditional BIM to become more innovative and powerful in order to provide new insights and innovations for facilitating the creation of more efficient buildings. With the growing interest in integrating design requirements for energy-efficient buildings (e.g., American Society of Heating, Refrigeration, and Air Conditioning Engineers (ASHARE) standard) and building energy codes with BIM, semantic information of the building models regarding building material (e.g., physical and thermal properties), building geometry information, quantities and

properties of building elements become possible to support the process of energy-efficiency design assessment of buildings in various purposes.

Thus, this research presents a BIM-based data model and integrated frameworks for building performance evaluation and environmental simulations. This thesis emphasizes on investigating methods to facilitate the assessment of building performance as follow: 1) indoor thermal comfort; 2) thermal performance of the building envelope; and 3) lighting design by using an integrated database and interoperable information of a building between the BIM database and tools, including environmental sensing data, infrared camera, visual programming interface, and virtual reality (VR). The main purpose of this thesis is to explore the possibility of sharing and connecting BIM database (e.g., geometry information, thermal and physical properties) created by BIM authoring software with visual programming interface tools (such as Dynamo and Grasshopper) and game engine software tools (such as Unreal Engine) to extend the capabilities of the current BIM to support building design improvement based on ASHRAE standard regarding the measurement of indoor environments, Illuminating Engineering Society of North America (IESNA) lighting design standard regarding illumination level requirement for working space, and Overall Thermal Transfer Value (OTTV) standard.

1.2 Problem statement and research gaps

The main problems of using the current BIM regarding the assessment of thermal performance of building envelopes, thermal comfort evaluation, and lighting design can be attributed to the following main issues:

(1) Regarding the assessment of thermal performance of building envelopes, the current BIM is not yet mature enough to be readily used for integrating thermal and environmental sensor information to assess thermal comfort. BIM requires tools to enable building professionals to effectively detect the location of thermal defects and to extend its ability to analyze thermal performance and thermal comfort by accommodating environmental information to be used in the analysis process. In addition, to effectively maintain a comfortable temperature in a building, the selection of material for the building envelope during the design stage requires careful attention to limit the heat transferred through the building envelope. The traditional method of calculating and assessing thermal characteristics of building envelopes is impractical and time-consuming. BIM represents the building as an integrated database of coordinated information (Rahmani Asl et al., 2015) that can be shared as the central model and it contains details of geometric and non-geometric information of the BIM model.

Although the previous research showed that utilizing BIM can benefit to verify and to analyze indoor thermal comfort and improve the thermal performance in different phases of the building process,

methods for integrating BIM with environmental sensing data have not been fully proposed yet. In addition, methods for direct extraction material properties from the BIM database for OTTV evaluation has not been explored in the previous studies. Therefore, our first system, a novel method to extend the capability of the current BIM to create interoperability between measurement data and the BIM database to support the evaluation of indoor thermal comfort of building is presented in this research. In addition, our second system, the development of a novel method to facilitate the access and extraction of required parameters regarding the thermal properties of materials from a BIM model to evaluate the performance of envelope construction materials is a challenge to improve the building envelope design based on OTTV standards.

(2) Regarding lighting design, integrating lighting simulation tools with BIM to support lighting designers in visualizing, identifying, and examining indoor lighting performance as well as simulating lighting energy consumption has become an integral technique for improving and optimizing lighting conditions at an early design stage. Although lighting tools enable quantitative and qualitative analysis and visualization of indoor lighting, they do not provide an interactive environment between the users and the design context. Moreover, when using traditional tools, designers are unable to directly experience some lighting phenomena that may affect the visual perception of the occupants (e.g., brightness, darkness, glare, or insufficient illumination). In addition, when using conventional BIM authoring software applications and their plugins, tasks related to preparing lighting simulations are very time-consuming (Huang, 2008). Furthermore, the rendering step for achieving a photo-realistic output is very time-consuming. On the other hand, virtual reality (VR) provides new perspectives for designers to visualize their design through an immersive experience (Weidlich et al., 2007). Game engines are designed for creating dynamic activities, interacting with objects (Edwards et al., 2015), and providing accurate and timely feedback when users interact with building elements in a virtual environment. Therefore, our third system of this thesis proposed a new method that uses BIM, game engines, and VR to facilitate lighting design and lighting energy performance analysis via an immersive and interactive user experience.

1.3 Research objectives

With the limitations and research gaps mentioned-above, in this research, we investigate methods to extend the capabilities of the current BIM by integrating with technologies, such as environmental sensing data, visual programming and VR to facilitate the evaluation of the performance of buildings (i.e., thermal performance of the building envelope, indoor thermal comfort, and lighting design). This research proposes methods and develops prototype systems based on the BIM database (e.g., geometry information, physical properties, and thermal properties of the BIM model) coupling with visual programming language applications and a game engine. Three frameworks for extending BIM's capabilities to address the aforementioned issues are proposed:

- (1) To develop a novel method and a system for integrating the BIM model with 4D thermal information (building surface temperature and air temperature) to help visualize the thermal information of building surfaces over time and evaluate the indoor thermal comfort condition in a building. This can be done by integrating thermographic images, environmental sensors, and BIM geometry information using developed visual scripting. Eventually, indoor building surface temperature can be extracted from thermographic images that are mapped on the BIM model, and thermal comfort variables can be automatically calculated using visual scripting.
- (2) To develop a BIM-based Overall Thermal Transfer Values calculation (BOTTVC) that provides an automatic calculation and assessment of the building envelope design for measuring the thermal performance of the building on the basis of OTTV regulations. BIM's visual programming is proposed to extract the physical and thermal properties of the BIM model to facilitate semi-automatic OTTV calculations.
- (3) To develop a prototype system called BIM-based lighting design feedback (BLDF) for realistic visualization of lighting conditions and calculations of lighting energy consumption with a user-friendly interface using an interactive and immersive VR environment.

The developed systems provide a flexible and easy approach to apply to several practical projects. The applicability of the proposed methods is evaluated and validated in a real-world case study. The limitations of the proposed systems are discussed and summarized. Finally, recommendations for future developments are demonstrated. The specific objectives of the research are: (1) to explore the possibility of integrating BIM with technologies for creating new systems using the BIM database in order to facilitate the evaluation of thermal performance of building envelopes and indoor thermal comfort during the operational phase, optimize the evaluation of the thermal characteristics of building envelopes during the design phase, and support interactive environments for lighting design and real-time and lighting energy feedback; and (2) to investigate the applicability of the proposed methods using real-world case studies.

1.4 Thesis organization

This dissertation consists of seven chapters as follows:

Chapter 1 Introduction: This chapter illustrates the background and research objectives that constitute the main purpose of this research.

Chapter 2 Literature review: This chapter presents an overview of the concept of using BIM as the central data model for the analysis of multiple purposes for building performance analysis, techniques, and the recent technologies that are used to integrate with BIM to create new functionalities of BIM in relation to the evaluation of the performance of buildings (i.e., thermal performance of building

envelopes, indoor thermal comfort, and lighting design). The literature review comprises the recent technologies that can be used to extend the capability of using the existing BIM, the concept of BIM technology, visual programming technologies, and BIM's Application Programming Interface (API). Using BIM and game engine technologies for lighting simulations, integrating sensing data with BIM, the literature related to thermal imaging, thermal performance, and thermal properties of building envelopes, the required variables for evaluating the thermal performance of building envelopes, and indoor comfort theories are also reviewed.

Chapter 3 Overview of the proposed methodology: This chapter presents the idea of connecting sensor data with a virtual BIM model and extracting physical and thermal properties from the BIM database using visual programming technology. In addition, the proposed system to integrate BIM with VR for an immersive VR system for interior and lighting design is also discussed. This chapter also briefly discusses the different frameworks of the proposed methodology including the contributions and a brief overview of each framework. It contains workflow summaries of the proposed systems.

Chapter 4 Integrating 4D thermal information with BIM for building envelope thermal performance analysis and thermal comfort evaluation: This chapter elaborates on the proposed approach to use BIM-based environment data to facilitate the visualization of the changes of thermal information of building surfaces and assessment of thermal comfort conditions. The main focus of this chapter is on the integration of visual programming technologies, thermographic images, sensing data, and BIM to create 4D thermal information for evaluating indoor thermal comfort of buildings and visualize the location of heat leakages on the building envelopes. The applicability of the system is validated in a real-world case study. The findings of the validation study and limitations of the system are summarized.

Chapter 5 Optimizing the Evaluation of Building Envelope Design for Thermal Performance using a BIM-based OTTV Calculation: This chapter elaborates on the proposed approach for a BIM-based overall thermal transfer value calculation system for an-automatic assessment of the OTTVs of building envelopes using thermal properties of building materials in the BIM database. Integrating BIM and a developed visual script to automatically extract thermal and physical properties from the BIM database in order to provide a real-time thermal transfer value calculation is presented. A case study is validated.

Chapter 6 Integrating BIM and VR development engines for building indoor lighting design: BLDF prototype system for realistic visualization of lighting conditions and the calculation of energy consumption is proposed to provide qualitative and quantitative outputs for lighting design by integrating BIM geometry information and immersive VR environment to simulate the illumination of lights in buildings and visualize realistic VR scenes using head-mounted displays (HMDs). The accuracy of the system is verified in a real-world building. This chapter includes a case study to demonstrate the BLDF usage flow and how the proposed system can be utilized.

Chapter 7 Conclusions and future work: This chapter summarizes the presented frameworks, and the findings of the study and suggests recommendations for future research.

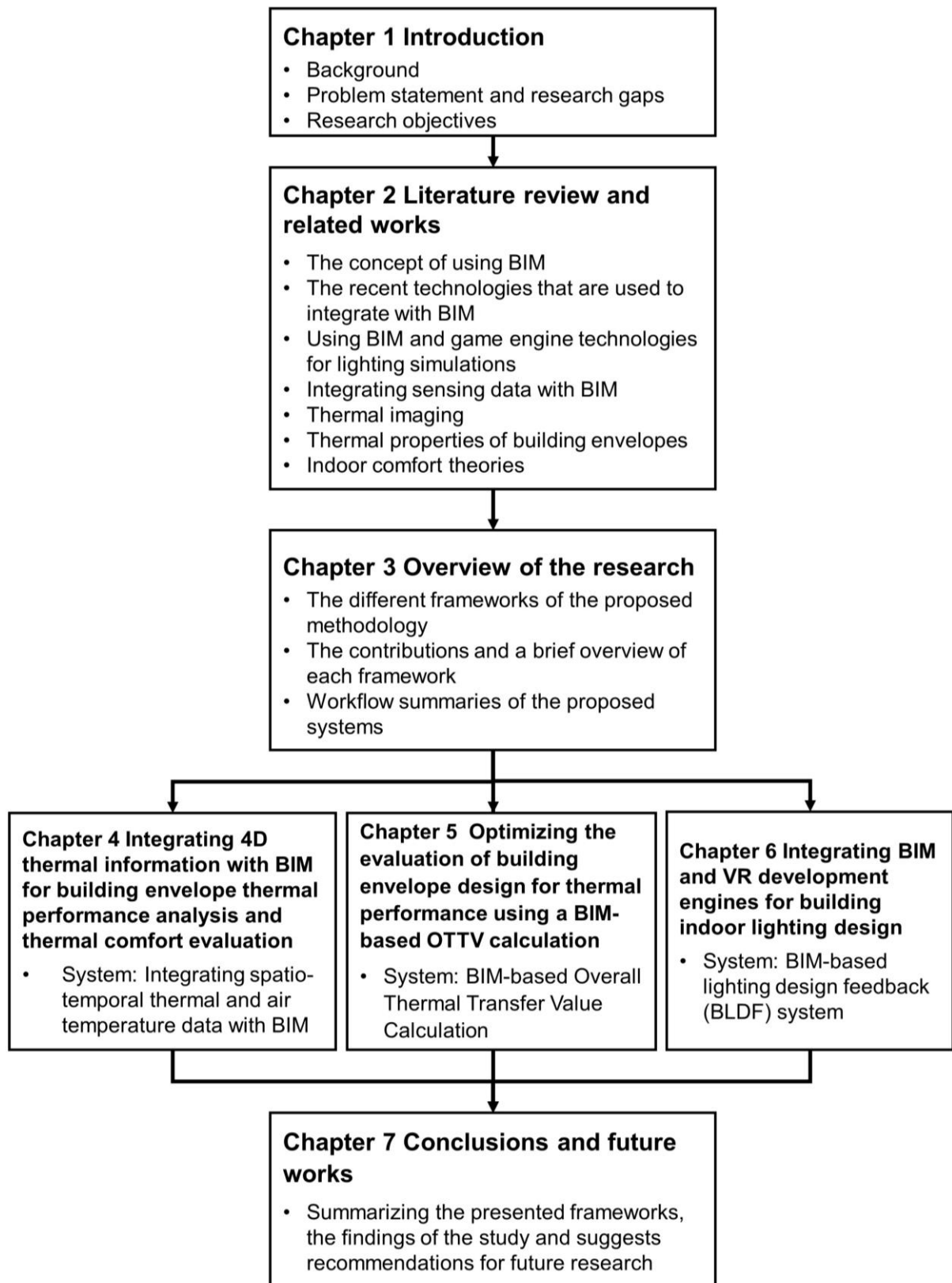


Figure 1 Thesis organization diagram

Chapter 2 Literature review

This chapter presents an overview of the concept of BIM technology and recent technologies that are popularly used to extend the capability of the existing BIM in the architecture, engineering, and construction (AEC) industry. The chosen technologies, (i.e., visual programming technologies, VR, and BIM's API) that are proposed to integrate with BIM for creating novel systems in this research are reviewed. The literature review also comprises the previous studies regarding coupling BIM with VR technologies for lighting simulations, integrating sensing data with BIM, and extracting useful information from the BIM to support better decision-making in selecting appropriate materials for building envelope assemblies. The literature related to various knowledge sources that support the evaluation of the performance of the buildings (i.e., thermal performance of building envelopes, indoor thermal comfort, and lighting design) is explained.

2.1 Building Information Modeling (BIM)

During the last two decades, the adoption of BIM technology has constituted a major paradigm shift in the AEC industry from the traditional computer-aided design (CAD) technology (Takim et al., 2013). BIM is an integrated digital process that provides coordinated reliable and sharable information about a project with other professionals in the design chain. BIM was developed to overcome the problem related to interoperability and data exchange between two distinct domains, design and analysis, and to support multiples exchanges or analyses based on one design model (Sanguinetti et al., 2012). The goal of BIM technology is to provide information about a building, including traditional building documents, such as drawings, specifications and construction details, as well as geometry information, and attributes of building models, as well as their relationship, to support the entire lifecycle data sharing among project participants (Eastman et al., 2008).

2.1.1 A definition of BIM

BIM refers to the development of a set of technologies and organizational solutions that are expected to increase interorganizational and disciplinary collaboration in the construction industry and to improve the productivity and quality of the design, construction, and maintenance of buildings (Miettinefn et al., 2014).

BIM is a digital representation of the physical and functional characteristics of building facilities and it is known as a tool for storing and sharing building information about a facility forming, which is a reliable basis for decisions during its lifecycle (BuildingSMARTalliance, 2015). The US General Service Administration (US General Service Administration (GSA), 2007) defines BIM as the development and use of a multi-faceted computer software data model to not only document a building design but also to simulate the construction and operation of a new capital facility or a recapitalized (modernized) facility. The use of BIM can create a building information model, which is defined as a data-rich, object-based, intelligent and parametric digital representation of the facility, from which views appropriate to various users' needs can be extracted and analyzed to generate feedback and improvement of the facility design (US General Service Administration (GSA), 2007). BIM offers benefits to all participants in a building's lifecycle management by facilitating multidiscipline collaboration, from primary design through the construction and operation phases (Sabol, 2008). BIM can therefore be defined as an integrated database and interoperable information of a project that covers all detailed information about each building component (e.g., geometry, spatial relationships, quantities, and properties of building components).

2.1.2 BIM interoperability and data exchange

Traditionally, project information was frequently exchanged and collaborated through a set of documents and 2D drawings. Some of the main issues involved in using 2D CAD are summarized as follows: (1) lack of central and reusable information; (2) difficulties in interoperability between different software application tools; (3) lack of interoperability of project-generated information and inadequate information sharing; (4) lack of semantic information or parametric information of components. It is known that the lack of flexibility in project collaboration and information communication using CAD technologies has contributed to the decline of construction productivity in the construction industry over decades (Hardin et al., 2014). BIM has been introduced as an innovative tool and techniques that facilitates information exchanges between the various parties involved in construction projects and it serves as a multi-disciplinary data repository, which potentially increases new opportunities to improve project collaboration in different purposes.

The crucial concept of the BIM is to provide interoperability and integrated wholly sharable information among different software application tools (Miettinen et al., 2014). Additionally, an important aspect of BIM development is to allow a large number of building data to be stored within a 3D building information model, where the data can be reusable. The interoperability of BIM has traditionally relied on file-based exchange formats (Eastman et al., 2008). BIM currently supports a wide range of file formats. This helped project teams handle the amount of building information and facilitate data transfer from one 3D modeling software application to another without loss of data fidelity (Autodesk, 2016c). Data exchange in the BIM process is often done using three neutral data file formats: Green Building

XML (gbXML), Industry Foundation Class (IFC), and Drawing Interchange Format (DXF). The IFC, gbXML, and DXF standards are used for sharing the physical and functional characteristics of a building between stakeholders throughout the entire project lifecycle.

2.1.3 BIM-based building performance simulation

BIM tools are increasingly being used to improve the design collaboration, and the modeling process through the construction of buildings with a promise of providing an effective design process and data sharing at all stages of the construction cycle (Jones et al., 2008). BIM has recently become an integral tool in the analysis of multiple performance measurements, including energy efficiency (e.g., Ahn et al., 2014; Hitchcock et al., 2011; Bazjanac, 2009), architectural design (e.g., Sanguinetti et al., 2012), structure design (Niggel et al., 2004; Ahuja et al., 2017; Zotkin et al., 2016), acoustics (e.g., Wu et al., 2013; Tan et al., 2017), and lighting (e.g., Shah et al., 2017; Kota et al., 2014).

Based on the previous studies that considered BIM as the central data model for buildings energy performance analysis are mainly focused on the automatic preparation of building models for various simulation tools (Rahmani Asl et al., 2015). Typical workflow and data exchange between the BIM and analysis software applications require the export of model geometry from the BIM to analysis applications depending on the analysis purposes (Aksamija et al., 2011). In the exchange model, one software system maintains the master copy of the data internally and exports a snapshot of the data for others to use (Isikdag et al., 2007). A neutral file that presents and contains the numerous information of a building is generated by System A. Then, another software system receives the neutral exchange file created by System A. System B will have to provide a functionality in its implementation for accessing the neutral file as well as for interpreting the contents and creating an internal representation of that information (Kemmerer, 1999).

Using BIM-based building performance analysis allows designers to efficiently generate and modify building model components in a single place and allows the system to propagate changes of model objects throughout all the views in a set of deliverables (Krygiel et al., 2008). To evaluate building performance in the early design stage, the information of the building contained in a BIM database, such as the geometry, material properties, and technical systems, needs to be accessed by design stakeholders (Schlueter et al., 2009).

Lee, (2012) surveyed the use of BIM for simulation and analysis to achieve green objectives in architectural and engineering companies. The result revealed that 67% of the used of BIM as an analysis tool was for energy performance, 60% for lighting analysis, 52% for heating ventilating and air conditioning (HVAC) design, and 48% for green building certification. Among the energy performance simulations are lighting and daylighting analysis (74%), whole building energy use (72%), and energy code compliance (70%).

2.2 Extending BIM capabilities

The use of BIM is well-known in various aspects of creating innovations for improving the process of design, construction, and management in the AEC industry. Efforts are being made to leverage BIM to be more powerful by extending its capabilities by adding new functionalities to the current BIM software application or/and integrating BIM database with technologies for various purposes. To leverage BIM capabilities, various technologies have been proposed to incorporate with BIM for different purposes, e.g., architectural visualization (Yan et al., 2011), integrating BIM and AR for design feedback (Fukuda et al., 2015), integrating BIM with sensing data to monitor building energy performance (Wang et al., 2013), fusing passive RFID and BIM for increased accuracy in indoor localization (Costin et al., 2015), Integrating BIM's API and visual programming for building performance optimization (Rahmani Asl et al., 2015), integrating BIM and GIS for developing a modeling method for algae powered neighborhood (Dutt et al., 2017), and integrating BIM and the photogrammetry technique with VR to provide an advanced method for experiencing of room views (Faltýnová et al., 2016).

In the following subsection, the technologies proposed to extend BIM capabilities in this research (i.e., graphical visual programming, BIM's API, environmental sensing data, game engines and VR technology) are described.

2.2.1 Graphical visual programming

Using an optimization algorithm through a visual programming interface is an integral tool for improving or optimizing building energy performance. A graphical programming interface allows users to extend the capabilities of the current BIM by using a graphical algorithm editor and can replace conventional coding tools with the visual metaphor of connecting small blocks of independent functionality into an entire system or procedure (Boeykens et al., 2009). An integrated visual programming interface with the existing BIM allows users to access and customize parameters of building elements more effectively than traditional coding tools allow. Moreover, users can easily establish relationships between building element parameters and any external data through a node-based visual programming language. The interface can provide a new workflow to make the building performance optimization more accessible for innovative energy-efficient building design (Rahmani Asl et al., 2015). Grasshopper for McNeel Rhinoceros and Dynamo for Autodesk Revit are examples of a visual programming environment that are compatible with BIM.

2.2.2 BIM's API

BIM's API is a set of codes that enables users to interact with a building model by connecting a source code to a reference element or a specific sub-element contained in the BIM database. API allows users to develop additional features and create custom tools, and plug-ins according to the desired needs on

a BIM modeling platform (Kensek, 2014) as well as it allows the access and customization all the parameters/properties of elements in a BIM project. Various BIM authoring software packages, such as Bentley ArchiCAD, Vectorworks, Tekla BIM, Catia, and MicroStation BIM, provide their own API. However, the Autodesk Revit API is a current popular software tool for application developers in the AEC industry. Revit API provides three methods to access its source code: (1) writing a program or script in the C# programming language using Visual Studio; this is the most prevalent and flexible method to utilize the API provided by Autodesk Revit in order to create Revit's add-ins; (2) using beginner scripting, such as Python, Visual Basic, and the C# to create Macros; (3) using graphical visual programming, such as Dynamo, which is an add-in for Autodesk Revit, to provide visual dataflow programming directly inside the Revit application (Boeykens, 2012). Programming experience is required to effectively use an API, which is not practicable for designers who are non-programmers. Visual programming is an option to take advantage of Revit API for users who have no programming experience.

2.2.3 Environmental sensing data with BIM

Environmental sensors, especially temperature sensors are crucial instruments that can be used to monitor minimum and maximum temperatures for maintaining thermal comfort conditions. Although collecting building environmental data using sensors provides valuable information for improving building performance, actual measurement data are not always available for use in conjunction with BIM. Efforts are being made to integrate environmental sensor (e.g., for sensing temperature, lighting, infrared, noise, humidity, and CO₂) with BIM for various purposes, such as building energy management by providing feedback of power usage (e.g., Wang et al., 2013; Hailemariam et al., 2010; Khan et al., 2011), design development (e.g., Kensek, 2014), and building performance analysis (e.g., Mauriello et al., 2015).

Based on a previous study as mentioned above, using computational logic in an advanced building information modeling environment can help to connect sensor data with a virtual BIM model. Visual programming interface tools are a method by which to bridge the hardware-software gap between sensors and 3D virtual models (Kensek, 2014).

2.2.4 Game engine and virtual reality technology with BIM

BIM has created an opportunity for stakeholders to collaborate and share multidisciplinary building information (Eastman et al., 2008) that can help designers to save time when creating new models (Ham et al., 2014). Integration with computer gaming environments is a new capability of BIM technology that allows users to better observe facilities and experience their surrounding environment before it is constructed (Figueroes-Munoz et al., 2015). Coupling of a game engine and the BIM can create a highly interactive environment with a digital geometry model derived from the BIM software. A number of previous studies have proposed methods for integrating game engine, BIM, and VR experience for

various purposes, e.g., design review (e.g., Shiratuddin et al., 2011; Wu, 2015), construction management (e.g., Bille et al., 2014), education (e.g., Wu, 2015; Goedert et al., 2011), energy conservation (e.g., Niu et al., 2015; Jalaei et al., 2014; Brewer et al., 2013), real-time architectural visualization (e.g., Yan et al., 2011), and design feedback (e.g., Hosokawa et al., 2016; Bahar et al., 2013; Motamedi, et al., 2017). Figueiras-Munoz et al. (2015) indicated that integration of BIM and gaming technology has the potential for combinatorial innovation.

2.3 Indoor thermal comfort analysis

ASHRAE standard 55 defines thermal comfort as a state of mind, which expresses satisfaction with the thermal environment (ASHRAE, 2013). There are three different methods for describing thermal comfort: predicted mean vote (PMV), predicted percentage of dissatisfied (PPD), and the adaptive method model (Fanger, 1970). Fanger (1970) proposed the PMV method for estimating thermal sensation and comfort based on a heat balance model. PMV is an index that predicts the mean value of the votes of a large group of people on a seven-point thermal sensation scale (3: hot, 2: warm, 1: slightly warm, 0: neutral, -1: slightly cool, -2: cool, -3: cold) (ASHRAE, 2013; Fanger, 1970). The main factors related to PMV are air temperature, clothing level, and MRT. PPD is a quantitative measure of thermal comfort in a particular environment based on occupants' votes and is related to the PMV method (ASHRAE, 2013; Fanger, 1970). The concept of adaptive method is applicable to naturally ventilated buildings with no mechanical cooling and heating system (Center for the Built Environment, 2013). The adaptive method is based on the fact that such buildings achieve thermal comfort across a wider range of indoor temperature because of the increased level of personal control over operable windows (de Dear et al., 2013).

2.3.1 Thermal comfort determinants

Thermal comfort measurable influential factors can be divided into physical, physiological, and psychological factors (Fanger, 1973). The main factors include four objective parameters: air temperature (°C), relative humidity (%), MRT (°C), air velocity (m/s), and two subjective parameters: metabolic rate, and clothing insulation. One of the most difficult parameters to analyze is MRT (La Gennusa et al., 2005). Evaluating MRT should take into account not only thermal radiation from surfaces but also the thermal radiation impinging on the human body (La Gennusa et al., 2005). MRT accounts for approximately 50% the occupants level of perceived comfort. There are different methods for evaluating MRT, including calculation methods using equations and measurement methods using globe thermometers or sensors. MRT is defined as the uniform surface temperature of surrounding walls and surfaces of an enclosure that affect the rate of radiant heat loss from the human body.

2.3.2 3D mean radiant temperature calculation

Manual calculation methods to derive MRT (T_{mrt}) are complicated and are not suitable for practical use due to angle factors, which are the influences of surrounding surfaces (Zmrhal et al., 2003). In order to calculate MRT by considering conical angles of building surfaces with respect to the position of the human body, the variables are the average of the surrounding surfaces temperature (T_i) and the angle factor between the person and surrounding surfaces ($F_{(p-N)}$). 3D MRT calculation can be performed using the following equation (ISO 7726, 1998):

$$T^4_{mrt} = T_1^4 F_{p-1} + T_2^4 F_{p-2} + \dots + T_i^4 F_{p-i} + \dots T_N^4 F_{p-N} \quad (1)$$

The angle factor between the person and the surface can be computed using the following equation:

$$F_{p-i} = F_{max} [1 - e^{-(a/c)/\tau}] [1 - e^{-(b/c)/\gamma}] \quad (2)$$

where

$$\tau = A + B(a + b)$$

$$\gamma = C + D(b/c) + E(a/c)$$

a is the width of the surface

b is the height of the surface and

c is the distance between the person and the target surface.

The coefficients F_{max} , A , B , C , D , and E describe difference values for two postures: seating or standing (Babiak et al., 2007).

Based on the literature, the evaluation of thermal comfort based on the correlation between the surface temperature of a building and the air temperature can be performed using two different tools: adaptive method chart (Center for the Built Environment (CBE), 2013) and a chart of the correlation between indoor air temperature and surface temperature (Sedlbauer et al., 2005; Gut et al., 1993).

The building envelope is one major factor that contributes to the thermal environment achieved inside the building. Building envelopes primarily comprise both opaque and transparent walls and roofs, which have a major effect on the heating and cooling loads required to maintain a satisfactory interior environment (Warren, 2003). Improving internal thermal comfort can be achieved by a high level of occupant satisfaction through an appropriate thermal design of the building envelope. Absorptivity, heat capacity and thermal conductivity of the building envelope have a profound effect on indoor thermal comfort. Evaluation of thermal comfort in a confined space depends on more than simply air temperature. Combining the radiant heat of each surface in the room with the air temperature to obtain

the operative temperature is also important. The operative temperature is defined as a uniform temperature of an imaginary black enclosure in which a person would exchange the same amount of heat by radiation and convection as in an actual non-uniform environment. The operative temperature is the average of the MRT and dry-bulb temperatures and can be obtained as follows:

$$T_o = \frac{T_{mrt} + T_{dry-bulb}}{2} \quad (3)$$

where

T_o is the operative temperature and
 T_{mrt} is the MRT, and $T_{dry-bulb}$ is the air temperature

2.3.3 Infrared thermography

Infrared thermography or thermal imaging and environmental sensors are currently available tools for diagnosing building issues, recognizing problems, prioritizing building maintenance, inspecting hidden problems and predicting required maintenance. Infrared thermography has been widely used to help identify potential problematic areas that need to be improved (Grinzato et al., 1998) by identifying thermal performance, precisely detecting heat sources in a building, measuring heat emissivity by transforming hidden characteristics to visible images (Eads et al., 2000), recording potential defects and apparent temperature readings, which can be interpreted for the propose of predictive maintenance, and assessing the energy efficiency of buildings. An infrared camera or thermographic camera can detect the intensity of radiation and converts invisible radiation emitted from a heated surface into temperature, which is then displayed as a thermal image (thermograph) (Rao, 2008). Infrared thermography has proved to be an adequate technique for measuring surface temperature in a continuous manner (Lagüela et al., 2012). While using an infrared thermometer is useful for measuring a single spot temperature, an infrared thermal imaging camera can scan and measure an entire building. This can also be achieved using hundreds of infrared thermometers simultaneously (Lagüela et al., 2012). However, thermal cameras measure only surface radiation rather than the actual temperature. Surface temperature readings by a thermographic camera indicate apparent temperature values (Rao, 2008). Theoretically, the total radiation received by the infrared camera comes from three sources: the emission of the target object itself, the emission of the surroundings reflected by the object, and the emission of the atmosphere (Usamentiaga et al., 2014). According to the Stefan- Boltzmann law, the surface temperature can be obtained using the following equation (Danese et al., 2010; Ganem et al., 2016):

$$E = \varepsilon \sigma T^4 \quad (4)$$

where

E is the radiation emitted per unit of surface (W/m^2)

ε is the total hemispherical emissivity of the surface ($0 < \varepsilon < 1$) (non-dimensional)

σ is the Stefan-Boltzmann constant ($5.67 \times 10^{-8} W/m^2 K^4$)

T is the surface absolute temperature (K).

Usamentiaga et al. (2014) and Revel et al. (2014) proposed the following equation for calculating a more accurate surface temperature from infrared thermography:

$$T_{obj} = \sqrt{\frac{W_{tot} - (1 - \varepsilon_{obj}) \cdot \tau_{atm} \cdot \sigma \cdot (T_{refl})^4 - (1 - \tau_{atm}) \cdot \sigma \cdot (T_{atm})^4}{\varepsilon_{obj} \cdot \tau_{atm} \cdot \sigma}} \quad (5)$$

where

$W_{tot} = \varepsilon_{obj} \cdot \tau_{atm} \cdot \sigma \cdot (T_{obj})^4 + (1 - \varepsilon_{obj}) \cdot \tau_{atm} \cdot \sigma \cdot (T_{refl})^4 + (1 - \tau_{atm}) \cdot \sigma \cdot (T_{atm})^4$ ε_{obj} is

the average emissivity of the surface

τ_{atm} is the transmission coefficient of the atmosphere (assumed as a constant value of 0.99)

T_{obj} is the temperature of the target object measured by the infrared sensor, T_{refl} is the reflected temperature and

T_{atm} is the temperature of the atmosphere (indoor air temperature).

There are two main forms of using infrared thermography: steady and transient. A steady thermogram is a static snapshot of the temperature measurement, whereas transient thermography allows observation of changes in surface temperature over time from a single thermogram (Danese et al., 2010). Thermography is commonly used to qualitatively or quantitatively identify the distribution of radiant heat on a surface. Quantitative evaluation requires the quantification of temperature values in order to distinguish the severity of a problem. The amount of radiation emitted by an object is directly proportional to the surface temperature of the object. The qualitative method requires a visual evaluation of the color pattern of surface-heat variations by using a thermographic image, which presents different temperature distribution ranges on each surface.

2.4 Thermographic 3D modeling and RGB thermal textures

Conventional thermography for building energy auditing involves the acquisition of multiple 2D images, which has significant limitations. For example, it is difficult to identify problems without providing the building context, e.g., the location and geometry of the object and affected areas (Vidas

et al., 2013). Moreover, it is difficult to visualize the overall building layout from 2D images, and photographs cannot be attributed to a particular side of the building (Wardlaw et al., 2010). Conversely, a 3D thermal model provides more comprehensive 3D views of the thermographic data by integrating thermal imagery with the geometric model. A number of previous studies have proposed methods for 3D thermal modeling based on field surveys of thermal data of building envelopes (e.g., Ham et al., 2014; Lagüela et al., 2012; Schreyer et al., 2009; Borrman et al., 2012). However, these studies focused only on creating 3D thermal models for various purposes without considering the integration between temperature sensing data with the 3D thermal model for verifying the effect of thermal data on the indoor thermal condition.

Techniques for creating 3D thermal models for measuring the surface temperature of existing buildings can be divided into three categories. The first category includes techniques for mapping infrared images to a 3D model, and the second category involves image fusion and matching infrared images and digital images. Finally, the third category involves mapping infrared images to 3D point clouds (Wang et al., 2013). Furthermore, a structure from motion (SfM) technique can be used to generate a 3D reconstruction by combining a sequence of 2D thermographic images of a building (e.g., Hoegner et al., 2015). Thermographic images mapped on a BIM model can provide an accurate 3D geometry of a building with thermographic textures. Providing RGB color values in thermal images supports the interpretation of the different temperature values. The RGB value of each of the individual pixels in a thermal image refers to the apparent temperature value, which is useful for thermal verification of object temperatures.

2.5 Visual analytics for root-cause detection

Visual analytics is the science of analytical reasoning facilitated by interactive visual interface (Thomas et al., 2005). Visual analytics evolved from combining automatic data analysis techniques and information visualization for an effective understanding of very large and complex datasets (Keim et al., 2009; Keim et al., 2012). The goal of visual analytic techniques is to make the best possible use of the huge amount of information involving multiple processes and a variety of applications by appropriately combining the strengths of intelligent automatic data analysis with the visual perception and analysis capabilities of the human user (Kohlhammer et al., 2011). The development of such techniques enables users to: 1) synthesize information and derive insight from massive, dynamic, ambiguous, and often conflicting data; 2) detect the expected and discover the unexpected; 3) provide timely, defensible, and understandable assessments; and 4) communicate assessments effectively in order to take appropriate actions (Thomas et al., 2005).

By integrating the analytical ability of humans and information visualization, visual analytics methodology can significantly support the process of the root-cause detection of building defects

captured by infrared thermography. Spatiotemporal data generates abnormal temperature profiles of surfaces. Thermographic data is displayed primarily using false colors, which serve as a basis for distinguishing the areas of the lowest temperature and highest temperature. Danese et al. (2010) confirmed that the visual analytics method can be used to facilitate the interpretation of multi-temporal thermographic imagery and can serve to identify spatial and spatio-temporal patterns that could provide valuable information about the building structure, the level of decay of material, and the presence of other physical phenomena in the building envelope.

2.6 Evaluating thermal performance of building envelopes

The building envelope plays a significant role in regulating indoor temperature and minimizing the amount of energy required for heating and cooling. To effectively maintain a comfortable temperature in a building, the selection of materials for the building envelope requires careful attention to limit the heat transferred through the building envelope. Globally, there are two building standards that are popularly used to measure the thermal performance of a building envelope: (1) thermal insulation standards, which are used in cold climates (using this standard, thermal transmittance values (U-values) of the envelope material are measured) and (2) OTTV building regulations, which are used in hot climates, especially in Southeast Asia (Li et al., 2010). OTTV regulation is applicable to mechanically cooled buildings. The aim of the OTTV code is to prescribe the thermal characteristics of the building envelope (Szokolay, 2004).

2.6.1 Building envelopes

The evaluation of building performance can be divided into five aspects: (1) the building envelope, (2) the air conditioning and ventilation, (3) the water heating system, (4) the dynamic equipment, and (5) the illumination (Egwunatum et al., 2016). A building envelope is a physical separator between the internal and external environments. Building envelopes are required to perform a combination of structural roles, such as space-enclosing and environmental protection (e.g., heat and noise) or modification roles (Murthy, 1978). Materials utilized for the building envelope are typically considered to be thermal storage components. Building envelopes include the exterior walls, roofs, and floors. A thermal barrier (or insulation) and an air barrier are the two components of a building envelope. The thermal barrier is a boundary for heat flow, and the air barrier is a protective, air-resistant material that controls air leakage in and out of the building envelope (Kruger et al., 2013).

To maintain comfortable indoor conditions, the entire building envelope must provide a good thermal barrier and prevent heat losses and gains. The building envelope has been considered to be the most important factor affecting energy efficiency (Egwunatum et al., 2016). A number of studies have shown that the thermal properties of building enclosure materials have a major impact on the proportion of

operational energy required by the buildings, especially for cooling and heating systems (Kruger et al., 2013; Noori et al., 2015; Sadineni et al., 2011).

Noori et al. (2015) proposed strategies to minimize heat gain through the envelope by enhancing the design and choosing appropriate building materials, including (1) redesigning the envelope, (2) using alternative materials, (3) using insulation materials, (4) installing shading devices and enhancing the surrounding microclimate, and (5) selecting an optimum building orientation and area of windows. An appropriate choice of the combination of envelope materials is one strategy that can lower the thermal impact, minimize solar heat transmission, and help architects achieve high energy efficiency in buildings (Sadineni et al., 2011).

2.6.2 Building regulations worldwide for energy-efficient building envelope design

Regulations to control building envelope design are a set of rules that specify the minimum/maximum acceptable limit of heat gain penetrating through envelopes, to help a designer obtain an energy-efficient design with optimal thermal characteristics of materials, for example, the U-value, thermal resistance (R-value), and Solar Heat Gain Coefficient (SHGC). Prescriptive requirements for building envelope designs for evaluating thermal performance have been established in many countries worldwide. Different standards cover different climate conditions. For example, Li et al. (2010) stated that there are two standards that are popularly used to measure the thermal performance of building envelopes worldwide: the U-value for countries with cold climates and the OTTV for countries with hot climates. An example of the minimum requirements of the U-value of building envelopes in cold-climate countries (i.e., in Europe) is shown in Table 1. The Perimeter Annual Load (PAL), adopted in Japan, is another standard to evaluate the envelope performance of buildings. PAL refers to the annual thermal load of perimeter spaces per unit area and is expressed in MJ/m²yr (Energy, Act, & Program, 2016). Prescriptive requirements for heat transfer coefficients and the resistance of insulation materials were adopted in Japan only for residential buildings (Laustsen, 2008). In the U.S., the American Society of Heating, Refrigerating and Air-Conditioning Engineers (ASHRAE) 90.1 and the International Energy Conservation Code (IECC) are used as standards for designing high-performance buildings. ASHRAE 90.1 provides a minimum prescriptive/mandatory requirement for R-values and a maximum requirement for U-values of building envelopes for thermal performance assessment in different climate zones (McGuerty et al., 2013).

Table 1 Example of the minimum requirement for the U-value of building envelopes in cold-climate countries (i.e., Europe)

	United Kingdom	Denmark	Finland	Sweden	Germany	Ireland	
Source	(HMG, 2013) (B. Anderson, 2006)	(The Danish Ministry of Economic and Business Affairs Danish Enterprise and Construction, 2015)	(Decree of Ministry of the Environment on thermal insulation in a building, 2002)	(The Swedish National Board of Housing Building and Planning, 2011)	(Federal Ministry of Transport, 2009)	(Government of Ireland, 2011)	
Year released	2010	2015	2003	2011	2009	2011	
Status	Mandatory	Mandatory	Mandatory	Mandatory	Mandatory	Mandatory	
Standard	The Building Regulations 2010 Conservation of fuel and power in new dwellings (L1A) and in new buildings other than dwellings (L2A) British Standard (BS) EN ISO 8990 is used as the measurement standard for the U-value of the building components, i.e., walls, roof, and floor, BS EN ISO 12567-1 for windows and doors, and BS EN ISO 12567-2 for rooflights	Danish Building Regulations (BR) 15	C3 National Building Code of Finland	Building and Planning Building Regulations (BBR)	Energy Conservation Regulations (EnEV)	Building Regulations: Part L Conservation of Fuel and Energy: Dwellings and Part L - Conservation of Fuel and Energy Buildings other than Dwellings.	
The minimum requirement of U-value (W/m ² °K)	Walls Windows Roofs Floors Skylight Outside doors	0.30 2 0.20 0.25 2 -	0.30 0.18 1.50 0.15 1.40 0.14-0.15	0.25 1.40 0.16 0.20 1.50 1.40	0.18 1.20 0.13 0.15 - 1.20	0.28 1.30 0.20 0.35 1.40 1.80	0.21 1.60 0.16 0.21 1.60 1.60

2.6.3 Measurement of the thermal performance of a building envelope

To measure the performance of a building envelope in a hot climate, an important regulation, known as the OTTV, was developed to reduce external heat gains through the building envelope and the electricity demand of an air-conditioning system (Chan et al., 2014). The OTTV calculation method was initially created in 1975 by the ASHRAE. The OTTV concept has been described in the U.S. with the aim of determining heat gains and losses of a building (Janda et al., 1994). Since then, it has been employed in many countries. However, the OTTV is only applicable to mechanically cooled buildings (Li et al., 2010; Sadineni et al., 2011). A number of countries have created mandatory building energy efficiency standards and used the OTTV as part of their requirements. The maximum OTTVs for non-residential and residential buildings in various countries are shown in Table 2.

Table 2 OTTV standards in various countries

	Singapore	Thailand	Malaysia	Hong Kong	Philippines	Indonesia
Source	(Commissioner of Building Control, 2004)	(Ministry of Energy, 2009)	(GBI, 2010; GBS, 2011)	(Buildings Department, 2016)	(Philippine Green Building Council, 2013)	(Loekita et al., 2015)
Location	1° 20' N	13° 45' N	3° 7' N	22° 18' N	14° 35' N	6° 10'S
Year released	2008	2009	2010	2016	2013	2011
Status	Mandatory	Mandatory	Voluntary	Mandatory	Voluntary	Proposed
Standard	BCA	Building Energy Code	Green Building Index (GBI), MS1525,	B(EE)R	BERDE	SNI 03-6389-2011
Maximum OTTV for wall (W/m ²)	Non-residential buildings (air-conditioned area more than 500 m ²)	≤ 50 ≤ 50, ≤ 40, ≤ 30 Office and education buildings, department stores, hospitals, and hotels, respectively	≤ 50 ≤ 50 Office and education buildings, department stores, hospitals, and hotels, respectively	≤ 50 ≤ 50 Building tower and podium, respectively	≤ 24, ≤ 56 ≤ 24, ≤ 56 Building tower and podium, respectively	≤ 45 ≤ 45 N/A
	Residential building	≤ 25	N/A	≤ 50	≤ 14	≤ 45
Maximum OTTV for Roof (W/m ²)	Non-residential buildings (air-conditioned area more than 500 m ²)	≤ 50 ≤ 15, ≤ 12, ≤ 10 Office and education buildings, department stores, hospitals, and hotels, respectively	≤ 25 ≤ 25 Non-residential buildings	≤ 25 ≤ 25 Building tower, and podium, respectively	≤ 45 ≤ 45 N/A	≤ 35 ≤ 35 N/A
	Residential buildings	≤ 50	N/A	≤ 25	≤ 4	≤ 45

Building envelope design parameters related to OTTV control

The two principles of heat transfer that are taken into consideration for OTTV assessments are conduction and radiation. Conduction is the transfer of heat flow through solid opaque walls and glass windows, due to a difference in temperature between the two sides of the envelope. Radiation is the transmission of heat waves of electromagnetic radiant heat energy through glass windows. To control the rate of heat being conducted into the building, the following attributes of the building envelope must be considered while selecting materials for construction the building enclosure components (i.e., opaque and fenestration):

1. The U-value is the overall coefficient of thermal transmittance. It is used to measure the rate of transfer of heat through an envelope material and is measured in I-P units, by $\text{Btu}/\text{h}\cdot\text{ft}^2\cdot^\circ\text{F}$, and in SI units, by $\text{W}/\text{m}^2\text{K}$. Although a low U-value implies good insulation and low annual energy consumption, Masoso et al. (2008) stated that a low U-value alone is not always sufficient to reduce energy consumption, and other factors should be considered, including the combination of the cooling set-point temperature and internal gains.
2. The R-value is the converse of the U-value. It affects the ability of a material to resist heat flow and is expressed in I-P units, by $\text{ft}^2\cdot\text{h}\cdot^\circ\text{F}/\text{BTU}$ and in SI units, by $\text{m}^2\cdot\text{K}/\text{W}$. A higher R-value indicates greater thermal resistance.
3. The absorptivity of the external surfaces is expressed quantitatively by the absorption coefficient, which varies with the color of the exterior envelopes.
4. The shading coefficient (SC) of glass is a measure of the total solar gain passing through glass. SC depends on the color of the glass and the degree of reflectivity. The range of SC is 0.00–1.00. A low value implies that less solar heat is transmitted through the glass.
5. The external SC of shading devices is a measure of the solar control of shading to limit radiant and re-radiant solar gain.
6. The SHGC is a measure of the fraction of solar heat gain transmitted through glass. SHGC is measured on a scale of 0-1 (0: no heat is transmitted through the glass; 1: the highest amount of heat energy can pass through the glass).
7. With respect to the building's location or latitude, the building orientation and window-to-wall ratio (WWR) are particularly important for minimizing the amount of solar radiation received in a specific orientation, which affects the ambient temperature and ventilation.

Theoretical calculation of the OTTV

The OTTV calculation procedure for a wall and a roof divides the building enclosure into two types: opaque and glazing. Individual walls with the same orientation and same construction are first computed. Then, the OTTV of the entire envelope can be obtained by calculating the weighted average of the OTTVs of individual walls for all orientations (Lam et al., 1996). Building envelopes with high

OTTVs have high heat absorption by the building and quick heat transfer into the building. This means that the building requires high electricity consumption for cooling. Based on the available literature and building energy standards of various countries in Southeast Asia (see Table 2), the forms of OTTV equations in different countries have been modified to eliminate irrelevant terms and include additional variables depending on each location (Lam et al., 1996), as shown in Table 3, which compares the OTTV requirements and coefficients for six countries.

Table 3 Comparison of the forms of OTTV equations of different countries in Southeast Asia

Country	Building types		OTTV equations
			$OTTV = \frac{(A_{01})(OTTV_1) + (A_{02})(OTTV_2) + \dots + (A_{0i})(OTTV_i)}{A_{01} + A_{02} + \dots + A_{0i}}$
where OTTV = overall thermal transfer value from wall/roof for orientation i (W/m^2), A_{0i} = gross area of exterior wall or roof for orientation i (opaque wall/roof area + fenestration area) (m^2)			
			Opaque Fenestration
Singapore	Non-residential	Wall	$OTTV_i = 12(1 - WWR)U_w$ + 3.4(WWR)U_f $\quad + 211(WWR)(CF)(SC)$ (6)
		Roof	$OTTV_i = 12.5(1 - SKR)U_r$ + 4.8(SKR)U_s $\quad + 485(SRR)(CF)(SC)$ (7)
	Residential	Wall	$OTTV_i = 3.4(1 - WWR)U_w$ + 1.3(WWR)U_f $\quad + 58.6(WWR)(CF)(SC)$ (8)
		Roof	N/A
Thailand	Non-residential	Wall	$OTTV_i = (1 - WWR)(U_w)(TDeq)$ + (WWR)(U_f)(\Delta T) $\quad + (WWR)(SHGC)(SC)(ESR)$ (9)
		Roof	$OTTV_i = (1 - SRR)(U_r)(TDeq)$ + (SRR)(U_s)(\Delta T) $\quad + (SRR)(SHGC)(SC)(ESR)$ (10)
Hong Kong	Non-residential	Wall	$OTTV_i = (1 - WWR)(U_w)(\Delta T)(TDeq)$ + (WWR)(SC)(ESM)(SF) (11)
		Roof	$OTTV_i = (1 - SRR)(U_r)(\Delta T)(TDeq)$ + (SRR)(SC)(ESM)(SF) (12)
	Residential	Wall	$OTTV_i = 3.57(1 - WWR)U_w \alpha G_w$ + 0.64(WWR)U_f G_w $\quad + 41.75(WWR)(SC)(ESC)G_w$ (13)
		Roof	$OTTV_i = 3.47(1 - SRR)U_r \alpha G_r$ + 0.40(SRR)(U_s)(G_s) $\quad + 41.10(SRR)(SC_r)(G_s)$ (14)
Malaysia	Non-residential	Wall	$OTTV_i = 15 \alpha (1 - WWR)U_w$ + 6(WWR)U_f $\quad + 194(WWR)(SC)(CF)$ (15)
		Roof	$OTTV_i = (A_r)(U_r)(TDeq)$ + (A_s)(U_s)(\Delta T) $\quad + (A_s)(SC)(SF)$ (16)
Philippines	Non-residential	Wall	$OTTV_i = (A_w)(U_w)(TDeq)$ + (A_f)(U_f)(\Delta T) $\quad + (A_f)(SC)(SF)$ (17)
		Roof	$OTTV_i = (A_f)(U_f)(TDeq)$ + (A_s)(U_s)(\Delta T) $\quad + (A_s)(SC)(SF)$ (18)
Indonesia	Non-residential	Wall	$OTTV_i = \alpha [U_w (1 - WWR)(TDeq)]$ + (U_f)(WWR)(\Delta T) $\quad + (SC)(WWR)(SF)$ (19)
		Roof	$OTTV_i = \alpha [U_r (1 - SRR)(TDeq)]$ + (U_s)(SRR)(\Delta T) $\quad + (SC)(SRR)(SF)$ (20)

Nomenclature **OTTV for wall**

WWR - window to wall ratio (A_f/A_{0i})
 U_w - thermal transmittance of opaque wall ($W/m^2 K$)
 U_r - thermal transmittance of opaque roof ($W/m^2 K$)
CF - solar correction factors for walls/roof
SC - shading coefficient of external shading device
ESM - external shading multiplier for overhang projections to windows
TDeq - equivalent temperature difference for opaque wall
 ΔT - temperature difference between glazing surface and air
SF - solar shading factor of external shading devices (W/m^2)
 α - absorptivity of the wall
 G_w - wall orientation factor and
ESR - effective solar radiation,

OTTV for Roof

G_s - roof orientation factor
 α - absorptivity of the roof
ESC - roof orientation factor,
SRR or SKR - skylight to roof ratio (skylight area / gross area of roof)
 U_r - thermal transmittance of opaque roof (W/m^2)
 U_s - thermal transmittance of skylight glazing ($W/m^2 K$)
SHGC - solar heat gain coefficient
 A_w - area of opaque wall (m^2)
 A_f - area of fenestration (m^2)
 A_s - area of the skylight part of a roof (m^2)
 A_r - area of opaque roof (m^2)

As discussed, different countries use varying forms of OTTV equations with different choices of variables and calculation methods. Our prototype system provides a flexible approach to enable different OTTV calculation methods applicable to the systems used in different countries.

2.7 Lighting design analysis using BIM and VR technology

2.7.1 Integrating building information modeling (BIM) with a game engine

Using BIM-based simulations are increasingly being used to assess the success or failure of indoor lighting design. Lighting simulation plugins for BIM applications help users to analyze design options in order to provide sufficient lighting for occupants and improve building energy efficiency and overall building performance (Aksamija et al., 2010). Two types of lighting simulation plugins are compatible with the BIM: external plugins and internal plugins (e.g., Lighting Analysis in Revit, Lighting Assistant in 3ds Max, Radiance, Daysim, Diva, and DesignBuilder). Internal plugins or internal extensions can be added to BIM applications, e.g., Revit, to enable the highest degree of interoperability (Nasyrov et al., 2014). External plugins are needed for data exchange across platforms to perform simulations and visualizations. Generating quantitative results is the main use of such plugins. However, qualitative results of lighting design, which refers to the illumination of an entire scene and has complex characteristics, such as aesthetics, are difficult to quantify (Sorger et al., 2016).

A few studies have focused on using game engines and VR for lighting design visualization. For example, Gröhn et al. (2001) presented a method for visualizing indoor climate and visual comfort in a 3D VR environment. In their method, photo-realistic visualization was used to visualize the lighting distribution on the surfaces of the architectural model. However, they did not include real-time control of lighting conditions. In addition, Sik-lányi. (2009) studied how using different types of lights influences the development of realistic VR scenes. Sampaio et al. (2010) developed a virtual interactive model as a tool to support building management by focusing on the lighting system. Santos et al. (2003) developed an immersive VR system for interior and lighting design using the cave automatic virtual environment (CAVE). This system provided users with an interface to change the design elements of the building, e.g., walls, floor, furniture, and decoration, in a virtual environment. However, their system focused only on the appearance of lighting design using ray tracing as the rendering algorithm, which did not provide a function to simultaneously generate quantitative outputs of lighting design, e.g., illuminance level and energy consumption feedback.

2.7.2 Lighting design metrics in the game environment

Lighting plays an important role in indoor environmental conditions. Lighting performance depends on several factors, such as energy cost, energy savings, illuminance, and energy consumption (Deru et al., 2005). Designers want to achieve an optimal design with minimum energy consumption. The design of daylighting and artificial light rely on a combination of specific scientific principles, established

standards and conventions, and aesthetic (Benya et al., 2001). The following five physical parameters that influence occupants' visual comfort in architectural spaces should be considered: lighting illuminance levels, lighting distribution (diffusion), correlated color temperature (CCT), brightness ratio, and glare (Fielder, 2001; Descottes et al., 2011). Designers must ensure that the visual comfort parameters comply with the standard of lighting design. Regarding human visual perception, the most important variables are CCT and illuminance level (Shamsul et al., 2013). Visual perception is defined as an interpretation capability of visual sensation when people visually perceive their surrounding environment. As mentioned above, illumination level and CCT are two variables that have a significant influence on human perception. The illuminance value is an indicator for verifying the quantity of light in a given environment. International lighting standards and building regulations specify the level of illuminance required for providing visual comfort to facilitate human visual performance. Correlated color temperature describes the characteristics of light colors. Color temperature plays a particularly important role in both the physical properties of light and the physiological and psychological response of humans when light enters the eyes (Descottes et al., 2011; Shamsul et al., 2013).

VR experience is based on users' perception of the virtual world (Mihelj et al., 2013). VR technology enables the creation of realistic models and makes scenes look real (Stahre et al., 2006). Immersion (perception) and real-time interaction (action) are two properties of VR. VR allows users to experience an artificial environment through human senses (Souha et al., 2005). Head-mounted displays (HMDs) have been used as 3D immersive tools to provide an experience that is close to the human perception of reality (Ciribini et al., 2014; Scarfe et al., 2015).

In the game environment, lighting plays a significant role in making scenes look realistic. Game engine technology has lighting features that resemble real-world lightings (Shiratuddin et al., 2011). Lighting simulation for gaming and VR presentations relies on a mixture of rendering algorithms, including path tracing and photon mapping. It is possible to effectively and physically simulate indoor illuminated environments at a level of quality where concepts of photorealism and perceptual accuracy can be discussed and measured (Murdoch et al., 2015). Lighting simulation in game engines can produce realistic scenes based on the inverse square law, which states that illumination intensity varies directly with luminous intensity on a surface and is inversely proportional to the square of the distance between the light source and the lighted surface (IESNA, 2000; de Rousiers et al., 2014). Other lighting metrics, such as luminous flux and light color, are also provided in the game engine. Luminous flux (light output or intensity), measured in lumens (lm), determines the quantity of light emitted from the lamp to illuminate the entire scene. Light color is expressed as color temperature (kelvins or the SI abbreviation "K"). Another parameter for measuring light is luminance, measured in foot lamberts (fL) or candelas/m² (cd/m²). Luminance refers to perceive brightness which describes the amount of light delivered into space and reflecting off of a surface in a space that affects human ability to see (The Energy and Resources Institute (TERI), 2004). Luminance measurement affects the measurement of

exterior/interior design and finishes in reflecting light rather than measuring lighting quality. Luminance is a useful baseline metric to identify sources of glare within a person's field of view. The advanced dynamic lighting feature in game engines allows pre-visualization of various designs. Consequently, lighting features in game engines replace conventional methods and enable faster lighting simulation when changing parameters. Moreover, it is possible for players to perceive the characteristics of light in order to determine which design pattern is more appropriate for the users.

2.7.3 Human visual perception through VR technology

A number of previous researches have studied visual perception dimensions of VR technology. Menshikova (Menshikova et al., 2012) studied the Simultaneous Lightness Contrast (SLC) illusion and the results of their study showed that VR technologies may be effectively used in studies of lightness perception. Their study showed that the VR technology enables reproducing visual illusions in depth and to construct complex 3D scenes with controlled parameters to create articulated effects. Scarfe et al. (2015) stated that immersive VR opens up new possibilities for studying visual perception in much more natural conditions.

The quality of an HMD display screen depends on its resolution as well as luminance and contrast ratio of the screen, field of view (FOV), exit pupil, eye relief, and overlap (Vince, 2004). The contrast is the ratio between higher luminance and the lower luminance that defines the feature to be detected, a value of 100:1 is typical. Luminance is the amount of light energy emitted or reflected from a screen in a specific direction (Fuchs, 2017) and a measure of a screen's brightness, and ideally should exceed 1000 cd/m² (Vince, 2004). The luminance that can be observed in nature covers a range of 10⁻⁶ to 10⁶ cd/m² and the human visual system can accommodate a range of about 10⁴ cd/m² in a single glance (Fuchs, 2017). The FOV is a measure of the horizontal and vertical angle of view. The horizontal FOV of HMDs is restricted to about 100–120 degrees for each eye (Fuchs, 2017).

VR has a great potential to become a usable design tool for the planning of lighting design in buildings (Stahre et al., 2006). However, due to the technological limitations, there are still problems in representing realistic lighting condition. A virtual world may produce semi-realistic lighting phenomena, however, precisely perceiving illuminance and glare of scenes in HMD is impossible with the current technology. The FOV of a typical head based-display is limited and the resolution can vary from the relatively few pixels offered in the early system to very high resolution (Sherman et al., 2003). The screen of VR headset should display a huge number of pixels about 6000 pixels horizontally and 8400 pixels vertically, which are not compatible with the current technology (Fuchs, 2017). Although the visual perception is still different from the reality using the current technology, there are many visual details in the luminous environment that cannot be expressed through numerical information, such as misaligned luminaries and disturbing light-shade patterns (Inanici, 2007).

2.7.4 Discomfort glare indices

Glare refers to a physical discomfort and is caused by non-uniform luminance distribution within the visual field (Fasi et al., 2015). Glare occurs in two ways; excessive brightness and the excessive range of luminance in a visual environment (IESNA, 2000). Glare is typically divided into three categories: 1) disability glare, which is caused by excessive brightness areas in the field of view of a person with greater luminance than that of which eyes can adapt to; 2) veiling glare, which is caused by reflections on specular or diffusive materials that might reduce the contrast and visibility of the task; 3) discomfort glare, a psychological sensation that does not necessarily impair vision in short term and can remain unnoticed to observers, it can cause annoyance, headaches or eyestrain after long exposure (Abraham, 2017). Discomfort glare is caused by luminance that is high relative to the average luminance in the field of view (IESNA, 2000). A glare index is a numerical evaluation of the acceptability of the presence of glare using a mathematical formula.

Several principal indices of discomfort glare have been proposed to quantify discomfort glare generated from small lighting sources (e.g., artificial lighting) and large luminous sources (e.g., windows) (Abraham, 2017). For discomfort generated by small sources, examples of discomfort indices include visual comfort probability (VCP) (Guth, 1963), unified glare rating (UGR) (Sorensen, 1987), and CIE glare index (CGI) (Einhorn, 1973). Example of discomfort indices generated by large luminous sources includes daylight glare index (DGI) (Chauvel et al., 1982) and daylight glare probability (DGP) (Wienold et al., 2006).

VCP is a rating that evaluates lighting systems in term of the percentages of people that will find a given discomfort glare (IESNA, 2000). VCP is defined as a number that corresponds to the percentage on a scale of 0–100. UGR is used to measure glare possibility in a given environment. UGR is the logarithm of glare from electric light sources (Boyce, 2003). UGR value ranging from 10 for low levels of discomfort glare to 28 for high levels of discomfort glare. DGI index was developed to predict glare from large area sources, such as a window. The DGI uses categorical rating to explain quantitative value between 16 for just noticeable to 28 for intolerable glare (Hirning et al., 2014). DGP is a metric for an estimate of the appearance of discomfort glare in daylit spaces. DGP considers the vertical illumination at the eye level as well as on the glare source luminance, its solid angle and its position index (Wienold et al., 2006).

Recently, most architect and lighting designers prefer not to be guided by glare indices (Hirning et al., 2014). However, preventing glare is important for design consideration (Reinhart et al., 2012) such as work safety. Various studies have investigated that there are other potential subfactors which influence the large variations in individual glare sensitivity, such as age of the person (Reinhart et al., 2011; Van den Berg et al., 2009), gender (Wolska et al., 2014), culture (Amirkhani et al., 2016), and physical differences (Pulpitlova et al., 1993). Although various metrics have been developed attempting to

quantify glare, a major obstacle in quantifying discomfort glare is the difficulty in analyzing complex lighting distributions due to the dynamic nature of daylight (Hirning et al., 2014). Every equation evaluate glare differently, and the evaluation of discomfort glare indices in practice is complicated (Stone et al., 1973; Clear, 2012). However, in the advanced lighting research, the assessment of discomfort glare in spaces increasingly involves the use of simulated high dynamic range (HDR) images (Boyce, 2003; Giraldo et al., 2016).

A number of studies have focused on using HDR images for discomfort glare analysis from daylight, e.g., (Clear, 2012; Suk et al., 2017; Mcneil et al., 2016). Existing glare assessment studies were typically based on real-world building. A few studies have proposed methods to simulate light illuminance and glare in a virtual environment, (e.g., Mangkuto et al., 2014; Inanici et al., 2003). HDR images store luminance data on a pixel scale, which enable the possibility of detecting glare sources to compute discomfort glare metrics. With the digital evaluation of HDR, it is possible to integrate the HDR rendering scenes generated by a game engine with glare evaluation tools, such as Evalglare, Photolux, Find- glare, to improve the lighting design and discomfort glare measurement during the design process.

Chapter 3 Overview of the research

3.1 Introduction

This chapter presents an overview of the proposed methodology. This thesis proposed a BIM-based data model and integrated frameworks for building performance evaluation and environmental simulations. This research comprises three main systems. As mentioned in Section 1.3, this research aims to extend the capabilities of the current BIM for aiding the evaluation of building performance with respect the requirements in building energy-efficient standards (i.e., ASHARE standard, IESNA lighting standard, and OTTV standard). Four main technologies have been proposed to integrate with BIM: graphical visual programming software, environmental sensing data, infrared thermography, and VR technologies. Figure 2 shows the overall structure of the dissertation and content relationship of this research, and it also presents how the literature review sections are related to the subsequent chapters.

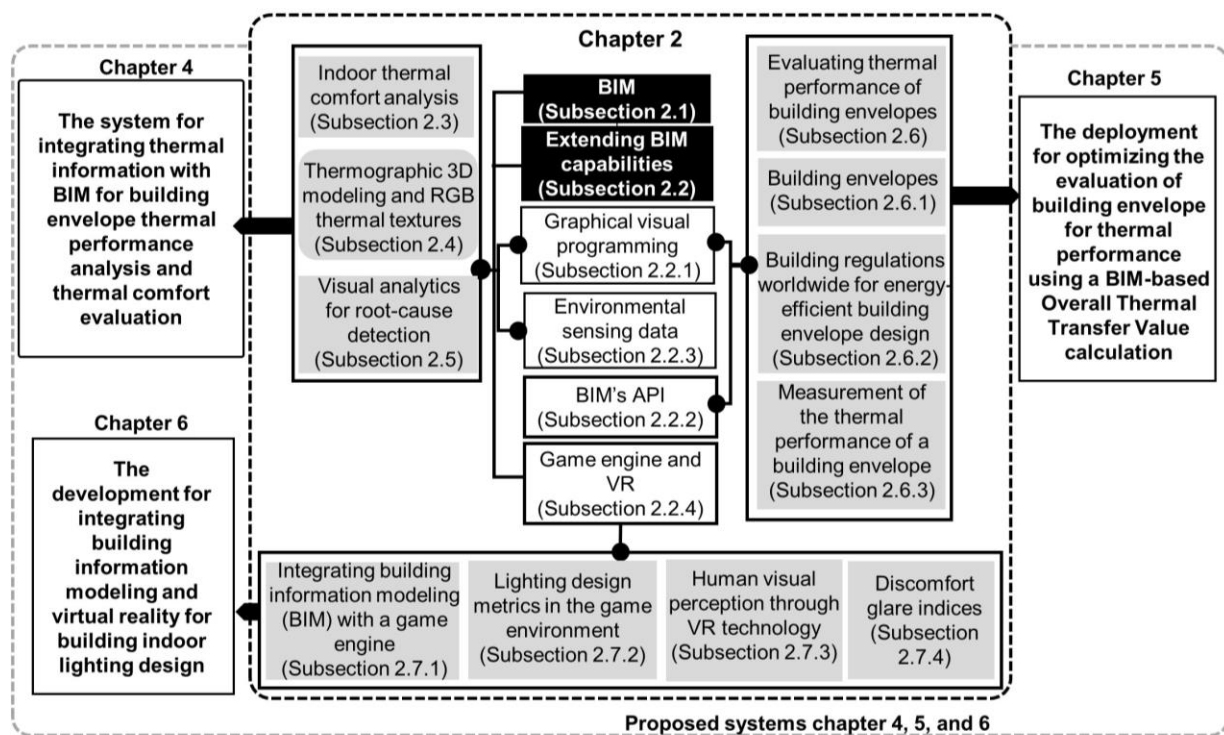


Figure 2 Content relationship

3.2 Overview of the proposed methodology

In this research, the BIM technology is used as a central data repository of building information that facilitates interoperability between BIM and the technologies mentioned in Section 3.1 proposing the evaluation of the thermal performance of building envelopes, indoor thermal comfort, and lighting design. As shown in Figure 3, for evaluating the thermal performance of building envelopes, two systems have been developed on the basis of different phases of a building project. In this research, the systems for evaluating building envelopes for thermal performance during the design stage and operational stage have been developed. For lighting design feedback, a system has been developed to couple BIM and game engines to create a highly interactive environment with a digital geometry model that is derived from the BIM software and to simulate daylighting and artificial lights of a designed building.

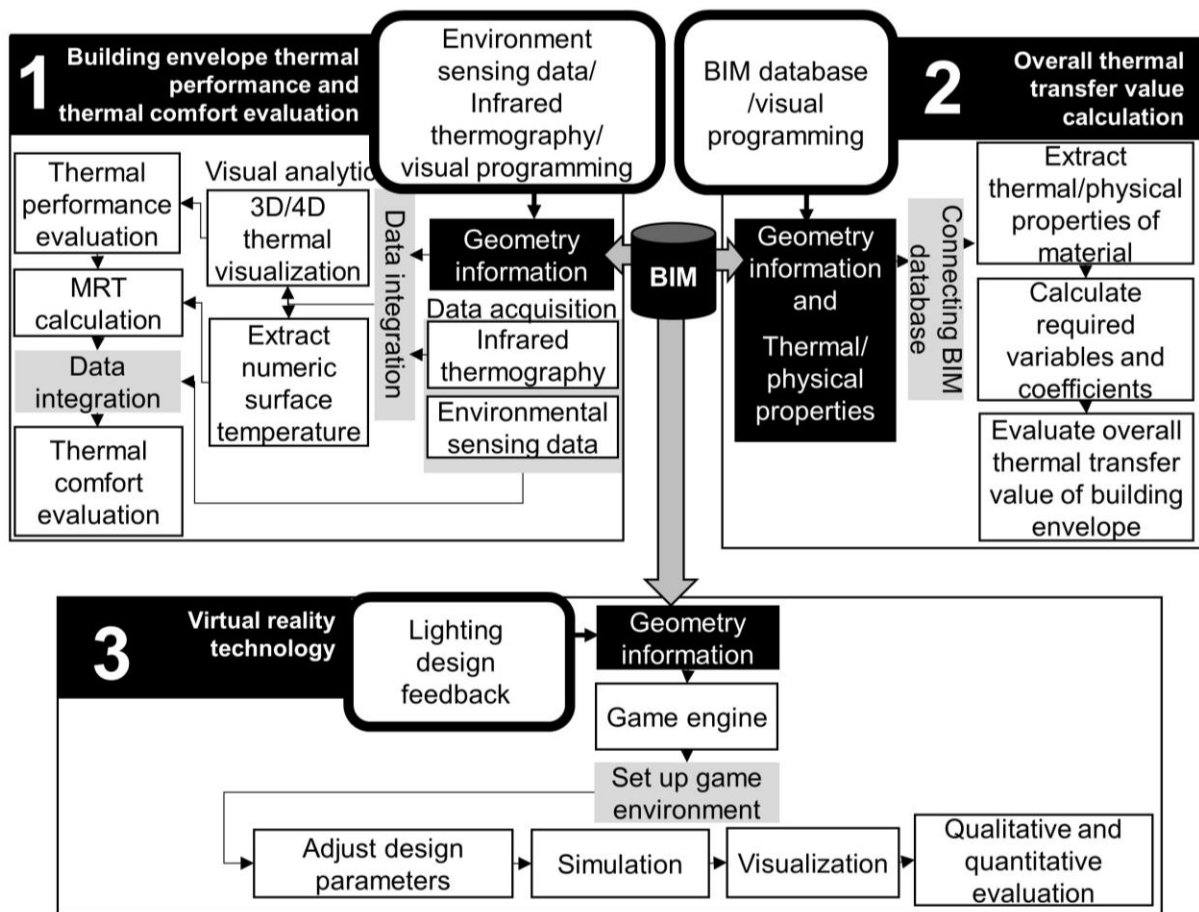


Figure 3 Overview of the proposed methodology

3.3 Integrating thermal data with BIM for evaluating thermal performance of building envelope and indoor thermal comfort in the operational stage

The first developed a method is to systematically collect environmental and thermal data and to integrate them with the BIM model in order to be used for various applications during the operation and maintenance phase of the building lifecycle. Surface temperature values are extracted from thermographic images and are geometrically referenced using a BIM model. This is done by mapping time coded thermal images on modeled surfaces. Additionally, time-coded thermal data together with an as-built BIM model are used to calculate variables to evaluate the thermal comfort. Furthermore, the integrated thermographic images on the surface of building envelope assist spatio-temporal analysis through 4D visualizations. The proposed method does not aim to reconstruct the BIM model from thermal images, however, it proposes mapping such images on the surfaces of an existing BIM model.

The proposed methodology comprises six main steps as shown in Figure 4. The first step is BIM modeling and data collection. Thermal and environmental data, including surface temperature reading (i.e., thermographic images), sensors reading (i.e., air temperature and humidity values), and weather condition descriptions, are collected for a building, and a 3D BIM model of the building is then created (Figure 4a). The second step is to map the thermographic images to the BIM and to integrate sensor data with the BIM model (Figure 4b). The integrated thermal images provide information for the visual analysis and can be used to create a database of numerical thermal data. The third step is data extraction and data processing. The obtained raw data are processed to support thermal comfort evaluation (explained in Section 4.2.4) (Figure 4c). The fourth step is to create appropriate outputs from the BIM to be used for thermal performance analysis and thermal comfort measurement. In this step, 3D (spatial), 4D (spatio-temporal) visualizations, and statistical outputs are obtained (Figure 4d). In the fifth step, the analysis of spatio-temporal thermal data is performed using visual analytics to investigate spatial thermal data, and to identify root causes of problems, defects, and inefficiencies. In addition, calculation of thermal comfort variables and measurement of the thermal comfort level are also performed in this step (Figure 4e). The sixth step is to execute improvement scenarios (Figure 4f).

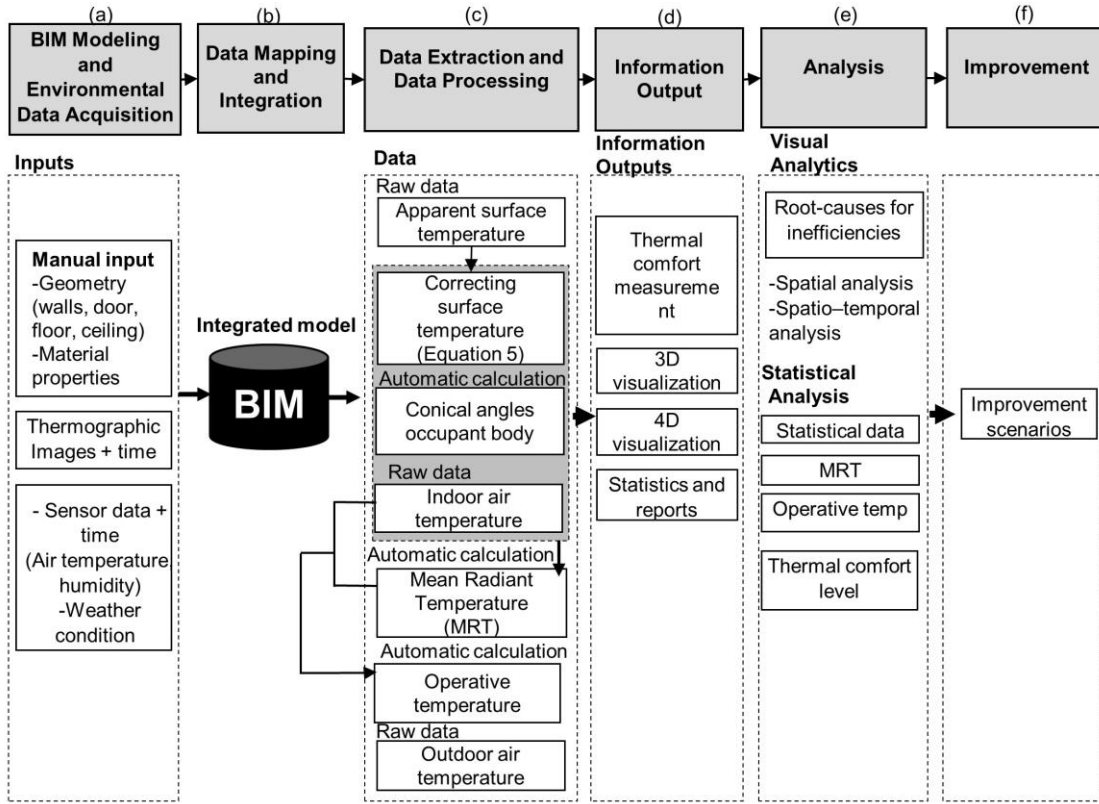


Figure 4 Overview of the system for integrating infrared thermography and sensing data with BIM model

3.4 Extracting BIM database for overall thermal transfer value calculation

The second system focuses on extending BIM using its visual programming to better select an appropriate thermal characteristic of envelope materials. Graphical visual programming provides the opportunity to extend the capability of BIM. BIM can also be used as a central repository of information related to the thermal characteristics of building envelopes. Integrating BIM with its graphical algorithm editor can aid designers in accessing and extracting the required parameters regarding the thermal properties of materials from a BIM model to evaluate the performance of envelope construction materials.

The BOTTVC prototype system was developed as an integrated framework to establish a relationship between a BIM model and physical/thermal assets that are available in the BIM database, in order to optimize the evaluation of the thermal performance of building envelopes during the design process. The BOTTVC system is proposed to help users reduce the time required to test and examine the potential to control the thermal transmittance of multiple building envelope design alternatives.

The proposed methodology comprises seven main steps, as shown in Figure 5. The first step is BIM modeling. After the multiple building envelope design alternatives (e.g., type of construction material, material thickness, type of insulation, and thickness of material) are proposed in the design stage, building envelope elements (e.g., opaque and fenestration walls, external doors, roofs, floors, and shading devices) are modeled and their geometric and non-geometric information (e.g., thermal

properties and physical assets of materials) are created using BIM authoring software (e.g., Autodesk Revit) (Figure 5a). The second step is to create effective interoperability between a 3D BIM model and its database by connecting the BIM database with a visual programming interface (e.g., Dynamo) to access the material properties available in the BIM model (Figure 5b). The third step is to extract the building information stored in the BIM database to calculate variables relevant to the OTTV estimation (Figure 5c). In this step, deriving coefficients to calculate the OTTV from the BIM model information using BOTTVC can be divided into three categories: (1) coefficients that can be directly extracted from thermal and physical properties in a BIM model (e.g., U-value, R-value, specific heat, thermal conductivity, SHGC, width, and thickness of the building envelopes); (2) the extracted database information from the BIM model that is to be used as input data to calculate coefficients (e.g., WWR and SSR); (3) the extracted information from the BIM model combined with a constant coefficient given by OTTV standards through equations to calculate OTTV coefficients (e.g., TDeq, ESC, SC, ESR, and SF). The fourth step is to calculate OTTV coefficients (Figure 5d). The fifth step is to accommodate all relevant coefficients from the previous step to compute the OTTV. The sixth step is to generate the OTTV result (Figure 5f). The seventh step is to evaluate and analyze the thermal performance of a building envelope by comparing the output of the OTTV with the relevant OTTV code/standard (Figure 5g). If the OTTV of the building fails to comply with the OTTV standard, then the system provides an ability to change the new material and its thermal and physical properties via a visual programming interface, which enables designers to efficiently choose an appropriate combination of building enclosing materials to control thermal transfer into their design building.

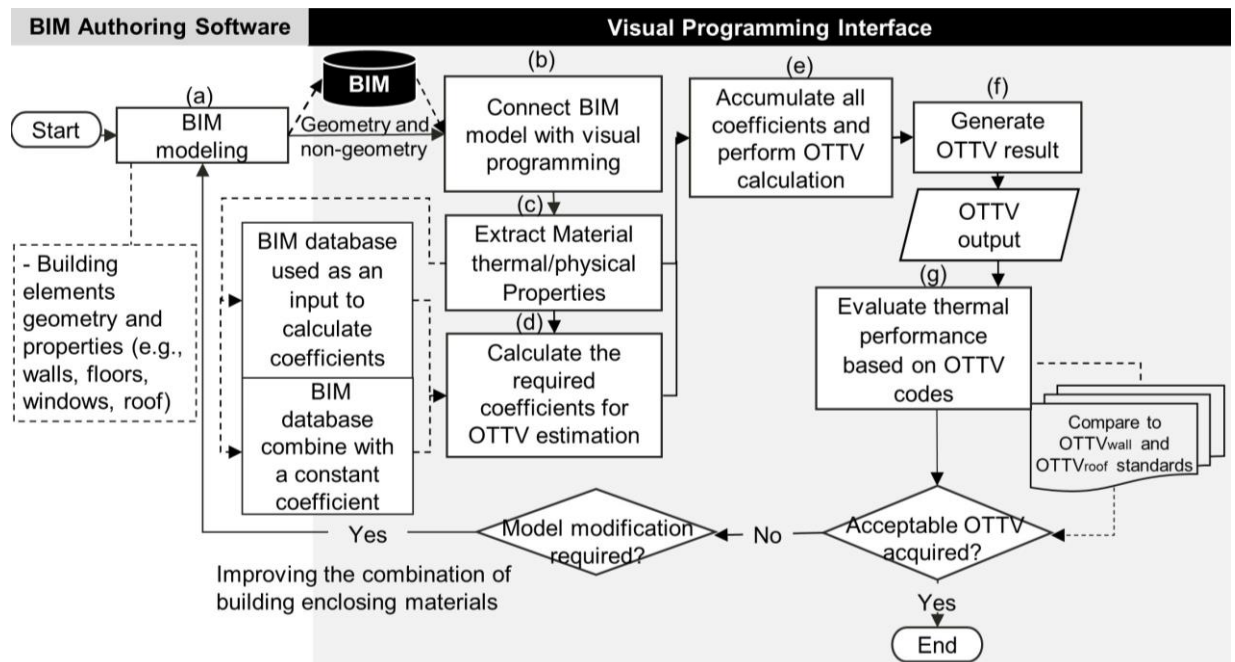


Figure 5 Overview the proposed method of BOTTVC

3.5 Integrating BIM and VR for lighting design feedback

The goal of this study is to develop a system for visualizing lighting design that allows users to experience, analyze, and assess the lighting quality of their designed space in an immersive environment. The proposed methodology comprises seven major steps, as shown in Figure 6. The first step is to create the building model using a BIM authoring software application. In this step, a 3D BIM model comprising the virtual equivalents of veritable building elements is created using a BIM tool, e.g., Autodesk Revit. Building elements (e.g., walls, columns, ceiling, floor, furniture, light bulbs, and fixtures), and their geometric and non-geometric information (e.g., material and properties) are created in the BIM software (Figure 6a). The model is then exported to a game engine (Figure 6b). The next step is to adjust the model in the game environment and to set initial values using the user interface (Figure 6c). Then, visualizations such as lighting illumination (shown with realistic scenes or false-colors), lighting atmosphere, and energy consumption feedback are provided (Figure 6d). In this step, lighting simulation is performed in the game environment using an embedded physics engine. The fifth step is to use immersive visualizations provided in the system to identify and analyze the conditions of the lighting design by visually analyzing the lighting conditions, examining visual comfort to achieve an optimum lighting design, and analyzing and comparing quantitative information (Figure 6e). If the design is not satisfactory, the system provides options to change and update the parameters for simulating new scenarios and visualizing lighting results via its graphic user interface (GUI) widgets (Figure 6f). Once a satisfactory design is achieved, new design parameters are updated in the BIM software (Figure 6g).

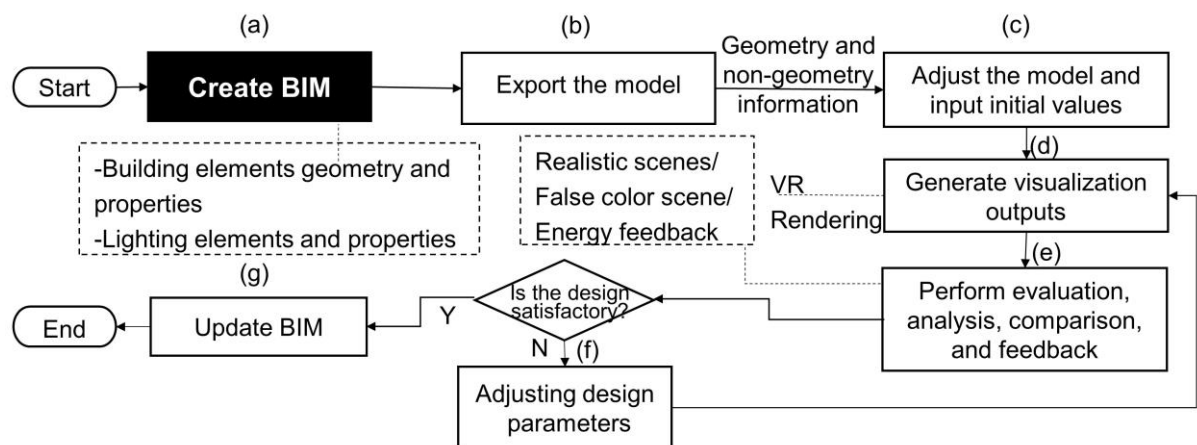


Figure 6 Overview of the proposed method for integrating BIM and VR for lighting design feedback

3.6 Chapter conclusions

An overview of the proposed methodology of this thesis is provided in this chapter. This chapter also contains details on the concept of combining BIM with infrared thermography images, environmental sensing data, graphical visual programming, and VR technology to provide a tangible evaluation of the performance capability of the design building. The overview of each system is explained in this chapter to show the procedure of system development.

Chapter 4 Integrating 4D thermal information with BIM for building envelope thermal performance analysis and thermal comfort evaluation

4.1 Introduction

This chapter investigates the use of BIM technology to enable building professionals to effectively detect the location of thermal defects and analyze the thermal performance and indoor thermal comfort by accommodating environmental information to be used in the analysis process. In this chapter, a novel method and a system for integrating the BIM model with 4D thermal information (building surface temperature and air temperature) are proposed to help visualize the thermal information of building surfaces over time and evaluate the indoor thermal comfort condition in a building. The proposed method uses time-coded thermographic images that are acquired by infrared thermographic survey and indoor/outdoor dry-bulb temperature collected by sensors. The acquired data are integrated with a BIM model. Visual scripting is used for extracting and then mapping spatio-temporal thermal data to a 3D BIM model. The proposed system converts the collected thermal images into numeric surface temperatures, integrates the collected environmental data in the BIM, calculates thermal comfort variables, such as mean radiant temperature (MRT), and assesses the thermal comfort level for various locations inside the building. The developed prototype system provides valuable visualization information and statistical data for analyzing thermal performance and assessing the thermal comfort level.

The objectives of this chapter are: (1) to develop a method for integrating spatio-temporal thermal and environmental sensor data with the BIM model; (2) to calculate the thermal comfort index and evaluate the occupants' thermal comfort level for each space using the integrated data; and (3) to analyze thermal performance using 3D and 4D thermographic visualizations in order to identify the root causes of problems and inefficiencies of building envelopes.

4.2 Proposed system

The proposed system uses visual programming to integrate sensor data (i.e., air temperature and thermal information) with BIM. The prototype system expands the capabilities of BIM to visualize and analyze thermal data over time in a 3D environment. Data collected from sensors (e.g., air temperature) and

thermal data are used as inputs to automatically calculate thermal comfort variables (MRT and operative temperature) based on equations (explained in Section 2.3) using visual scripting. The details of the developed prototype system are described in the following subsections.

4.2.1 3D BIM modeling and environmental data acquisition

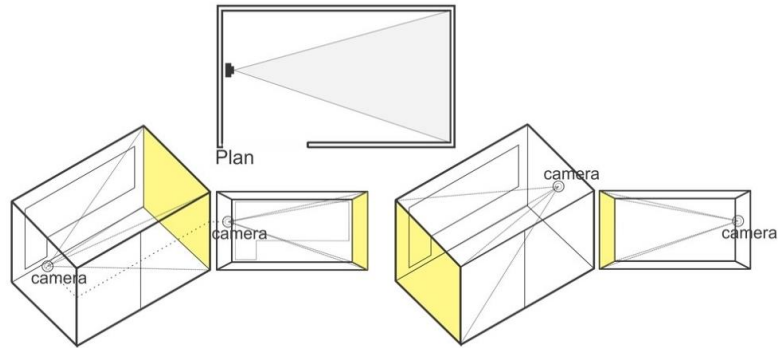
A 3D BIM model of a building is created using a BIM authoring software application such as Autodesk Revit. The geometry of building elements, e.g., walls, ceiling, windows, and doors, and their material properties, are modeled. The model data are then exported to Rhinoceros, which is a BIM compatible application.

Environmental data collection

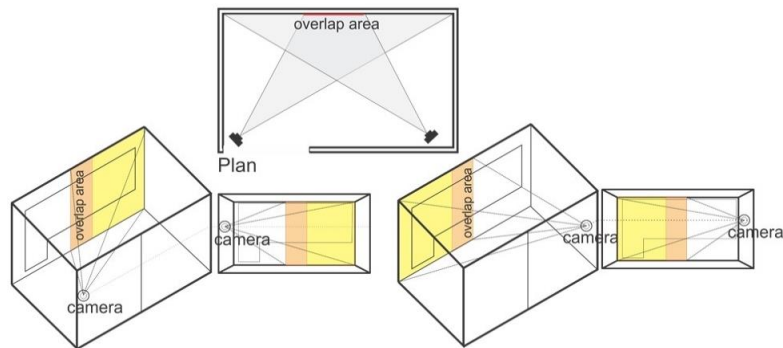
Several types of environmental data, e.g., air temperature, humidity, air-flow, lighting levels, and solar radiation patterns, can be collected. In the present study, air temperatures and humidity are required to be collected with sensors at regular intervals. The collected raw data contain numeric values of dry-bulb temperatures, relative humidity, and timestamps.

Thermographic data acquisition

In order to acquire the surface temperature of a building, periodic data collection of surface temperatures variation is using a thermal camera. The interior thermographic images should not be captured during rainy weather condition as water and excessive humidity on building envelope affects the results (unless the target analysis is specific to rainy conditions). Additionally, thermographic imaging should be done in sunny, mostly cloudy, overcast, or at night. This is because the changes of radiation patterns of sunlight on building surfaces affect the results. The description of weather condition is recorded for each image capturing round. In order to perform a thermographic survey of the interior of a typical rectangular room, the following general guidelines are proposed: 1) if the target surface can be covered in one shot, the camera should be perpendicular to the surface with its focus on the surface (Figure 7a); 2) if multiple shots are required to cover a surface, thermographic images must have at least 30% overlap with each other while covering the entire surface (Figure 7b); however, the perspective distortion should be corrected at a later stage; and 3) a fixed coordinate system should be used for identifying locations of the thermal camera when capturing thermographic images.



(a) A single shot with a straight view of the surface



(b) Multiple shots to cover the wall surface

Figure 7 Capturing thermographic images

Additionally, obstacles and assets blocking the target surface should be cleared. If 2D thermographic images are not taken with a parallel view of the surface, a step to automatically remove the perspective distortion is required. Additionally, after fixing the perspective distortion, if multiple images of one surface are acquired, they must be adjusted and stitched together to create a seamless image (Figure 8). These changes are performed using a raster graphics editor, such as Adobe Photoshop. In this step, considering the dimensions of the surface is important, because the size of the combined images should correspond to that of the surface. Combined images for each surface are then mapped into the BIM model. In order to avoid the temperature legend from changing when capturing multiple thermographic images, the temperature range of the thermal camera should be fixed to be constant.

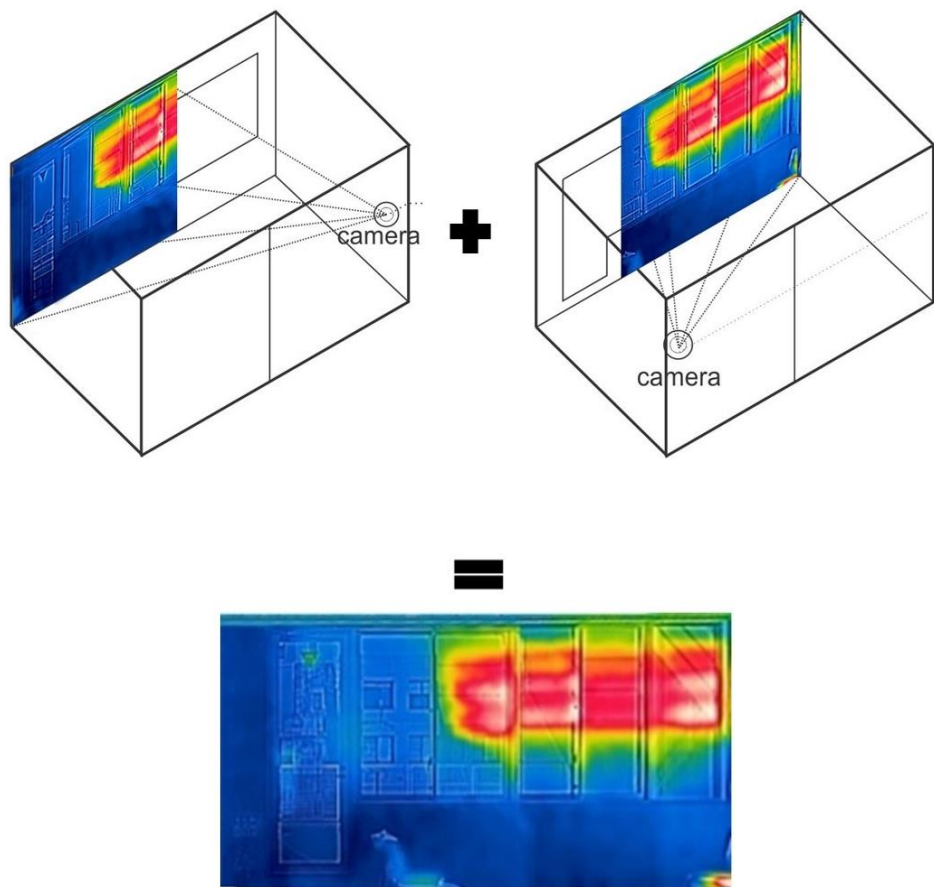


Figure 8 Adjusting the perspective distortion and stitching multiple thermographic images

4.2.2 Mapping thermal data on a BIM model and preparing environmental data

After creating an as-built 3D BIM model of the building and assigning materials and thermal properties (Figure 9a), the BIM model is imported into BIM compatible software, such as Rhinoceros (Figure 9b). The thermographic data and sensor data are also collected (Figures 9c and e). In order to integrate thermographic images of the building envelope with the 3D BIM model, a series of thermographic images that are captured at various times are adjusted (Figure 9d) and processed for mapping. A developed visual script is used in this step (Figure 9g) (explained in Section 4.2.3). Additionally, in order to transfer the collected data, such as sensor readings, to the model, a visual script is used to retrieve sensor readings from spreadsheet files (Figure 9f). The spreadsheet contains air temperature values, coordinates of sensors, and timestamps. Consequently, the prototype system produces an integrated BIM model having thermographic textures with color codes, coordinate references, and the environment sensor data (Figure 9h).

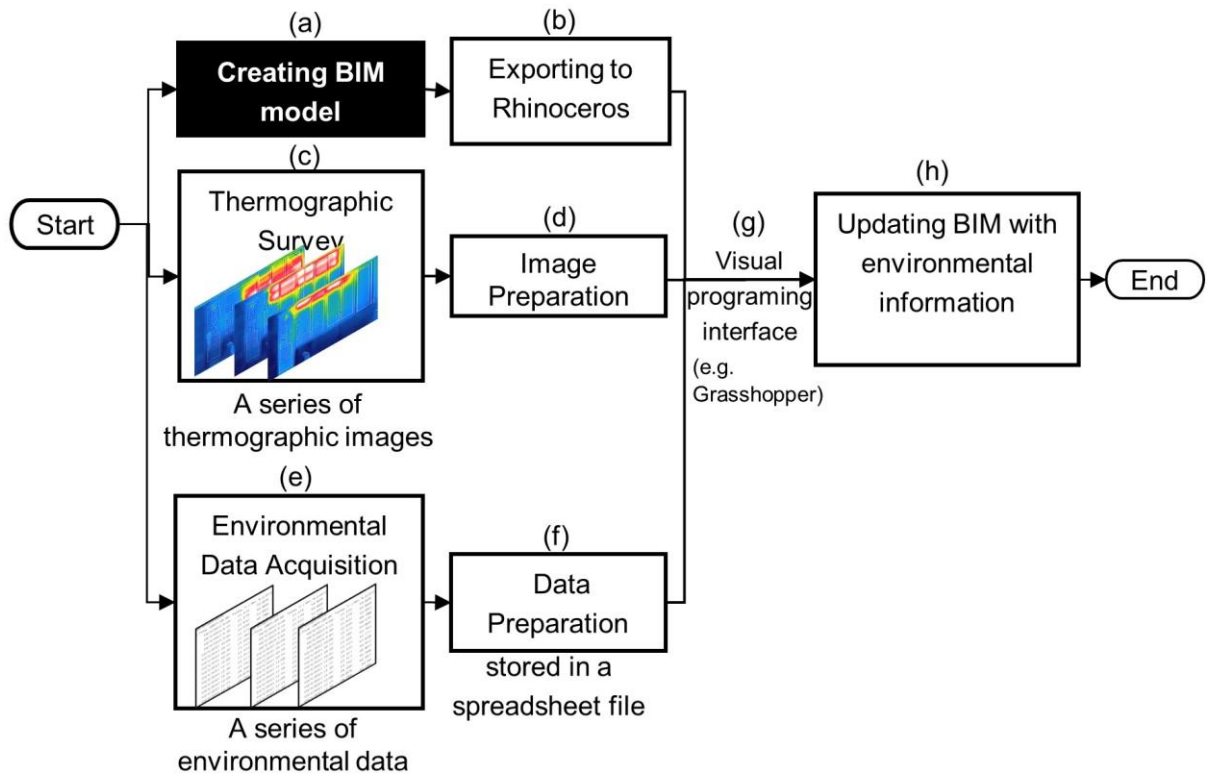


Figure 9 Workflow for integrating sensor data and thermographic data with BIM

4.2.3 Creating 4D thermal information

4D thermal visualizations were created in Rhinoceros using its visual scripting in Grasshopper. The visual script integrates thermographic images and their timestamps with geometric information in the BIM model. A series of thermal images are loaded and displayed on the 3D model by using a file path of the ImageSampler component in Grasshopper (Figures 10a and b). In order to visualize the thermal information over time, a series of static thermal images that entirely cover each interior surface of the building envelope are overlaid on the surface of the model according to the sequence of thermal image timestamps (Figure 10c). Consequently, a 3D BIM model with time coded thermal images is created (Figure 18). In the prototype system, a sidebar control in Rhinoceros is used to visualize thermal patterns at different times.

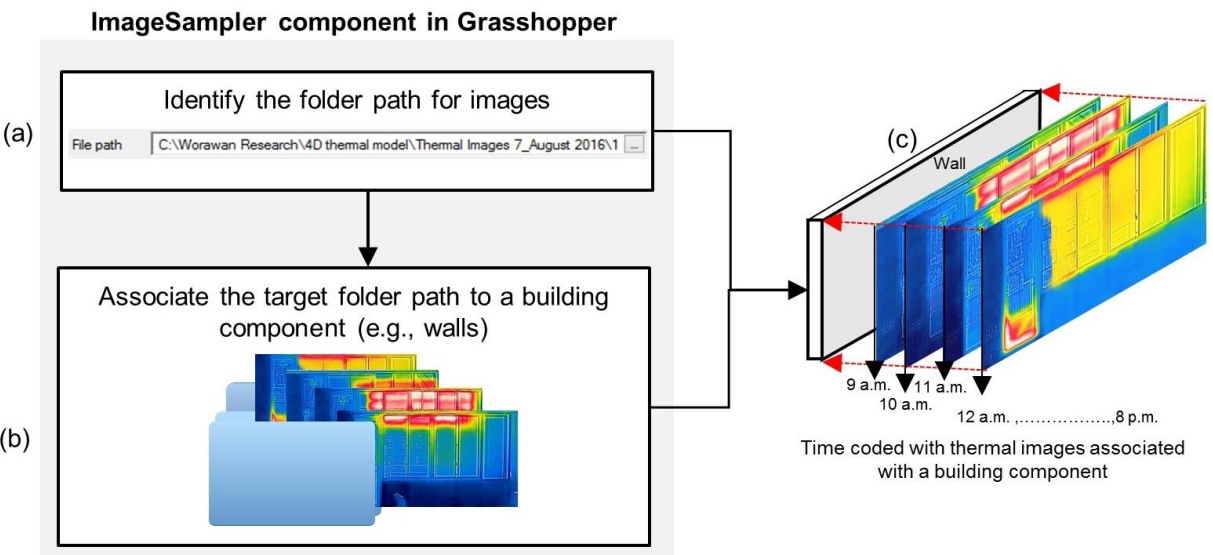


Figure 10 Process flow for creating 4D thermal information

4.2.4 Data extraction and data processing

Figure 11 shows the workflow for data extraction and data processing. Visual scripting (Figure 12a) is used to acquire temperature data from thermographic images that are mapped onto the BIM model in Rhinoceros (Figure 11a). Visual scripting extracts numeric RGB values from images with their coordinates (x,y,z). The RGB values are extracted based on a planar grid of pixels that contain temperature values (Figure 12b).

The size of a grid can be adjusted to suit the requirements of the user. The RGB values are translated to temperature values using a Visual Basic for Applications (VBA) script. The correct values from the RGB conversion step are then used to compute the surface temperature using Equation (5) (described in Section 2.3.3). In the next step, the computed surface temperatures are used as input to calculate MRT considering angle factor of the user and the operative temperature. Calculation of the angle factor between the user and the surrounding surfaces is also performed in this step. Consequently, these variables are used to assess the thermal comfort level (Figures 11c and d).

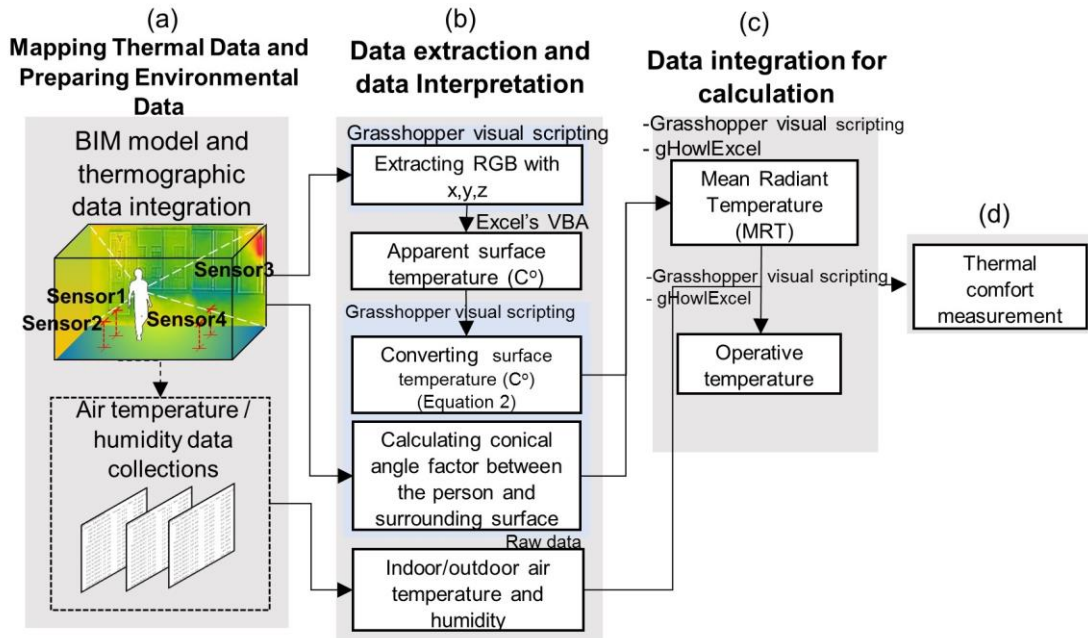
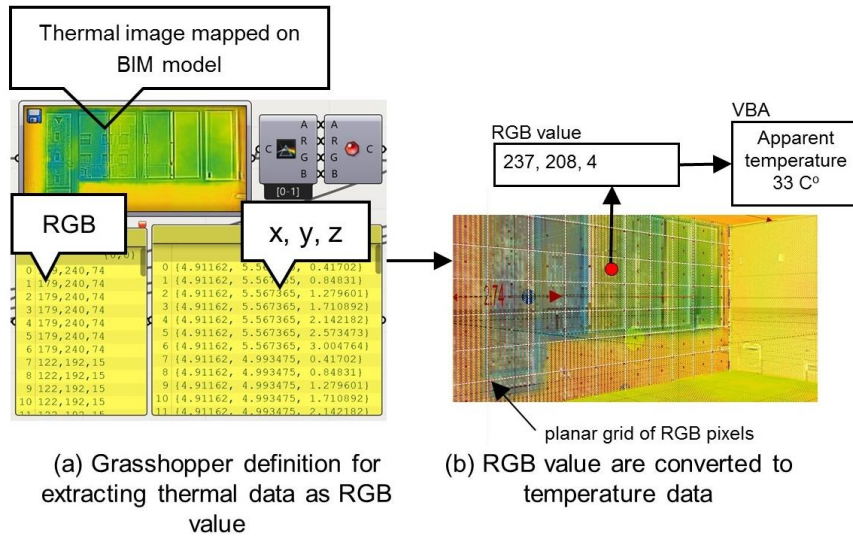


Figure 11 Workflow for data extraction and data interpretation



Temperature range °C	Color legend	R	G	B
34-35		255	255	255
33-34		255	0	0
32-33		255	127	0
31-32		255	255	0
30-31		127	255	0
29-30		0	127	255
28-29		0	0	255
27-28		0	0	127
26-27		0	0	0

(c) The relationship between temperature and R, G, B values

Figure 12 Data extraction and data interpretation

4.2.5 Calculating thermal comfort variables using visual scripting

As explained in Section 2.3.2, a 3D calculation method is required in order to calculate MRT considering the conical angles ($F_{(p-i)}$) of building surfaces with respect to the position of the occupant. A visual programming interface is used to calculate a/c , b/c , τ , and γ , which are factors used in calculating the conical angles ($F_{(p-i)}$) in Equation (2). The six enclosing surfaces are divided into smaller surfaces by referencing the center position of the occupant's body (Figure 13a). Each of these surfaces has its own angle factor and average temperature. With the help of scripting, the width of the surface (a), the height of the surface (b), and the distance between the person and the target surface (c) are measured automatically (Figure 13b). Figure 13c shows specific equations for calculating τ and γ . Using this system enables the calculation of conical angles in a 3D environment while the position of the occupant changes.

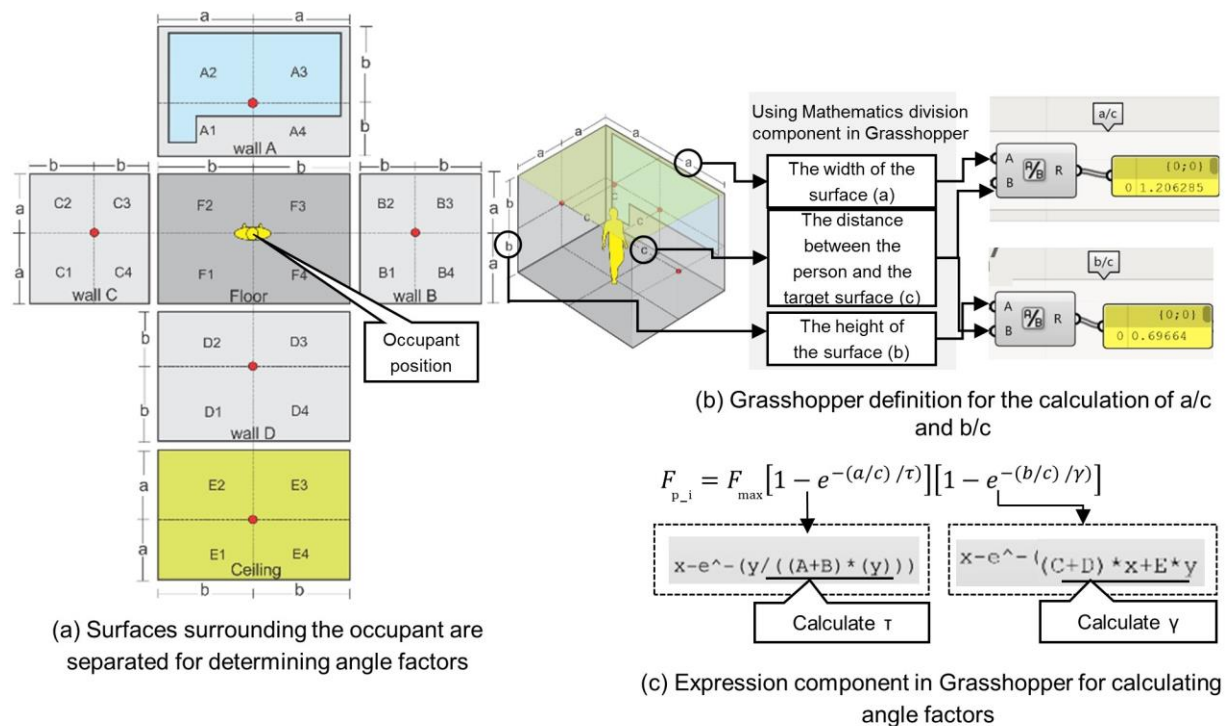


Figure 13 Dividing surfaces for calculating MRT and corresponding Grasshopper setup

4.2.6 Data integration for assessing thermal comfort level

The indoor/outdoor air temperature and humidity data acquired by sensors are imported into the visual programming application (i.e., Grasshopper). Data logger software, i.e., HOBO Ware, is used to read and export the sensor reading file to a spreadsheet file in .csv format (Figure 14a). Each spreadsheet file contains dry-bulb air temperature, relative humidity, and a timestamp (Figure 14a). The spreadsheet files are connected to Grasshopper using the file path function and the gHowl plug-in (Figure 14b). In order to use the recorded data as input information for thermal comfort assessment, the average values of four sensors are computed. After calculating the average MRT and the average indoor air

temperature, the operative temperature is calculated using Equation (3). Ladybug (a plug-in for Grasshopper (Sadeghipour et al., 2013)) is used to evaluate the thermal comfort level based on the adaptive method. The adaptive method parameters are based on ASHRAE standard 55-2013. The output is a series of integers indicating a three-point scale: -1 (the input condition is too cold for the occupants), 0 (the input condition is comfortable for the occupants), and 2 (the input condition is too hot for the occupants).

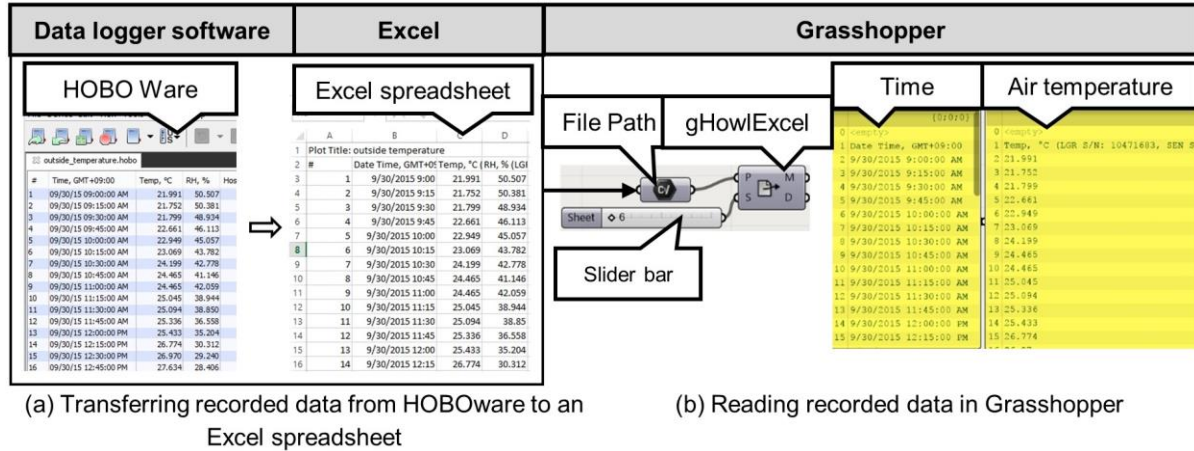


Figure 14 Reading the recorded data by the data processing module

4.2.7 Information output

After integrating the timestamped thermographic images with the BIM model and importing a set of data series from sensors into our system, various outputs can be generated. The possible outputs are:

- 3D thermal data, which show the building envelope with added thermographic images as textures. Surface temperatures of building envelopes are extracted from RGB values of thermographic images.
- 4D visualizations, which shows changes of thermal values over time.
- Statistical data outputs, e.g., MRT, and operative temperature
- The result of the measurement of thermal comfort levels over time, which is reported as ASHRAE comfort chart for naturally ventilated buildings (adaptive method).

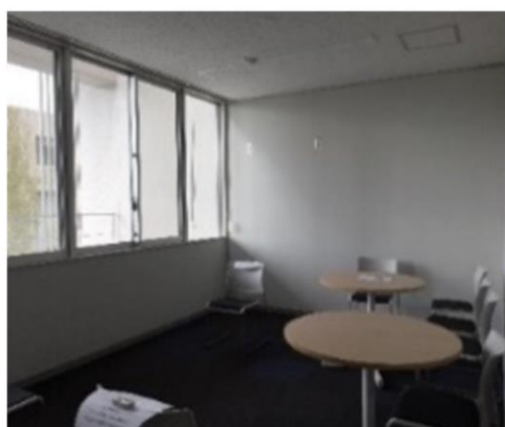
4.2.8 Visual analysis

The 3D BIM model that is integrated with thermal information of the temperatures of interior surfaces can help users to visually observe the surface temperature of different areas and identify patterns of inefficiency or sources of problems using color coding. Each part of the thermal scene can be used in surface temperature measurement, detecting exact locations of heat sources, monitoring the performance of the building envelope, and visualizing potential problem areas by showing the locations of heat leakages on the building envelope. 4D thermal visualization allows users to view changes in thermal information over time and can provide a basis for spatio-temporal analysis.

4.3 Case study

4.3.1 Experimental room

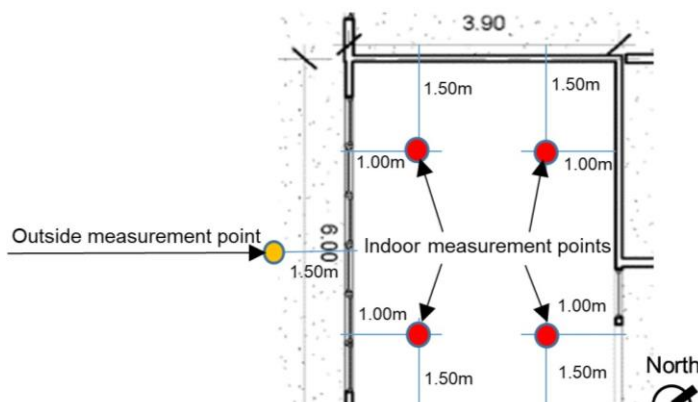
The student lounge on the 4th floor of the M3 building at Osaka University, Japan, was chosen as the experimental area. The latitude and longitude of the building are 34°410'N and 135°300'E, respectively. The case study room is a naturally ventilated area with no HVAC system installed that is directly connected to a corridor with no doors. The room for the case study is naturally ventilated and has no HVAC system. The horizontal sliding sash windows of the room are of double-pane glass with an aluminum frame. The opaque wall is constructed of a lightweight material and is insulated. Environmental data collection was executed in the summer (August) and the autumn (October) under both cloudy and clear weather conditions from 9 a.m. to 8 p.m. During the experimentation period, the windows were all closed. Figures 15a and 15b show photographs of the room in cloudy and sunny weather conditions, respectively. The experimental room has a typical rectangular shape, as shown in Figure 15c.



(a) the room in cloudy sky



(b) the room in clear sky



(c) 2D room Plan

Figure 15 Experiment room and placement of air temperature and humidity sensors

4.3.2 BIM modeling and environmental data collection

The BIM model of the room was created using Autodesk Revit Architecture 2015. The BIM model contains geometric and non-geometric information of the building components. The model data are then exported to Rhinoceros with Grasshopper scripting via an IFC file format (Figure 16).

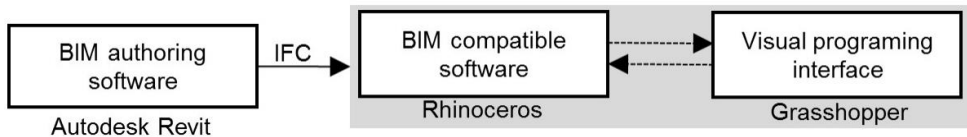


Figure 16 Process of BIM model transfer

2D thermographic images were captured using a thermographic camera (i.e., FLIR C2) with an infrared sensor 80×60 pixels (4800 measurement pixels). The temperature range of the camera is -10°C to $+150^{\circ}\text{C}$ with an accuracy of $\pm 2^{\circ}\text{C}$ and a field of view of $41^{\circ} \times 30^{\circ}$. The interior thermographic survey for the entire surfaces of the experimentation area was performed using eight images following our proposed guideline (described in Section 4.2.1). Air temperature and relative humidity data were collected using data loggers (i.e., HOBO UX100, temperature sensor - 0.21°C at 50°C , relative humidity - 2.5% from 10% to 90% RH). In our case study, five temperature and humidity sensors are used for a 24m^2 room. One sensor was used to measure outdoor temperature and four sensors were used for indoor air temperature. The measurement points were chosen at the working-level height, i.e., approximately 1.0 m above the floor, distances of 1.0 m and 1.5 m from their adjacent walls. Sensors were set to collect real-time temperature and humidity measurements at time intervals of 15 min. The location of each sensor in the experiment room is shown in Figure 15c.

4.3.3 Integrating thermographic images and temperature data with BIM

Acquired thermographic images were adjusted in order to remove perspective distortions (especially for the southwest wall due to large angles). The images were combined to obtain seamless thermographic images with a straight view that covers the entire wall by considering the dimensions of the respective wall using Adobe Photoshop CS4. In order to present 4D thermographic models, thermographic images that were captured over time were added to the building envelope as textures. Rhinoceros and its Grasshopper plug-in were used for mapping time-coded thermographic images in the imported BIM model and for simulating the 4D thermal dynamic.

Visual scripting in Grasshopper is used to extract thermal values from thermographic images (Figure 17b), which can visualize the changes of thermal information over time. The dimensions of the planar grid are $0.50\text{m} \times 0.50\text{ m}$. The RGB values of the pixel in the center of each planar grid are used in the calculation (Figure 17b). A color map is used to interpret temperature values. The coordinates (x,y,z) of each extracted RGB pixel are also obtained (Figure 17b).

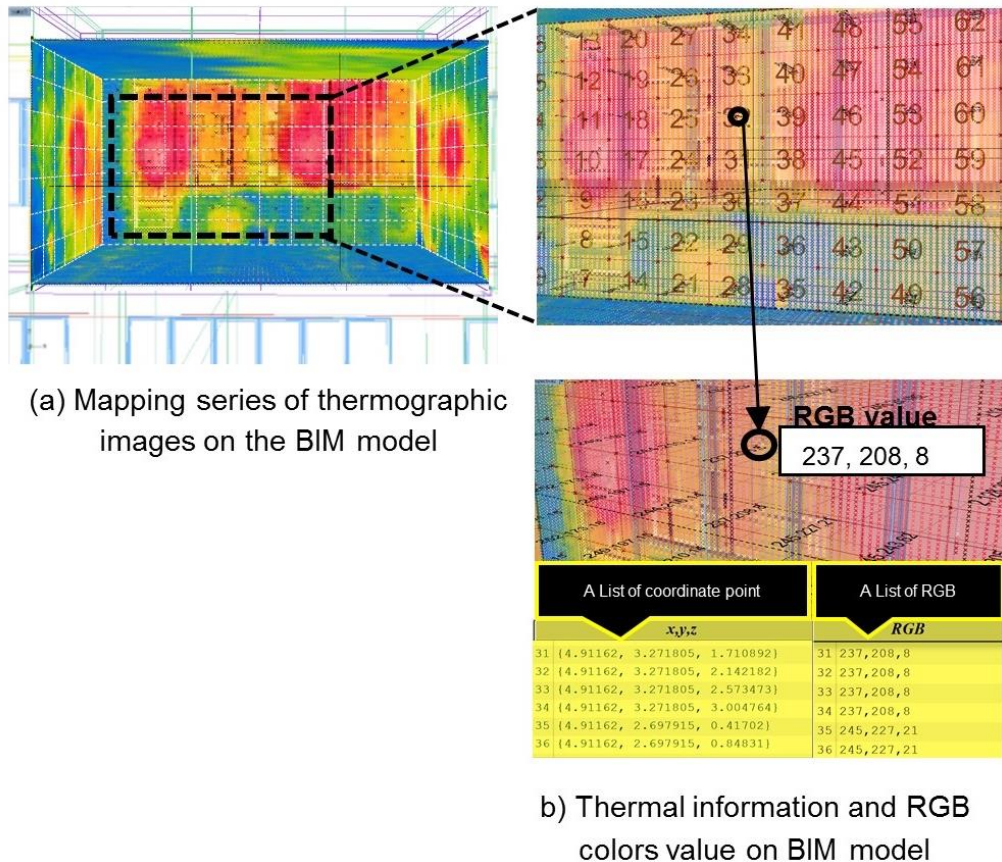


Figure 17 Visualization of thermal information

4.3.4 4D thermal model visualization output

Figure 18 shows an example of the visualization output in the summer (August) in clear weather condition. The changes in the locations of high-temperature areas at different times can be visualized through the 4D thermographic model which is useful for planning improvements. The outer wall of the case study room faces southwest, which receives the highest amount of sunlight in the summer. The spatio-temporal thermal data showed that the main heat source is the window area. The temperature range on the window glass surface is 30 °C - 35 °C over time. From 12 noon to 4 p.m., the temperature of part of the window surfaces and frames reaches 35 °C. The wall surface temperature could be reduced by adding insulation or changing the building envelope component and adding internal/external shading devices to prevent direct heating. In addition, several factors, such as the thermal capacity, thermal resistance, the color of the material, solar heat gain control, visible light transmittance (VLT), and solar heat gain coefficient (SHGC), must be considered for the improvement of the opaque and fenestration envelopes.

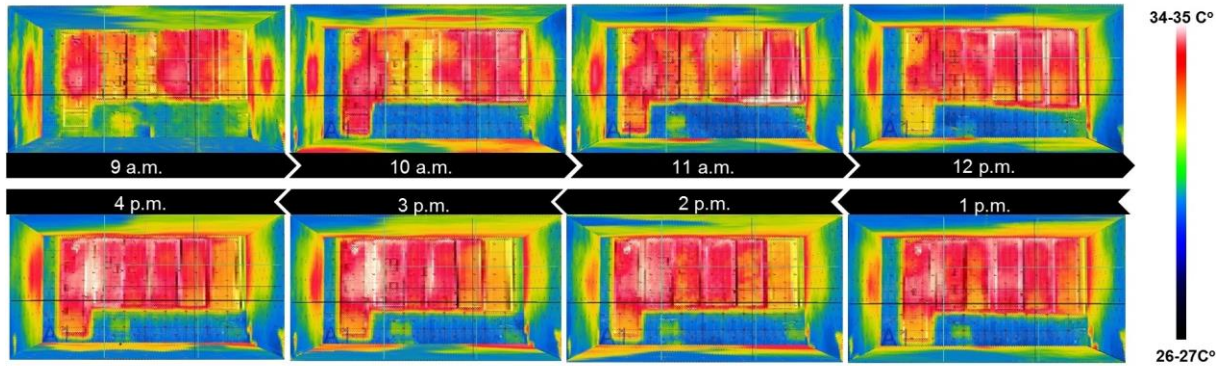


Figure 18 Example of 4D thermographic visualization

4.3.5 Calculating thermal comfort variables

Six locations in the model were chosen for calculating the MRT and the operative temperature and for evaluating thermal comfort during working hours (from 9 a.m. to 8 p.m.). The BIM model of the experimental room ($6 \text{ m} \times 3.90 \text{ m} \times 3.2 \text{ m}$) with windows ($4.80 \text{ m} \times 2.00 \text{ m}$) is shown in Figure 19.

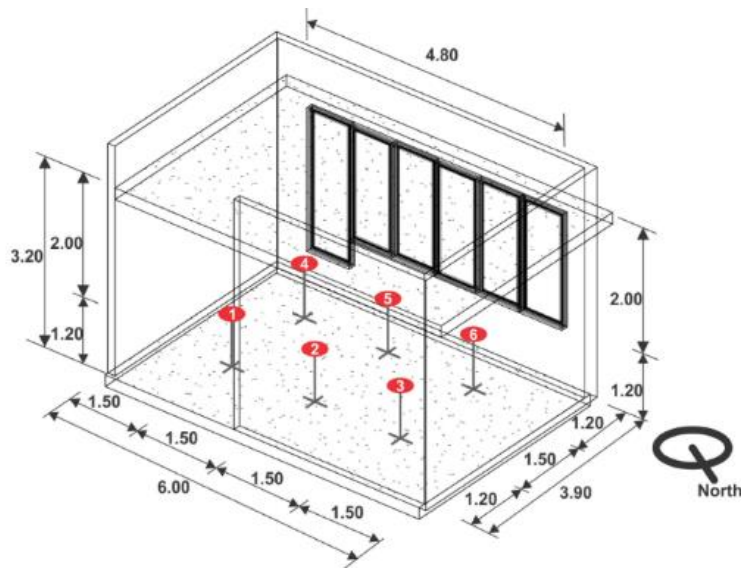


Figure 19 Locations of assessment points

The surface temperature values of each wall are extracted from the thermal model and are converted to the actual surface temperature. As described in Section 4.2.4, the average surface temperatures are used as input data for calculating the MRT and the operative temperature. Visual scripting by Grasshopper in Rhinoceros is used to automatically calculate the corresponding angle factors between the occupant and the surrounding surfaces based on Equations (1) and (2) (described in Section 2.3). This automatic calculation method helps experts to save time in calculating the comfort level when occupants change their position in the room. The values of MRT considering the occupant position and operative temperature are computed and are shown in Figures. 20-22.

Figures 20 - 22 show examples of variables used in thermal comfort analysis at six locations in the room. The results show that there was no significant difference between the six locations in the experiment room. However, the influence of MRT is the greatest at locations 4, 5, and 6, which are close to the windows. In summer, the average MRT is approximately 29 °C, and the operative temperature is approximately 30.41 °C. In autumn, the average MRT is approximately 21.96 °C, and the operative temperature is approximately 23.76 °C. The changes in the MRT and the operative temperature over time allow the evaluation of comfort conditions throughout the selected days.

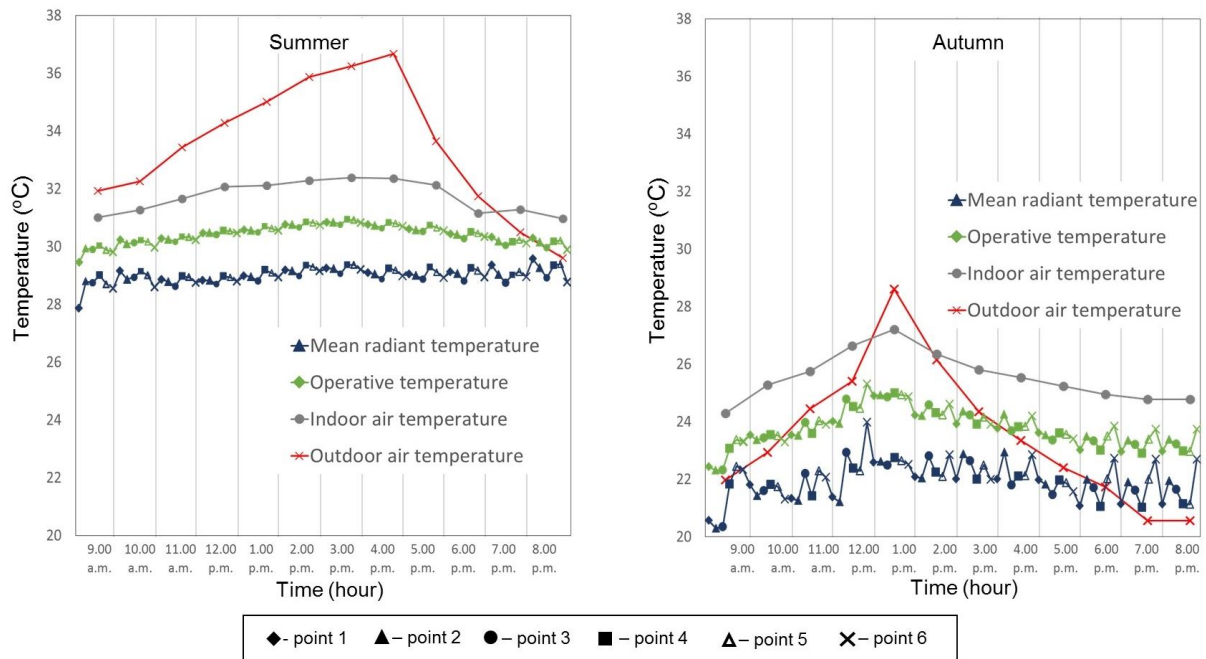


Figure 20 Indoor/outdoor air temperature and calculated value of MRT and operative temperature considering angle factors of six occupant locations in summer and autumn

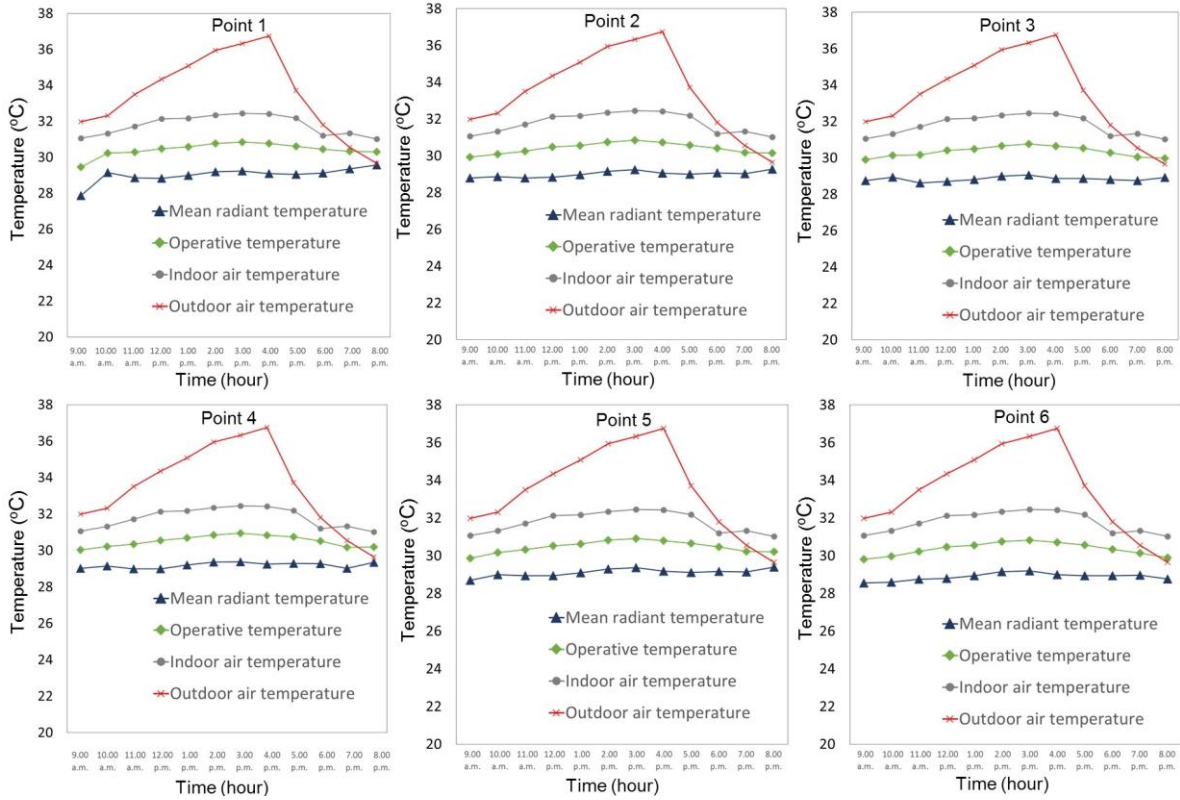


Figure 21 Results of MRT and the operative temperature calculations at six locations in the room in summer (August), Osaka, Japan

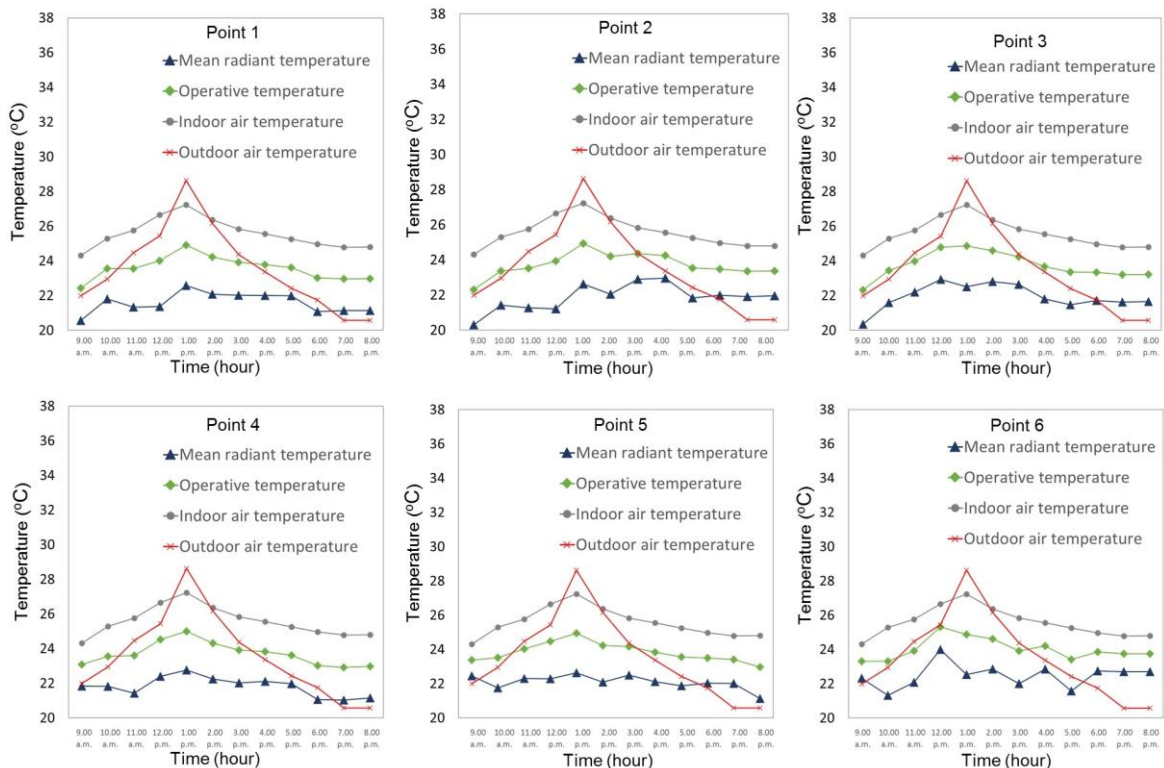


Figure 22 Results of MRT and operative temperature calculations at six locations in the room in autumn (October), Osaka, Japan

4.3.6 Thermal performance and thermal comfort analysis

For assessing thermal comfort, the Ladybug plug-in and the adaptive method model were used to determine acceptable thermal conditions in a naturally conditioned room. The thermal comfort at different locations and times was evaluated using the adaptive comfort chart to identify whether the conditions of measurement positions fall within the acceptable range. If the indoor thermal condition is not acceptable, improvements should be proposed.

The results of the indoor thermal comfort analysis are shown in Figure 23. The ASHRAE standard recommends a comfortable temperature between approximately 23 °C and 28 °C in the summer and between 20 °C and 25.5 °C in winter. For autumn, a comfortable temperature is between approximately 24.1°C and 26.8 °C (Rijal et al., 2015). The results for summer (Figure 23a) indicates that in the morning (9 a.m. to 10 a.m.), comfortable conditions are maintained based on recommendations by the ASHRAE standard (within 90% acceptability limits). However, from 11 a.m. to 5 p.m., the condition fails to comply with the ASHRAE standard (uncomfortable, too hot for occupants). The poorest thermal conditions occurred in the afternoon between 3 p.m. and 4 p.m. During this time, indoor temperature, outdoor temperature, MRT, and the operative temperature reached 32.45 °C, 36.75 °C, 29.29 °C, and 30.74 °C, respectively.

Consequently, an approximately 5 °C – 6 °C reduction in the operative temperature and MRT helps to maintain thermal comfort during this period. From 6 p.m. to 8 p.m., the input conditions reached the comfortable range, which shows within 80% acceptability limits at 6.00 p.m. and 7.00 p.m. and 90% acceptability limits at 8 p.m. The case study room requires an improvement plan in order to achieve a higher degree of thermal comfort for occupants in summer (e.g., adding shading devices and considering the thermal properties of the opaque and fenestration envelopes). In autumn, the indoor thermal conditions complied with the ASHRAE standard (Figure 23b).

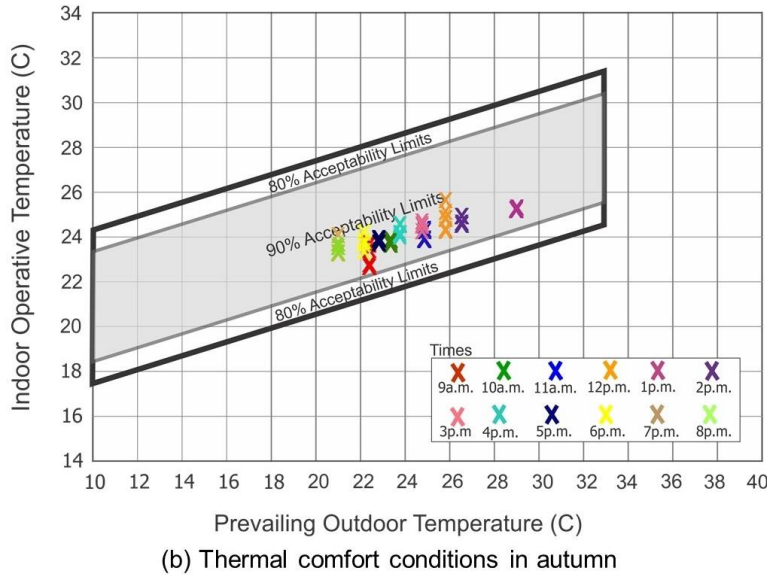
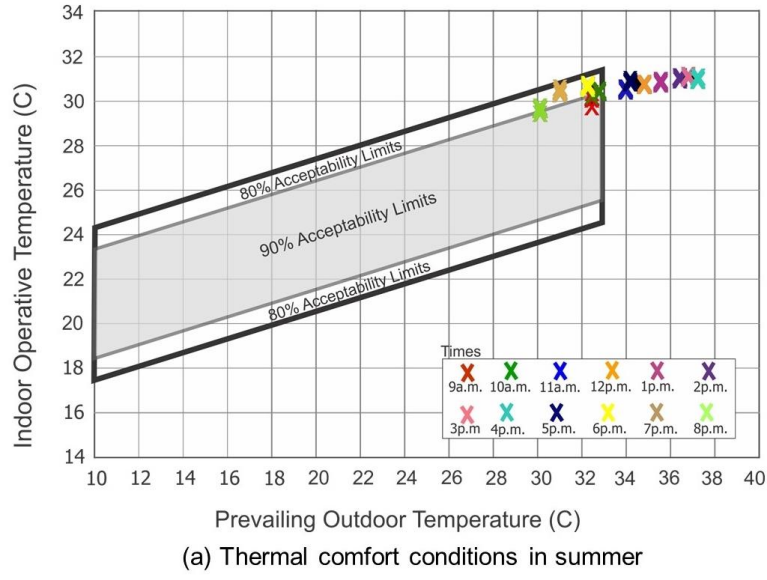


Figure 23 Thermal comfort conditions in the adaptive comfort standard

4.4 Discussion

Section 4.5 described the implementation of the proposed system by demonstrating how the system can be used to assess thermal comfort conditions and thermal performance in a real-world case study. The findings of the aforementioned study provide several new insights into integrating thermographic images and environmental data with a BIM model for visualizing and locating heat leakages on building surfaces and evaluating indoor thermal comfort. The findings of the validation study are summarized as follows:

- Although the thermal camera provided accurate thermal imaging, a high-resolution camera should be used. Correcting the perspective distortion of acquired images during post-processing

can lower the quality of data. Alternatively, using photogrammetry techniques for 3D reconstruction of a thermal model can solve this problem.

- Although BIM-compatible software (i.e., Rhinoceros) was successfully used in our case study, direct integration of sensor data and the BIM software (e.g., Autodesk Revit) is possible using Dynamo visual scripting.
- The proposed system uses the .csv file format to store temperature data collected by sensors. However, in order to fully support BIM information exchange requirements, such data can be stored using IFC resources.
- The proposed system provides a flexible and easy approach for the calculation of MRT not only for rooms with a rectangular layout but also for rooms of any complex shape.
- The ability to analyze the thermal performance of the building is limited only to visual analysis of the location areas of heat loss and heat sources through a series of color-coded thermographic textures applied to the BIM model. Therefore, the ability to measure the thermal transfer values of the envelopes for an efficient analysis should be developed.
- Although relative humidity data were collected by the sensors, in our case study, such data have not been used to assess thermal comfort, because the adaptive method does not require relative humidity as an input for measuring thermal comfort level. However, in order to evaluate the comfort level in an air-conditioned building using the PMV and PPD methods, relative humidity data should be integrated into the system.
- Occupant standing posture was considered in calculating the angle factor in the proposed system. However, the comfort levels should be compared between standing and seating postures.
- The ASHRAE comfort chart for naturally ventilated buildings (adaptive method model) was used in the present study. Thus, another method (such as PMV and PPD) by which to evaluate thermal comfort in an air-conditioned room should also be developed.
- In the case study, thermal images are captured in clear and overcast weather condition. Hence, the change of radiation pattern of sunlight on the building surface is not considered. Capturing images in semi-cloudy condition makes the assessment of the performance of the envelope difficult.

4.5 Chapter conclusions

A method for integrating BIM model with 4D thermal information for thermal performance analysis and indoor thermal comfort evaluation has been proposed in this chapter. The developed system has five main steps: 1) creating a BIM model; 2) collecting environment data; 3) mapping thermal data to the BIM model; 4) calculating thermal comfort variables; and 5) evaluating indoor thermal comfort.

The proposed method investigated a tool for visualizing qualitative and quantitative thermal information and evaluating the indoor thermal comfort conditions at different locations in a building.

A BIM compatible application (Rhinoceros and its Grasshopper plug-in) was used to develop the prototype system. The proposed method has been validated and verified in a student lounge at Osaka University. The developed system enabled users to visualize changes in thermal information mapped to the BIM model and automatically calculates indoor thermal comfort values. In addition, the proposed system simplifies the process of calculating MRT for a complex environment. Furthermore, the proposed system helps users to examine the thermal comfort conditions of buildings and to identify potential problems in order to achieve a higher degree of comfort for occupants. The proposed method allows only visual analysis the surface temperature of building envelopes in order to identify patterns of excessive heat loss or heat generation over time. In order to better analyze the thermal performance of the building envelope, a system by which to calculate the overall thermal transfer value (OTTV) using a BIM thermal properties database should be developed.

Chapter 5 Optimizing the evaluation of building envelope design for thermal performance using a BIM-based OTTV calculation

5.1 Introduction

This chapter proposes a method to access the materials' thermal properties from the BIM database for assessing the rate of heat transfer through building envelopes. The development of a BIM-based approach to provide an automatic assessment of the OTTV of building envelopes is demonstrated in this chapter. The OTTV standards are popularly used worldwide for assessing the rate of heat transfer through building envelopes. However, manual calculation methods for OTTV involve functions with various variables and coefficients that need to be considered. Furthermore, computing multiple functions using manual calculation methods can be time-consuming and human error can occur throughout the completion of the calculation process. Applying the OTTV to assess the thermal performance of building envelopes requires tools that enable designers to automatically measure the thermal performance and effectively determine the optimum combination of envelope materials. This study proposes integrating BIM and a developed visual scripting to automatically extract thermal and physical properties from the BIM database for supporting thermal transfer value calculation.

The objectives of this chapter are (1) to investigate a method to extend the capability of the current BIM to access thermal and physical properties of materials available in the BIM database for the OTTV calculation and (2) to create a robust prototype system that saves considerable time when calculating an OTTV, thus saving time when measuring the average heat transfer into a building. The system aims to achieve the most appropriate building envelope characteristics to cut down on external heat gain, reduce the energy demand of air-conditioning, and help building professionals ensure that the thermal performance of a building envelope complies with OTTV requirements in the design stages.

5.2 Development of the BOTTVC system

Autodesk Revit (Autodesk, 2016d) and the Dynamo 0.9.1 visual programming interface (Autodesk, 2016b) are used to develop the BOTTVC system. Dynamo is an open-source visual programming application that is embedded into Autodesk Revit.

5.2.1 3D BIM modeling

A 3D BIM model comprising the virtual equivalents of veritable building elements is created using Autodesk Revit, in which the geometries of building elements (e.g., opaque and fenestration walls, windows, doors, roofs, floors, shading devices, and their material properties) are modeled. Building enclosing constructions and material thermal and physical assets are transferred into a BOTTVC prototype system developed using Dynamo.

5.2.2 Acquisition of required thermal properties and physical assets from the BIM database

Performing the automated OTTV calculation requires information of the thermal properties of different material combinations in an envelope system available in the BIM database, including the U-value, R-value, SHGC of glass, absorptivity, density, and specific heat capacity. The BOTTVC prototype system proposes two methods for acquiring such information from the BIM database in order to measure the overall thermal performance of the building envelope (Figure 24): (1) defining arbitrary variables in the *Code Block* node and (2) using Python scripting (detailed in Subsection 5.2.3).

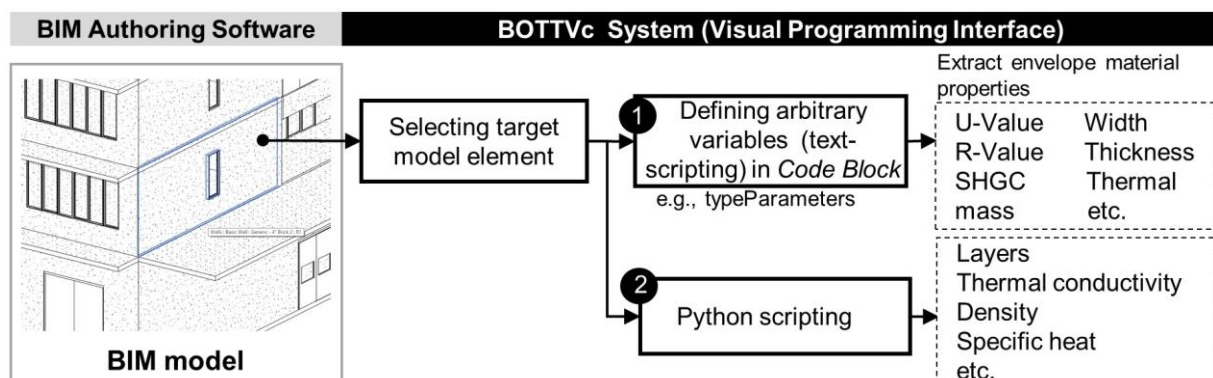


Figure 24 Process flow for acquiring OTTV coefficients from the BIM database

5.2.3 Text-scripting in *Code Block* node

Accessing and extracting the thermal properties of a material from the BIM database requires the BIM model to be connected with a visual programming environment using *SelectModelElements*, which is a basic node of Dynamo. The *SelectModelElements* node is used to select the target model elements in order to acquire material properties. After selecting a target element, material properties and their coefficient values in the BIM model are accessible and are extracted using text-scripting in *Code Block*. At this step, *typeParameters* is specified as an input in *Code Block* in order to access and display a list of material property identifiers (IDs) in the properties box. A parameter ID is determined to derive the required variables, which include numerical data and their units. The parameters must be converted into pure numeric datasets. Coefficients regarding OTTV measurements, including the U-value, the R-value,

and the SHGC of the construction materials are extracted using the proposed visual scripting (Figure 25).

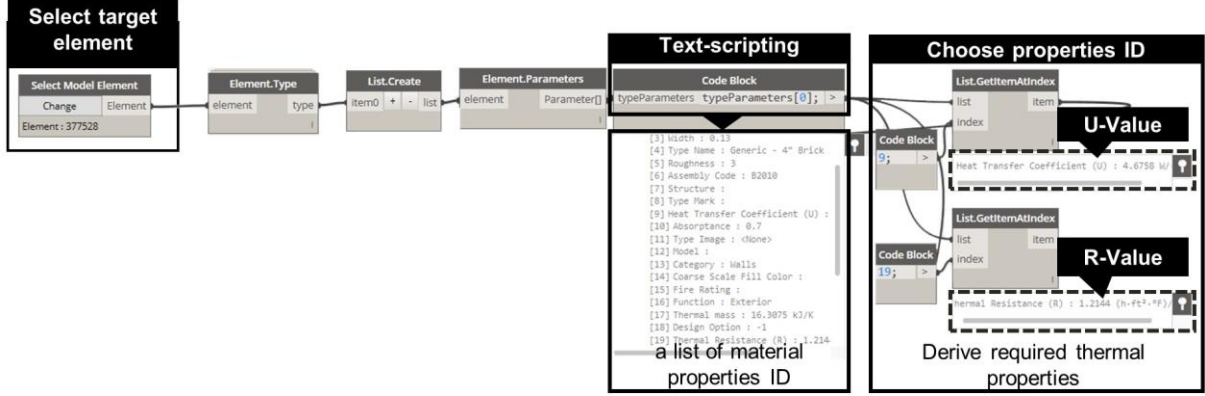


Figure 25 Example of extracting coefficients from the BIM thermal properties database

5.2.4 Python scripting

Although the current Dynamo (0.9) visual programming provides the ability to extract thermal properties from the BIM model, there is no function available to access some coefficients, including thermal conductivity, density, and specific heat of each individual material. Therefore, the BOTTVC prototype system uses Python scripting to access these coefficients from the BIM material assets. *ThermalAssetClass* in API for Revit is used. The *ThermalAssetId* class, which represents the properties of a construction material relevant to energy analysis, is used to access the thermal conductivity, density, and specific heat of the building material (Figure 26).

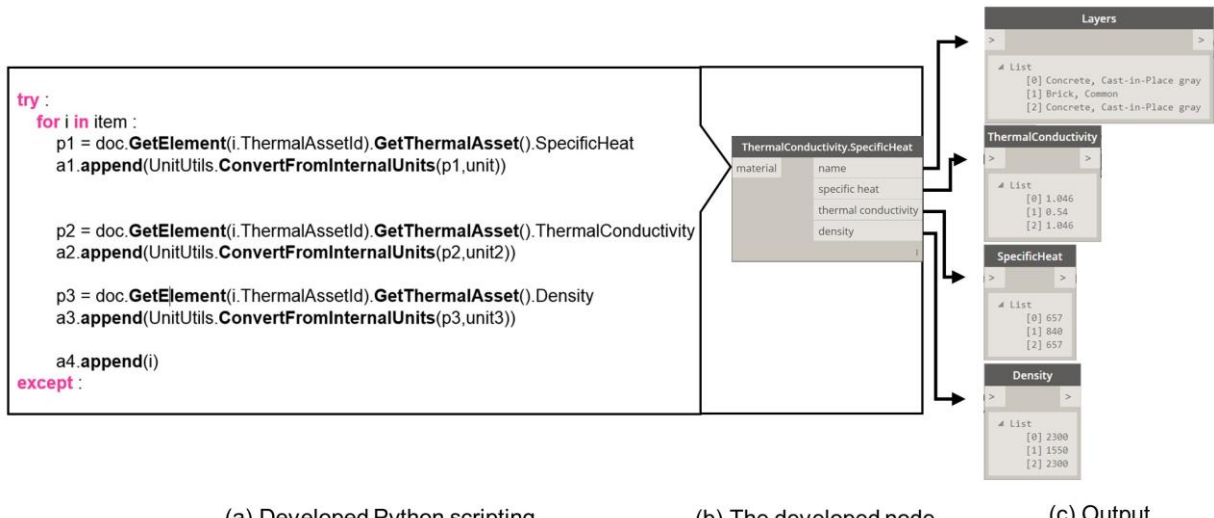


Figure 26 Example of extracting some coefficients from the BIM thermal properties database

5.3 Calculating OTTV coefficients using visual scripting

Further coefficients are required for OTTV calculations, including WWR, SSR or SKR, SC of external shading devices, ESC of external shading devices, TDeq, and SF, as well as physical properties (e.g.,

area of opaque and fenestration wall/roof, width, and height of external shading devices) of the model element.

5.3.1 Acquisition of WWR and SSR or SKR values

Data to derive the values of WWR and SSR or SKR are the total external surface areas of the target opaque walls, fenestration walls, and roof for each orientation. A target surface of a wall or a roof for each orientation is selected using the *SelectModelElements* node (Figure 27a).

The *Element.GetParameterValueByName* node is then used to extract physical parameters (i.e., the external surface area of a building envelope) from the BIM model by adding a *String* node to set a literal constant of the variable name. The required literal constant name is “Area” (Figure 27b). After deriving the gross surface area of the target surfaces (Figure 27c), *Math* function nodes are used to automatically calculate WWR and SSR or SKR values (Figure 27d). Figure 27 shows the proposed visual scripting to automatically calculate WWR and SSR or SKR.

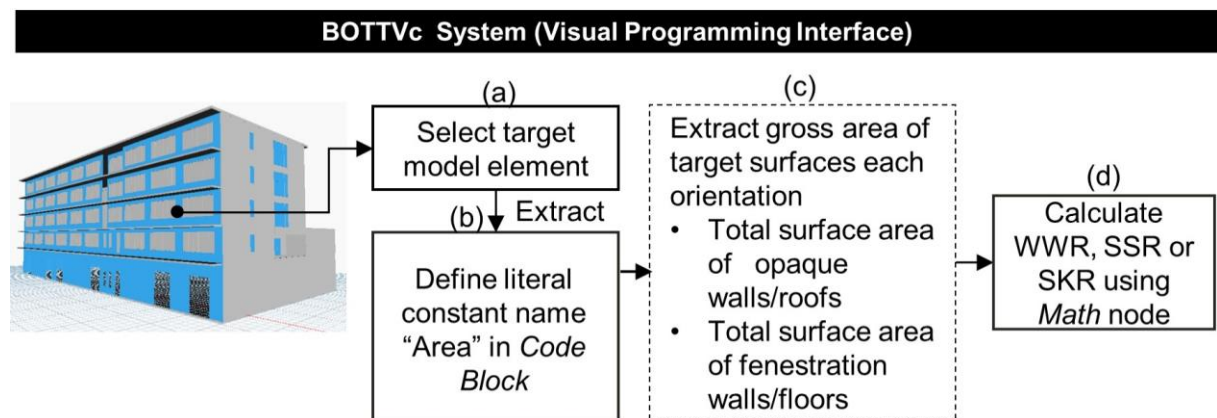


Figure 27 Workflow for extracting the total area of target surfaces of walls/roofs and calculating WWR and SSR or SKR values

5.3.2 Acquisition of SC or ESM coefficients

In order to derive the SC or ESM coefficients for fixed external shading devices (e.g., vertical fin, horizontal shading device, and egg crate), the dimension parameters of each shading device (Figure 28a), such as the length and width of an overhang (W), the distance between the upper edge of a window and the bottom of the overhang (B), the exposed area of a window, and the shaded area of a window (A), are automatically measured from the BIM model using the proposed visual scripting (Figure 28b). The outputs can be used to find an accurate value of SC or ESM (Figure 28c) at different orientations according to the OTTV calculation guidelines given by the local governments

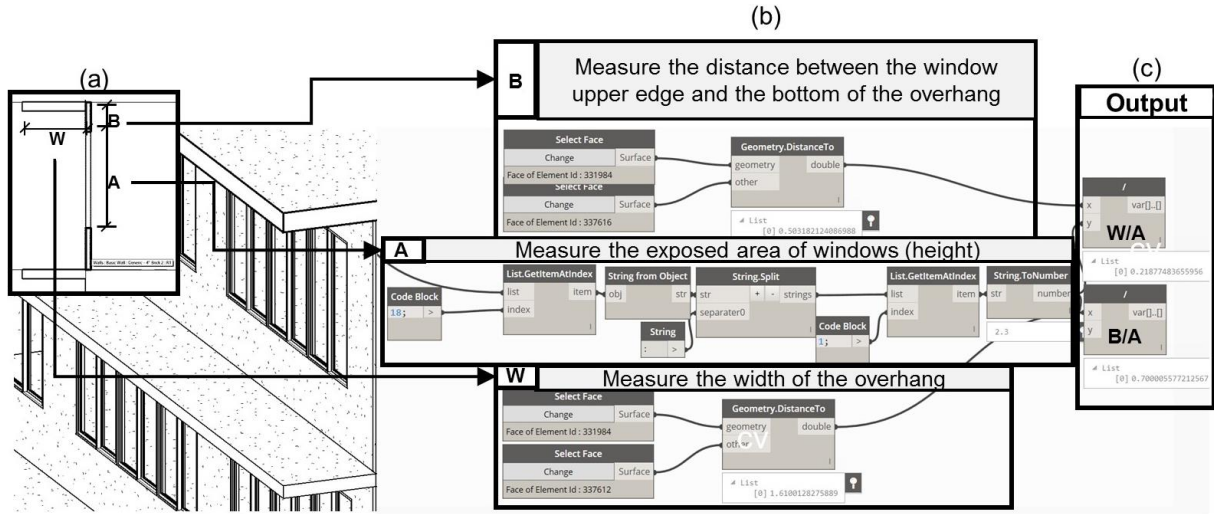


Figure 28 The proposed visual scripting to obtain variables for finding an SC or ESM value for external shading devices

5.3.3 Acquisition of TDeq and SF coefficients

As explained in Section 2.6.3, TDeq and SF coefficients are required for OTTV equations for some countries (e.g., Thailand, Hong Kong, the Philippines, Malaysia, and Indonesia). The equation for calculating TDeq differs depending on the OTTV code being applied. For example, in Thailand, TDeq involves three coefficients (i.e., density, specific heat, and wall thickness of construction materials). Material density and specific heat can be directly extracted from the thermal and physical properties in a BIM model (as explained in Sections 5.2.3 and 5.2.4). To derive the wall thickness, a *String* node is determined with a parameter name “Thickness”. Then, the Density Specific Heat (DSH) product of each material component of the building envelope is computed using *Math* function nodes using the following equation:

$$DSH_i = \rho_i \times c_{pi} \times \Delta x_i \text{ (kJ/m}^2\text{K}) \quad (21)$$

where

DSH is the DSH product with units $\text{kJ}/(\text{m}^2\text{K})$

ρ_i is the density of the material

c_{pi} is the specific heat of the material and

Δx_i is the thickness of the material.

Moreover, the colors of the external surfaces of the walls and roof are used to determine the solar absorption coefficient value. For Hong Kong, the Philippines, Malaysia, and Indonesia, after obtaining the density of a construction material from the BIM database, users can choose a constant TDeq value according to the density of the construction provided in the building energy code standards. Figure 29 shows the workflow for calculating TDeq using the BOTTVC system based on Thailand’s and Hong Kong’s OTTV codes. Although the proposed system aims to use extracted data from the BIM database

as inputs to calculate variables for verifying OTTV, there are some coefficients that do not require an input value from the BIM database, such as the SF value. Hence, in our developed system, we proposed using Dynamo's algebraic functions, which allow users to define numeric input values given by the code of practice to generate the output of the SF value. The SF value is required for OTTV calculation for the Philippines, Malaysia, and Indonesia. The SF value can be obtained using the following equation:

$$SF = 130 \text{ CF (W/m}^2\text{)} \quad (22)$$

where

CF is the correction factor with reference to the orientation of the façade and the pitch angle of the fenestration component.

For the case of Hong Kong, SF is provided as a constant coefficient, which users can choose the values for horizontal and vertical surfaces for each orientation from the solar factor table given by the OTTV calculation guideline of Hong Kong. Other coefficients, including ΔT , ESR, G_w , G_s , CF, and SC values, are constant coefficients that are given in the OTTV calculation guidelines. BOTTVC provides such constant coefficients in a spreadsheet file, which can be directly read using the BOTTVC system.

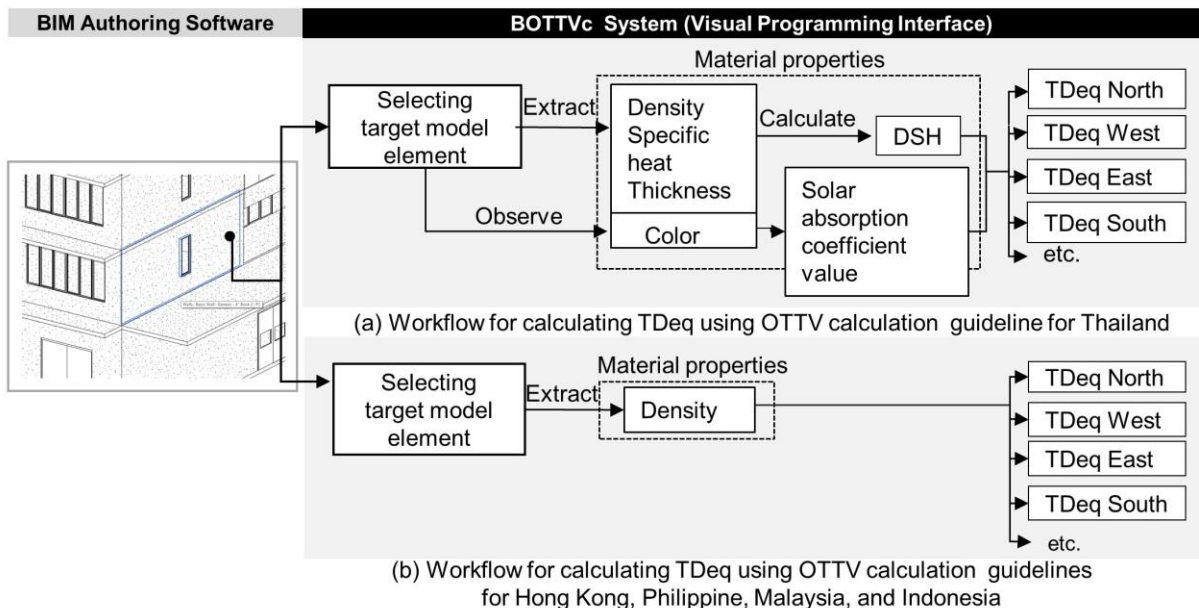


Figure 29 Workflow for calculating TDeq on the basis of OTTV standards in different countries

5.3.4 Accommodating OTTV coefficients for assessing the thermal performance of a building envelope

After deriving all the required coefficients related to the OTTV equation, all coefficients are accommodated and used as a set of input variables to compute the OTTV within our proposed system. The thermal performance is evaluated after acquiring the result of the OTTV calculation by comparing the output of the OTTV with OTTV standards. The designer must ensure that the OTTV of his/her building complies with the OTTV standard. If the OTTV does not meet the minimum requirement of the OTTV standard, then it is necessary to redesign the components of the building's enclosing material in the BIM authoring software.

5.3.5 Information output

After accessing the thermal properties, the physical properties from the BIM database are obtained using a visual programming language. A set of coefficients and OTTVs are computed with the various outputs obtained, including the following:

- The results of the measurement of the design of a building envelope for thermal performance reported as the OTTV, U-value, and R-value.
- Quantification of the effect of different envelope parameters, such as the U-value of opaque and fenestration materials, WWR, SC, TDeq, and SHGC on the heat gain through a building's external envelope.
- Thermal property information of construction materials to ensure that the proposed thermal performance design of the building envelope complies with the prescriptive requirements of OTTV standards.
- A 3D virtual context of the BIM model while calculating the OTTV.

5.4 Usage process flow for BOTTVC

In order to ensure that building envelopes are well-designed, provide suitable thermal properties to be operated in an air-conditioned environment, and meet the desired levels of thermal performance requirement, the verification and testing of the proposed envelope design solutions should be performed at the design stage. In the process of material selection for building envelopes, the BOTTVC system is proposed to help users initially verify the overall thermal transfer value of the various solutions for building envelope design.

The process flow of the BOTTVC system (as shown in Figure 30) is as follows: (a) the BIM model is created in Autodesk Revit, in which the geometry and material properties of building elements are modeled; (b) building information from the BIM model is linked with the BOTTVC system; (c) material

properties can be made accessible and a 3D geometry is automatically created after connecting the BIM model with Dynamo; (d) the required thermal and physical properties for OTTV calculation are extracted from the BIM model; (e) some OTTV coefficients are calculated using the BIM database as input data to obtain values through equations; (f) accumulation of all OTTV coefficients is performed and then all OTTV coefficients are set according to the calculation guidelines; (g) the OTTV calculation is executed, which enables users to immediately measure the OTTV of their design; in this step, the designer also evaluates the thermal performance of building envelopes by comparing the result to OTTV standards/codes; (h) the BIM model and its properties are saved. If the OTTV calculation result complies with the requirement of the *OTTV* standards. If the OTTV output does not meet the minimum requirement for the OTTV, then the user can change the combination of construction materials for the building envelope and run the calculations until the users find the optimal design solution and the overall thermal performance of the building envelope that complies with the OTTV requirements.

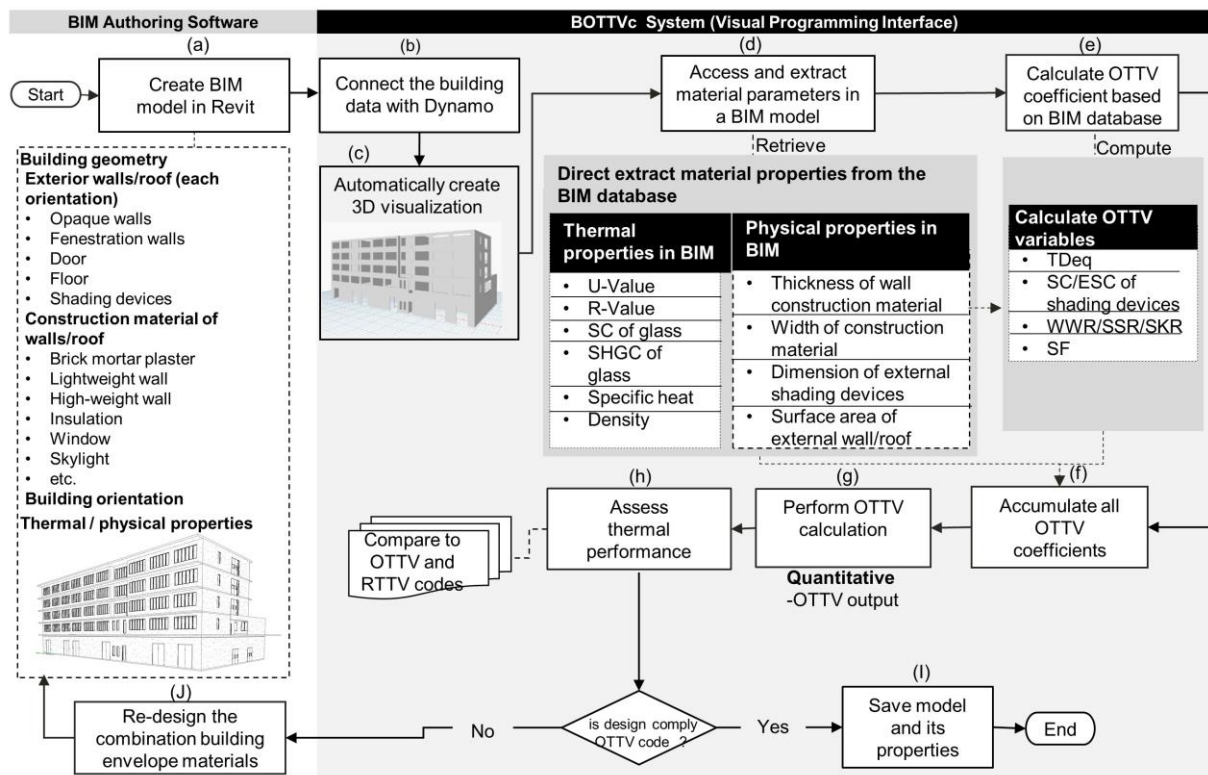


Figure 30 Usage process flow for BOTTVC

5.5 Case study

5.5.1 Baseline building

The applicability of the BOTTVC prototype system is validated in a non-residential building in the context of OTTV calculation methods for three countries that have employed the OTTV as a mandatory requirement for building energy conservation (i.e., Thailand, Hong Kong, and Singapore). The BOTTVC system is validated in a five-story building with a typical rectangular layout. The 3D BIM

model of the baseline building was created on the basis of its 2D drawings using Autodesk Revit Architecture 2015. The building was designed as offices, classrooms, laboratories, and student lounges. The case study building is a typical office building with a built in air-conditioned. The height of each floor is 3.20 m. Building information, such as the façade area and window area of all four elevations of the baseline building, was extracted from the BIM model using BOTTVC and used as a constant for OTTV calculations (described in Section 2.6.3). Specifications for the baseline building design were as follows: (1) the external wall material is opaque and has a 10-cm-thick brick wall with white plaster; (2) the windows are made of a single pane of glass ($SC = 0.7$) with aluminum used for the horizontal sliding sash windows; and 3) a reinforced concrete flat slab is used for the roof of the building.

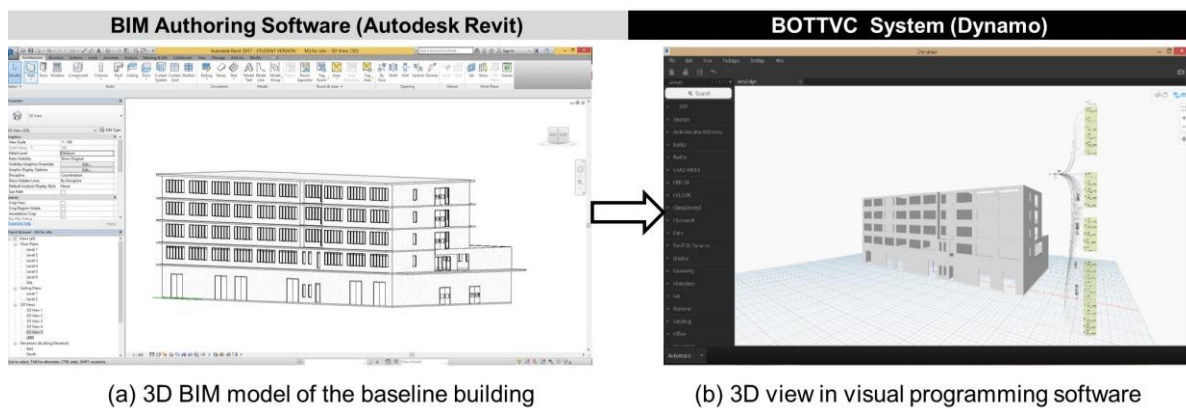


Figure 31 A 3D view of the model building in Revit (a) and in Dynamo (b)

5.5.2 Acquisition of OTTV coefficients using BOTTVC

The following subsections describe methods to acquire a set of coefficient data to be used as inputs to calculate the OTTV.

Extraction of building information from the BIM database

The BIM model of the baseline building contains details of the geometric and non-geometric information of components (e.g., building envelopes of both opaque and fenestration walls, windows, doors, roofs, and floors). An initial design of the thermal and physical properties of the building material was defined in the Material Library in Revit, and the orientation (e.g., North, South, East, West) of the building model was determined in Revit. After creating the BIM model for the case study, the BIM model and its properties were transferred into a visual programming environment.

Direct extraction of the OTTV coefficients

Performing direct extraction of information from the BIM model relevant to the OTTV calculation, including the U-value, R-value, specific heat, thermal conductivity, SHGC, and thickness of the building material, requires the proposed visual scripting to facilitate the sharing of such information with the BOTTVC system (explained in Section 5.2.2). Table 4 shows the required thermal and physical properties directly extracted from the BIM model using BOTTVC.

Table 4 Extracting thermal properties from the BIM database of the baseline building

Autodesk Revit	BOTTVC				
Material library involving thermal properties	Thermal properties				Physical properties
Opaque wall	U-value W/(m ² /k)	R-value m ² K/W	Specific heat KJ/(kg K)	Thermal conductivity W/(m/k)	Thickness (m)
Fenestration wall	Thermal properties				Physical properties
Fenestration wall	U-value W/(m ² /k)	R-value m ² K/W	SHGC	SC	Thickness (m)
					-
Opaque Roof	Thermal properties				Physical properties
Opaque Roof	U-value W/(m ² /k)	R-value m ² K/W	Specific heat KJ/(kg °C)	Thermal conductivity W/(m/k)	Thickness (m)

5.5.3 Calculating WWR and SSR or SKR coefficients

The total external surface area of opaque and fenestration walls and roofs in different directions was automatically measured to be used as input data to calculate WWR and SSR or SKR values in each orientation (e.g., North, South, East, West). The external wall orientation factor is a measure of the solar

radiation intensity that is received on building surfaces in a specific orientation. The external surfaces of buildings facing different orientations did not receive the same amount of solar radiation. Consequently, the value of WWR is an important coefficient that affects the total thermal transfer through walls in different directions. Large WWR and SSR or SKR values normally indicate a high amount of energy required for cooling a space. The computation of WWR and SSR or SKR in the baseline case with respect to different external surface orientations using the BOTTVC system is shown in Table 5.

Table 5 Calculating 1-WWR, WWR, 1-SSR, and SSR values using BOTTVC

Walls	North facade	South facade	East facade	West facade
Total façade area (m ²)	1499.043	1671.210	555.100	476.679
Total opaque wall area (m ²)	918.998	817.189	480.867	453.220
Total fenestration wall area (m ²)	580.044	854.020	74.232	23.459
1-WWR	0.613	0.322	0.548	0.592
WWR	0.386	0.511	0.133	0.049
Flat slab		0°		
Roof				
Total opaque roof area (m ²)		1983.511		
Total fenestration roof area (m ²)		-		
1-SSR		1		
SSR		-		

5.5.4 Integrating extracted BIM information with constant coefficients

As explained in Section 5.3, some coefficients for OTTV calculation require equations and constant coefficients to determine the values of the required coefficients (e.g., TDeq, SC or ESM, ESR, and SF). To acquire TDeq values of the baseline building based on the context of the energy code for Thailand, variables for TDeq calculation, including density, specific heat, and thickness of materials were, directly obtained from the material properties in BIM (explained in Section 5.3.3). The solar absorption coefficient for the white external walls of the baseline building is 0.3. According to the building regulations regarding OTTVs for Hong Kong, after acquiring the density of wall constructions for each orientation, the TDeq value was derived from the equivalent temperature difference table given by the

OTTV guideline. TDeq values of the case study building using BOTTVC are reported in Table 6. TDeq is not required for OTTV calculation in Singapore.

Table 6 TDeq values under the OTTV codes of Thailand and Hong Kong

Thailand								Hong Kong						
Wall	DSH1 mortar plaster				DSH2 masonry brick				DSH3 mortar plaster				DSH of all materials	Density
	DSH1	DSH2	DSH3	DSH of all materials	DSH1	DSH2	DSH3	DSH of all materials	DSH1	DSH2	DSH3	DSH of all materials		
	Density x y z	x*x*y*z; >	x*x*y*z; >	x*x*y*z; >	x y z	x y z	x y z	a+a+b+c; b>	DSH1 mortar plaster	DSH2 masonry brick	DSH3 mortar plaster	DSH of all materials	>	>
	15.111	130.2	15.111	160.422										
	TDeq	TDeq	TDeq	TDeq					TDeq	TDeq	TDeq	TDeq		
	North	South	East	West					North	South	East	West		
	7.90	9.70	9.80	8.70					1.70	1.40	2.40	2.10		
Roof	Concrete cast in place				DSH				Density				Roof construction	Density
	Density x y z	x*x*y*z; >	x*x*y*z; >	x*x*y*z; >					>	>				
	460.58328													
	TDeq 0°(Roof concrete flat slab)				TDeq 0°(Roof concrete flat slab)				TDeq 0°(Roof concrete flat slab)					
	16.2				9.75				9.75					

There are two types of SC: (1) the SC of glass provided by a manufacturer and (2) the SC of external shading devices. Singapore requires the SC ratio, which can be calculated using the SC of glass and the SC of shading devices, whereas Thailand only requires the SC of external shading devices. ESM is required for OTTV calculation for Hong Kong. The SC of glass can be directly obtained from material properties in the BIM database (as shown in Table 4). With respect to the SC or ESM of external shading devices, the measurement of an exposed area of a window and the shaded area of a window was performed (described in Section 5.3.2). There are some required constant coefficients provided in a spreadsheet file, including the ESR value and SF coefficient. The ESR value is only required for Thailand's OTTV calculation, whereas the SF coefficient is only required for Hong Kong's OTTV calculation. Such coefficients can be directly read in a spreadsheet file to be used in the calculation process via BOTTVC. Table 7 reports the SC or ESM values of external shading devices, ESR, and SF values of the baseline building.

Table 7 Results of SC, ESM, ESR, SF, and CF values for the baseline building

Thailand				Singapore				Hong Kong						
	North	South	East	West	North	South	East	West	North	South	East	West		
SC	0.95	0.94	0.97	0.97	SC	0.48	0.48	0.46	0.46	ESM	0.74	0.62	0.62	0.62
ESR	185.06	267.41	244.53	234.58	ESR	Not required			ESR	Not required				
SF_{wall}	Not required			SF_{wall}	Not required			SF_{wall}	121	197	183	157		
SF_{roof}	Not required			SF_{roof}	Not required			SF_{roof}	264					
CF	Not required			CF	0.80	0.83	1.13	1.23	CF	Not required				

5.6 Calculating OTTV for assessing the performance of a building envelope

Due to the fact that OTTV equations in various countries vary depending on their local climates, specific geographic locations, and OTTV standards, which have been established by the governments in different countries, the OTTV calculation method for each country requires different variable inputs as shown in Table 8. With the help of visual scripting, defining input variables in each equation can be flexible and easy for calculating OTTV under the methods given by the OTTV code of practice in different countries. All OTTV coefficients are accommodated in our system. The OTTV results of non-residential buildings in Thailand using Equation (9) and (10) and Hong Kong using Equations (11) and (12) were calculated using the BOTTVC system, as shown in Table 8. The OTTV calculation of a building envelope is divided into four orientations on the basis of the building orientation: North, South, East, and West.

Table 8 Summary of all input coefficients and OTTV outputs of the baseline building

External wall	Thailand				Singapore				Hong Kong			
	North	South	East	West	North	South	East	West	North	South	East	West
U _{wall}	4.89	4.89	4.89	4.89	4.89	4.89	4.89	4.89	4.89	4.89	4.89	4.89
U _{glass}	3.68	3.68	3.68	3.68	3.68	3.68	3.68	3.68	3.68	3.68	3.68	3.68
SHGC	0.78	0.78	0.78	0.78	Not required				0.78	0.78	0.78	0.78
SC _{glass}	0.7	0.7	0.7	0.7	0.7	0.7	0.7	0.7	0.7	0.7	0.7	0.7
SC or ESM shading device	0.95	0.94	0.97	0.97	Not required				0.744	0.620	0.620	0.620
SC _{glass} × shading devices	Not required				0.48	0.48	0.46	0.46	Not required			
1-WWR	0.613	0.322	0.548	0.592	0.613	0.322	0.548	0.592	0.613	0.322	0.548	0.592
WWR	0.386	0.511	0.133	0.049	0.386	0.511	0.133	0.049	0.386	0.511	0.133	0.049
TDeq	7.90	9.70	9.80	8.70	Not required				1.70	1.40	2.40	2.10
ESR	185.06	267.41	244.53	234.58	Not required				Not required			
SF	Not required				Not required				121	197	183	157
CF	Not required				0.80	0.83	1.13	1.23	Not required			
OTTV each orientation (W/m ²)	83.32	109.14	52.01	44.04	56.34	62.19	28.15	24.36	50.13	54.54	41.45	45.06
Overall OTTV _{wall} (W/m ²)	80.89				51.62				50.17			
Overall OTTV _{roof} (W/m ²)	76.18				42.80				167.30			

Table 8 (continue) Summary of all input coefficients and OTTV outputs of the baseline building

External roof	Thailand		Singapore		Hong Kong	
	0°(Roof concrete flat slab)					
U _{roof}	3.43		3.43		3.43	
U _{glass}	-		-		-	
SHGC	-		-		-	
SC _{glass}	-		-		-	
SC or ESM shading device	-		-		-	
1-WWR	1		1		1	
WWR	-		-		-	
TDeq	16.2		Not required		9.75	
SF	Not required		Not required		264	
CF	Not required		1		Not required	
Overall OTTV _{roof} (W/m ²)	76.18		42.80		167.30	

The different variables involved in OTTV equations can be explained as follows. For example, OTTV for external walls, $SC_{glass \times shading}$ devices and CF are not required for OTTV calculation in Thailand and Hong Kong, but they are required for Singapore. SHGC, TDeq, and SC or ESM shading device values are not required for Singapore's OTTV equation. However, such values are required for computing the OTTV in Thailand and Hong Kong. In addition, the ESR value is not included in Singapore's and Hong Kong's OTTV equations, but it is included in Thailand's OTTV equation. Additionally, the SF value is not required for OTTV equations in Thailand and Singapore. However, the SF value is an input for computing the OTTV in Hong Kong.

Regarding the OTTV for external roofs, the TDeq value is not a required input for calculating OTTV in Singapore, but it is required for Thailand and Hong Kong. The OTTV code of practice given by the government of Thailand and Singapore does not require the SF value as an input, whereas the CF value is required for calculating OTTVs in Singapore, but it is not required in Thailand and Hong Kong.

The results of the OTTV_{wall} assessment based on Thailand's and Singapore's legislations revealed that the building envelope with a southward façade shows the highest OTTV_{wall} (109.14 W/m² for Thailand and 62.19 W/m² for Singapore), followed by that with a northward façade (83.32 W/m² for Thailand and 56.34 W/m² for Singapore) and that with an eastward façade (52.01 W/m² for Thailand and 28.15 W/m² for Singapore). The case with a westward façade has the lowest OTTV_{wall} (44.04 W/m² for Thailand and 24.36 W/m² for Singapore).

For Thailand, the total OTTV_{wall} of the baseline building is 80.89 W/m², which is higher than the maximum allowable OTTV_{wall} for nonresidential buildings. Considering the baseline building, the major factors for heat transfer into the building were the higher WWR value and gross fenestration area facing South (0.511) and North (0.386) compared to East (0.133) and West (0.049). Hence, the major contribution to the thermal transfer value is by heat conduction and solar radiation through a fenestration wall. According to the OTTV_{wall} code of Thailand, the recommended total OTTV_{wall} for non-residential buildings (offices and education buildings) with a totally air-conditioned area of more than 2,000 m² should not exceed 50 W/m². The results reveal that the building envelope condition of the baseline building fails to comply with the OTTV standard. Consequently, an approximately 30.89 W/m² reduction in OTTV_{wall} is required to improve the performance of the building envelope to comply with the building code and to limit solar heat gain through the building envelope. For Singapore, the result revealed that the total OTTV_{wall} of the baseline building is 51.62 W/m², which is 1.62 W/m² greater than the OTTV_{wall} requirement of Singapore. In terms of the OTTV_{wall} calculation based on Hong Kong's building regulations for energy efficiency, the results revealed that the total OTTV_{wall} of the baseline building is 50.17 W/m². According to the OTTV_{wall} requirement for walls in Hong Kong, OTTV_{wall} should not exceed 24 W/m². Consequently, an approximately 26.14 W/m² reduction in OTTV_{wall} is required to reduce the electricity consumption for air-conditioning and to have an acceptable OTTV_{wall}.

The results of the OTTV_{roof} assessment based on the calculation methods for Thailand and Hong Kong revealed that the total OTTV_{roof} of the baseline building exceeded the requirements of 76.18 W/m² and 167.30 W/m², respectively. The OTTV_{roof} requirement specifies that it should not exceed 15 W/m² and 24 W/m² for Thailand and Hong Kong, respectively. Consequently, approximately 61.18 W/m² and 143.30 W/m² reductions in OTTV_{roof} are required for Thailand and Hong Kong, respectively.

5.7 Optimization scenarios

In order to achieve an acceptable OTTV, the design of the building envelope of the baseline building at the stage of material selection should consider the two basic components of heat gain through building envelopes (i.e., heat conduction through walls and windows and solar radiation through windows). Thus, the following optimization scenarios are proposed: (1) reducing the U-value for opaque walls and roofs, (2) lowering the windows' U-value and SHGC value, and (3) reducing the gross glazing area facing South/North. Each of the following scenarios was applied and BOTTVC was used to find the optimal building envelope system:

- Scenario 1: By reducing the U-value for opaque walls and roofs, this study proposed four solutions to improve the thermal performance of external walls and one solution for roofs, as follows:
 - (A) Increasing the thickness of the exterior wall (brick and mortar) from 0.10 m to 0.20 m with single glass (SC = 0.5)
 - (B) Changing the building envelope material from masonry brick to lightweight brick with single glass (SC = 0.5)
 - (C) Using normal masonry brick and installing a 150 mm wool insulation with 6 mm of gypsum board with a single pane of glass (SC = 0.5)
 - (D) Using lightweight brick and installing 150 mm wool insulator with 6 mm of gypsum board with a single pane of glass (SC = 0.5)
 - (E) Installing a 10 cm wool insulator under the roof material
- Scenario 2: By lowering the windows' U-value, SC, and SHGC, we propose replacing the single glass pane with genuine double-glazing and low-E glazing with one of the following options:
 - (F) Normal brick with cement plasters on both sides with double-glazing (SC = 0.3)
 - (G) Lightweight brick with double-glazing (SC = 0.3)
 - (H) Lightweight brick with low-E double-glazing (SC = 0.3)
 - (I) Lightweight brick with double-glazing (SC = 0.2)
- Scenario 3: In the scenario, the gross glazing area facing South/North is reduced:

- (J) The ratio of the WWR is restricted to 30% of the gross wall area. The building envelope material is masonry brick with double glazing (SC = 0.2)
- (K) The ratio of WWR is restricted to 30% of the gross wall area. The building envelope material is lightweight brick with double-glazing (SC = 0.2)

The optimization results for the proposed scenarios using the BOTTVC system are reported in Figure 32 and Table 9.

The calculation outputs of the improvement scenarios for the building envelope's thermal performance were generated by BOTTVC. In this study, eleven scenarios were proposed to improve the thermal performance of the case study building. The OTTV standards in the context of the building regulations of Thailand, Hong Kong, and Singapore were used in the validation of the proposed system. The OTTV improvement scenarios are shown in Figure 32 and Table 9.

Although the first scenario to reduce the U-value of opaque walls and roofs helps reduce the heat gain into the building, the OTTVs remain over the mandatory compliance values of 50 W/m^2 and 24 W/m^2 for Thailand and Hong Kong, respectively. This is because reducing the U-value for opaque walls alone without considering the properties of glazing is insufficient and the poor selection of the window material, that is, a single glass pane with an SC of 0.7, is the highest contributor to the overall thermal transfer of the building. Hence, the second scenario of lowering the windows' U-value, SC, and SHGC was proposed. The results revealed that the reduction of the U-value of glass using double-glazing and low-E double glazing significantly lowers the OTTV within the range of 43.89 – 60.56% for Thailand and 36.54 – 62.42% for Hong Kong. A fenestration system of a building envelope generally represents a significant impact on cooling load in a building. Thus, the third scenario to reduce the gross glazing area facing South/North was proposed. The WWR (North and South) is restricted to 30% of the gross wall area which decreases the OTTV from 0.326 W/m^2 to 0.231 W/m^2 . The results revealed that the OTTV in this scenario was in the range of $33.28\text{--}40.45 \text{ W/m}^2$ and $19.55\text{--}28.92 \text{ W/m}^2$ based on the context of the OTTV codes for Thailand and Hong Kong, respectively. This scenario helps reduce the OTTV by nearly 41.14 – 50.00% for Thailand and 38.96 – 57.64% for Hong Kong compared to the baseline building.

Based on the proposed optimization scenarios, lowering the U-value of walls/roofs, windows, SC, and SHGC is the most effective method to increase the thermal performance of the building envelope of the baseline building in order to comply with OTTV requirements. The most optimal combination of the building envelope of the baseline building based on the OTTV calculation methods is lightweight brick with double glazing (SC = 0.2) for Thailand and Hong Kong and lightweight brick and low-E double glazing (SC = 0.3) for Singapore. Reducing the gross glazing area facing South and North is another effective method to minimize heat transfer through the building envelope into the building that should also be considered during the design stage.

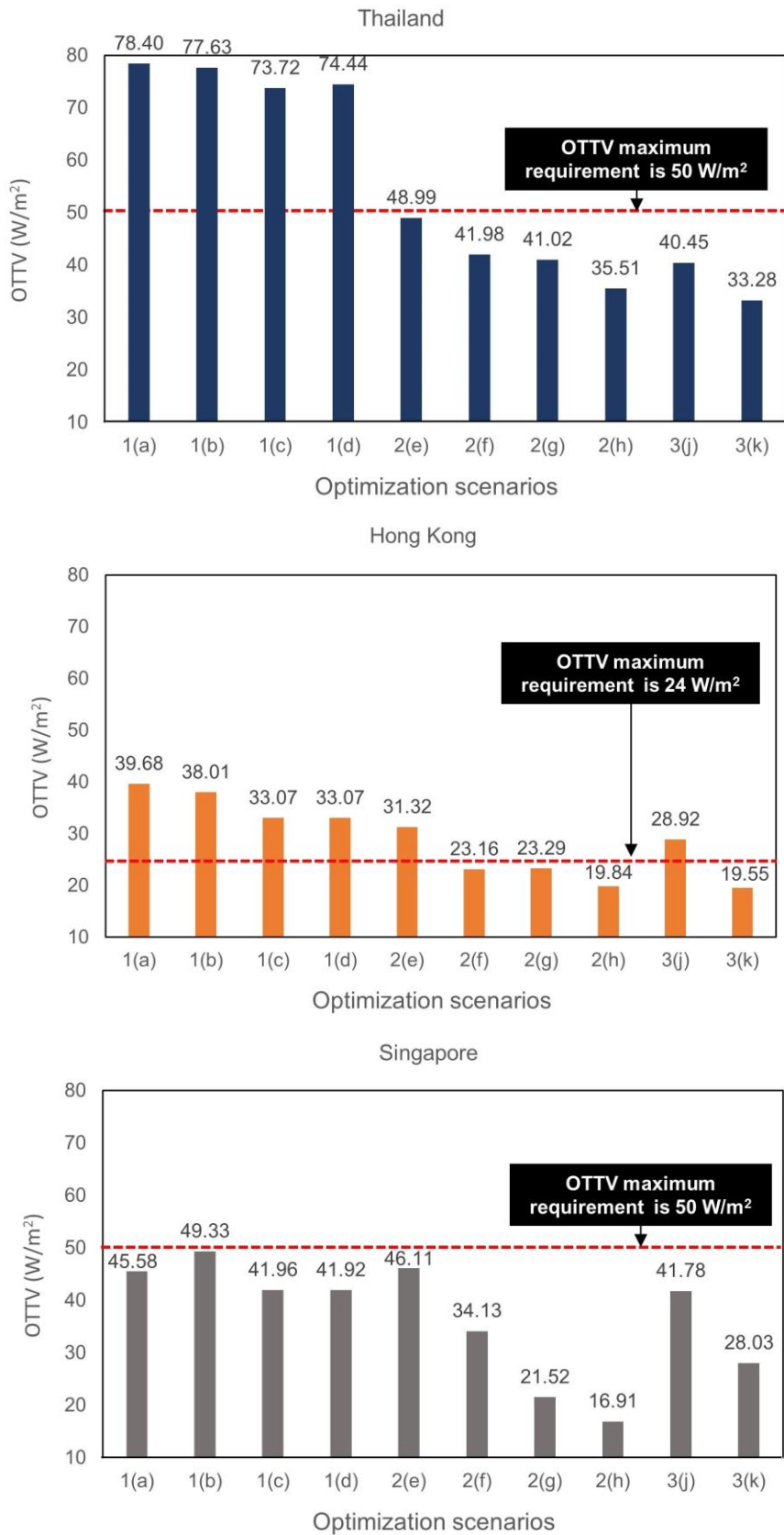
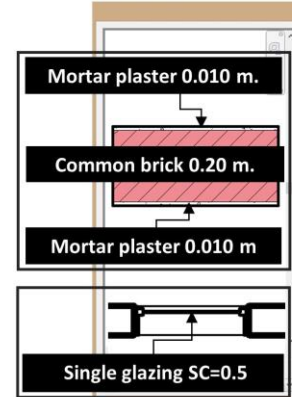
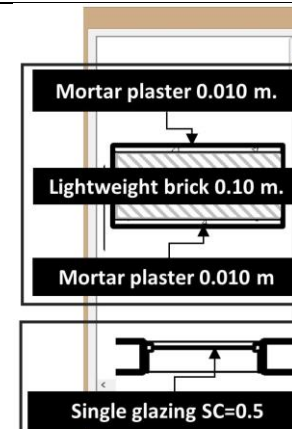
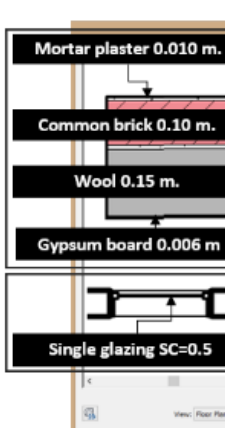
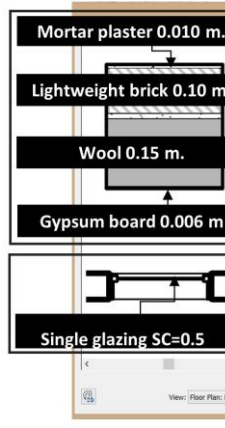


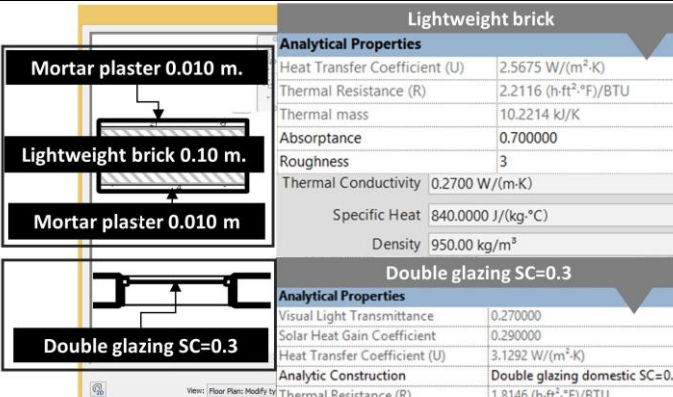
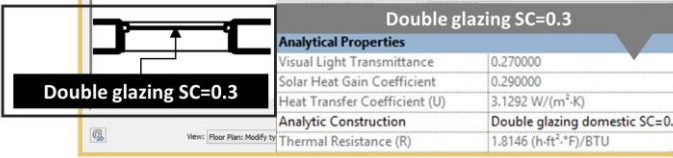
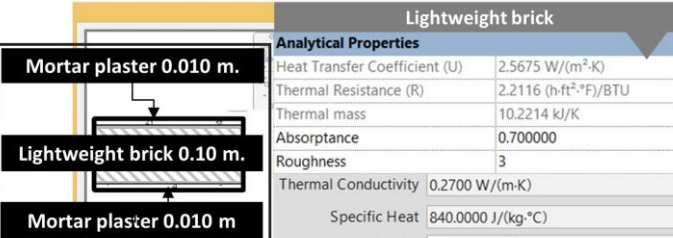
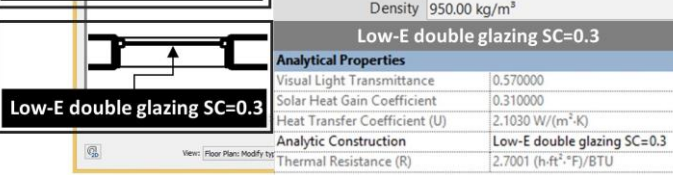
Figure 32 Comparing OTTV results of different optimization scenarios

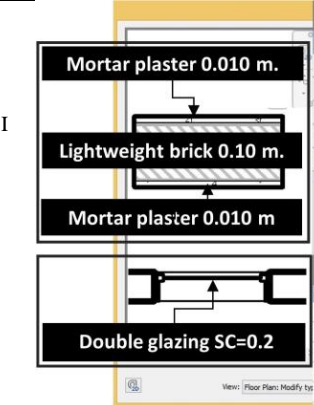
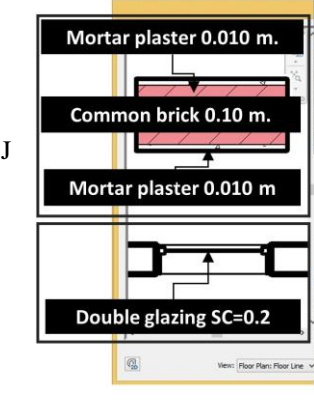
Table 9 OTTV outputs of different optimization scenarios

	Material layers	Material properties				Total OTTV _{wall} (W/m ²)																												
		U _{wall}	U _{glass}	SHGC	SC _{glass}	Thailand	Hong Kong	Singapore																										
Scenario (1) Reducing U-value for opaque wall and roof																																		
A	 <p>Common brick</p> <p>Analytical Properties</p> <table border="1"> <tr><td>Heat Transfer Coefficient (U)</td><td>2.5675 W/(m²·K)</td></tr> <tr><td>Thermal Resistance (R)</td><td>2.2116 (h·ft²·°F)/BTU</td></tr> <tr><td>Thermal mass</td><td>26.9997 kJ/K</td></tr> <tr><td>Absorptance</td><td>0.700000</td></tr> <tr><td>Roughness</td><td>3</td></tr> <tr><td>Thermal Conductivity</td><td>0.5400 W/(m·K)</td></tr> <tr><td>Specific Heat</td><td>840.0000 J/(kg·°C)</td></tr> <tr><td>Density</td><td>1,550.00 kg/m³</td></tr> </table> <p>Single glazing SC=0.5</p> <p>Analytical Properties</p> <table border="1"> <tr><td>Visual Light Transmittance</td><td>0.460000</td></tr> <tr><td>Solar Heat Gain Coefficient</td><td>0.590000</td></tr> <tr><td>Heat Transfer Coefficient (U)</td><td>6.7018 W/(m²·K)</td></tr> <tr><td>Analytic Construction</td><td>Single glazing SC=0.5</td></tr> <tr><td>Thermal Resistance (R)</td><td>0.8473 (h·ft²·°F)/BTU</td></tr> </table>	Heat Transfer Coefficient (U)	2.5675 W/(m ² ·K)	Thermal Resistance (R)	2.2116 (h·ft ² ·°F)/BTU	Thermal mass	26.9997 kJ/K	Absorptance	0.700000	Roughness	3	Thermal Conductivity	0.5400 W/(m·K)	Specific Heat	840.0000 J/(kg·°C)	Density	1,550.00 kg/m ³	Visual Light Transmittance	0.460000	Solar Heat Gain Coefficient	0.590000	Heat Transfer Coefficient (U)	6.7018 W/(m ² ·K)	Analytic Construction	Single glazing SC=0.5	Thermal Resistance (R)	0.8473 (h·ft ² ·°F)/BTU	2.567	6.701	0.59	0.5	78.40	39.68	45.58
Heat Transfer Coefficient (U)	2.5675 W/(m ² ·K)																																	
Thermal Resistance (R)	2.2116 (h·ft ² ·°F)/BTU																																	
Thermal mass	26.9997 kJ/K																																	
Absorptance	0.700000																																	
Roughness	3																																	
Thermal Conductivity	0.5400 W/(m·K)																																	
Specific Heat	840.0000 J/(kg·°C)																																	
Density	1,550.00 kg/m ³																																	
Visual Light Transmittance	0.460000																																	
Solar Heat Gain Coefficient	0.590000																																	
Heat Transfer Coefficient (U)	6.7018 W/(m ² ·K)																																	
Analytic Construction	Single glazing SC=0.5																																	
Thermal Resistance (R)	0.8473 (h·ft ² ·°F)/BTU																																	
B	 <p>Lightweight brick</p> <p>Analytical Properties</p> <table border="1"> <tr><td>Heat Transfer Coefficient (U)</td><td>2.5675 W/(m²·K)</td></tr> <tr><td>Thermal Resistance (R)</td><td>2.2116 (h·ft²·°F)/BTU</td></tr> <tr><td>Thermal mass</td><td>10.2214 kJ/K</td></tr> <tr><td>Absorptance</td><td>0.700000</td></tr> <tr><td>Roughness</td><td>3</td></tr> <tr><td>Thermal Conductivity</td><td>0.2700 W/(m·K)</td></tr> <tr><td>Specific Heat</td><td>840.0000 J/(kg·°C)</td></tr> <tr><td>Density</td><td>950.00 kg/m³</td></tr> </table> <p>Single glazing SC=0.5</p> <p>Analytical Properties</p> <table border="1"> <tr><td>Visual Light Transmittance</td><td>0.460000</td></tr> <tr><td>Solar Heat Gain Coefficient</td><td>0.590000</td></tr> <tr><td>Heat Transfer Coefficient (U)</td><td>6.7018 W/(m²·K)</td></tr> <tr><td>Analytic Construction</td><td>Single glazing SC=0.5</td></tr> <tr><td>Thermal Resistance (R)</td><td>0.8473 (h·ft²·°F)/BTU</td></tr> </table>	Heat Transfer Coefficient (U)	2.5675 W/(m ² ·K)	Thermal Resistance (R)	2.2116 (h·ft ² ·°F)/BTU	Thermal mass	10.2214 kJ/K	Absorptance	0.700000	Roughness	3	Thermal Conductivity	0.2700 W/(m·K)	Specific Heat	840.0000 J/(kg·°C)	Density	950.00 kg/m ³	Visual Light Transmittance	0.460000	Solar Heat Gain Coefficient	0.590000	Heat Transfer Coefficient (U)	6.7018 W/(m ² ·K)	Analytic Construction	Single glazing SC=0.5	Thermal Resistance (R)	0.8473 (h·ft ² ·°F)/BTU	2.567	6.701	0.59	0.5	77.63	38.01	49.33
Heat Transfer Coefficient (U)	2.5675 W/(m ² ·K)																																	
Thermal Resistance (R)	2.2116 (h·ft ² ·°F)/BTU																																	
Thermal mass	10.2214 kJ/K																																	
Absorptance	0.700000																																	
Roughness	3																																	
Thermal Conductivity	0.2700 W/(m·K)																																	
Specific Heat	840.0000 J/(kg·°C)																																	
Density	950.00 kg/m ³																																	
Visual Light Transmittance	0.460000																																	
Solar Heat Gain Coefficient	0.590000																																	
Heat Transfer Coefficient (U)	6.7018 W/(m ² ·K)																																	
Analytic Construction	Single glazing SC=0.5																																	
Thermal Resistance (R)	0.8473 (h·ft ² ·°F)/BTU																																	

Material layers	Material properties				Total OTTV _{wall} (W/m ²)																											
	U _{wall}	U _{glass}	SHGC	SC _{glass}	Thailand	Hong Kong	Singapore																									
Scenario (1) Reducing U-value for opaque wall and roof (continue)																																
C	0.216	6.701	0.59	0.5	73.72	33.07	41.96																									
 <div style="border: 1px solid black; padding: 5px; margin-top: 10px;"> Common brick Analytical Properties <table border="1"> <tr><td>Heat Transfer Coefficient (U)</td><td>0.2162 W/(m²·K)</td></tr> <tr><td>Thermal Resistance (R)</td><td>26.2637 (h·ft²·°F)/BTU</td></tr> <tr><td>Thermal mass</td><td>17.3976 kJ/K</td></tr> <tr><td>Absorptance</td><td>0.700000</td></tr> <tr><td>Roughness</td><td>3</td></tr> </table> Wool <table border="1"> <tr><td>Thermal Conductivity</td><td>0.5400 W/(m·K)</td></tr> <tr><td>Specific Heat</td><td>840.0000 J/(kg·°C)</td></tr> <tr><td>Density</td><td>1,550.00 kg/m³</td> </tr> </table> Single glazing SC=0.5 Analytical Properties <table border="1"> <tr><td>Visual Light Transmittance</td><td>0.460000</td></tr> <tr><td>Solar Heat Gain Coefficient</td><td>0.590000</td></tr> <tr><td>Heat Transfer Coefficient (U)</td><td>6.7018 W/(m²·K)</td></tr> <tr><td>Analytic Construction</td><td>Single glazing SC=0.5</td></tr> <tr><td>Thermal Resistance (R)</td><td>0.8473 (h·ft²·°F)/BTU</td></tr> </table> </div>	Heat Transfer Coefficient (U)	0.2162 W/(m ² ·K)	Thermal Resistance (R)	26.2637 (h·ft ² ·°F)/BTU	Thermal mass	17.3976 kJ/K	Absorptance	0.700000	Roughness	3	Thermal Conductivity	0.5400 W/(m·K)	Specific Heat	840.0000 J/(kg·°C)	Density	1,550.00 kg/m ³	Visual Light Transmittance	0.460000	Solar Heat Gain Coefficient	0.590000	Heat Transfer Coefficient (U)	6.7018 W/(m ² ·K)	Analytic Construction	Single glazing SC=0.5	Thermal Resistance (R)	0.8473 (h·ft ² ·°F)/BTU						
Heat Transfer Coefficient (U)	0.2162 W/(m ² ·K)																															
Thermal Resistance (R)	26.2637 (h·ft ² ·°F)/BTU																															
Thermal mass	17.3976 kJ/K																															
Absorptance	0.700000																															
Roughness	3																															
Thermal Conductivity	0.5400 W/(m·K)																															
Specific Heat	840.0000 J/(kg·°C)																															
Density	1,550.00 kg/m ³																															
Visual Light Transmittance	0.460000																															
Solar Heat Gain Coefficient	0.590000																															
Heat Transfer Coefficient (U)	6.7018 W/(m ² ·K)																															
Analytic Construction	Single glazing SC=0.5																															
Thermal Resistance (R)	0.8473 (h·ft ² ·°F)/BTU																															
D	0.218	6.701	0.59	0.5	74.44	33.07	41.92																									
 <div style="border: 1px solid black; padding: 5px; margin-top: 10px;"> Lightweight brick Analytical Properties <table border="1"> <tr><td>Heat Transfer Coefficient (U)</td><td>0.2187 W/(m²·K)</td></tr> <tr><td>Thermal Resistance (R)</td><td>25.9593 (h·ft²·°F)/BTU</td></tr> <tr><td>Thermal mass</td><td>11.3886 kJ/K</td></tr> <tr><td>Absorptance</td><td>0.700000</td></tr> <tr><td>Roughness</td><td>3</td></tr> </table> Wool <table border="1"> <tr><td>Thermal Conductivity</td><td>0.7600 W/(m·K)</td></tr> <tr><td>Specific Heat</td><td>840.0000 J/(kg·°C)</td></tr> <tr><td>Density</td><td>780.00 kg/m³</td> </tr> </table> Single glazing SC=0.5 Analytical Properties <table border="1"> <tr><td>Visual Light Transmittance</td><td>0.460000</td></tr> <tr><td>Solar Heat Gain Coefficient</td><td>0.590000</td></tr> <tr><td>Heat Transfer Coefficient (U)</td><td>6.7018 W/(m²·K)</td></tr> <tr><td>Analytic Construction</td><td>Single glazing SC=0.5</td></tr> <tr><td>Thermal Resistance (R)</td><td>0.8473 (h·ft²·°F)/BTU</td></tr> </table> </div>	Heat Transfer Coefficient (U)	0.2187 W/(m ² ·K)	Thermal Resistance (R)	25.9593 (h·ft ² ·°F)/BTU	Thermal mass	11.3886 kJ/K	Absorptance	0.700000	Roughness	3	Thermal Conductivity	0.7600 W/(m·K)	Specific Heat	840.0000 J/(kg·°C)	Density	780.00 kg/m ³	Visual Light Transmittance	0.460000	Solar Heat Gain Coefficient	0.590000	Heat Transfer Coefficient (U)	6.7018 W/(m ² ·K)	Analytic Construction	Single glazing SC=0.5	Thermal Resistance (R)	0.8473 (h·ft ² ·°F)/BTU						
Heat Transfer Coefficient (U)	0.2187 W/(m ² ·K)																															
Thermal Resistance (R)	25.9593 (h·ft ² ·°F)/BTU																															
Thermal mass	11.3886 kJ/K																															
Absorptance	0.700000																															
Roughness	3																															
Thermal Conductivity	0.7600 W/(m·K)																															
Specific Heat	840.0000 J/(kg·°C)																															
Density	780.00 kg/m ³																															
Visual Light Transmittance	0.460000																															
Solar Heat Gain Coefficient	0.590000																															
Heat Transfer Coefficient (U)	6.7018 W/(m ² ·K)																															
Analytic Construction	Single glazing SC=0.5																															
Thermal Resistance (R)	0.8473 (h·ft ² ·°F)/BTU																															

	Material layers	Material properties				Total OTTV _{wall} (W/m ²)																								
		U _{wall}	U _{glass}	SHGC	SC _{glass}	Thailand	Hong Kong	Singapore																						
	Scenario (1) Reducing U-value for opaque wall and roof (continue)																													
E	<p>Analytical Properties</p> <table> <tr><td>Heat Transfer Coefficient (U)</td><td>0.3098 W/(m²·K)</td></tr> <tr><td>Thermal Resistance (R)</td><td>18.3293 (h·ft²·°F)/BTU</td></tr> <tr><td>Thermal mass</td><td>43.4350 kJ/K</td></tr> <tr><td>Absorptance</td><td>0.700000</td></tr> <tr><td>Roughness</td><td>3</td></tr> </table> <p>Concrete cast in place</p> <table> <tr><td>Thermal Conductivity</td><td>1.0460 W/(m·K)</td></tr> <tr><td>Specific Heat</td><td>657.0000 J/(kg·°C)</td></tr> <tr><td>Density</td><td>2,300.00 kg/m³</td></tr> </table> <p>Wool</p> <table> <tr><td>Thermal Conductivity</td><td>0.0340 W/(m·K)</td></tr> <tr><td>Specific Heat</td><td>710.0000 J/(kg·°C)</td></tr> <tr><td>Density</td><td>200.00 kg/m³</td></tr> </table>	Heat Transfer Coefficient (U)	0.3098 W/(m ² ·K)	Thermal Resistance (R)	18.3293 (h·ft ² ·°F)/BTU	Thermal mass	43.4350 kJ/K	Absorptance	0.700000	Roughness	3	Thermal Conductivity	1.0460 W/(m·K)	Specific Heat	657.0000 J/(kg·°C)	Density	2,300.00 kg/m ³	Thermal Conductivity	0.0340 W/(m·K)	Specific Heat	710.0000 J/(kg·°C)	Density	200.00 kg/m ³	0.309	-	-	-	6.87	18.48	4.42
Heat Transfer Coefficient (U)	0.3098 W/(m ² ·K)																													
Thermal Resistance (R)	18.3293 (h·ft ² ·°F)/BTU																													
Thermal mass	43.4350 kJ/K																													
Absorptance	0.700000																													
Roughness	3																													
Thermal Conductivity	1.0460 W/(m·K)																													
Specific Heat	657.0000 J/(kg·°C)																													
Density	2,300.00 kg/m ³																													
Thermal Conductivity	0.0340 W/(m·K)																													
Specific Heat	710.0000 J/(kg·°C)																													
Density	200.00 kg/m ³																													
	Scenario (2) Lowering windows' U-value, SC, and SHGC																													
F	<p>Common brick</p> <p>Analytical Properties</p> <table> <tr><td>Heat Transfer Coefficient (U)</td><td>4.8946 W/(m²·K)</td></tr> <tr><td>Thermal Resistance (R)</td><td>1.1601 (h·ft²·°F)/BTU</td></tr> <tr><td>Thermal mass</td><td>14.9037 kJ/K</td></tr> <tr><td>Absorptance</td><td>0.700000</td></tr> <tr><td>Roughness</td><td>3</td></tr> </table> <p>Double glazing SC=0.3</p> <p>Analytical Properties</p> <table> <tr><td>Visual Light Transmittance</td><td>0.270000</td></tr> <tr><td>Solar Heat Gain Coefficient</td><td>0.290000</td></tr> <tr><td>Heat Transfer Coefficient (U)</td><td>3.1292 W/(m²·K)</td></tr> <tr><td>Analytic Construction</td><td>Double glazing domestic SC=0.</td></tr> <tr><td>Thermal Resistance (R)</td><td>1.8146 (h·ft²·°F)/BTU</td></tr> </table>	Heat Transfer Coefficient (U)	4.8946 W/(m ² ·K)	Thermal Resistance (R)	1.1601 (h·ft ² ·°F)/BTU	Thermal mass	14.9037 kJ/K	Absorptance	0.700000	Roughness	3	Visual Light Transmittance	0.270000	Solar Heat Gain Coefficient	0.290000	Heat Transfer Coefficient (U)	3.1292 W/(m ² ·K)	Analytic Construction	Double glazing domestic SC=0.	Thermal Resistance (R)	1.8146 (h·ft ² ·°F)/BTU	4.894	3.129	0.29	0.3	48.99	31.32	46.11		
Heat Transfer Coefficient (U)	4.8946 W/(m ² ·K)																													
Thermal Resistance (R)	1.1601 (h·ft ² ·°F)/BTU																													
Thermal mass	14.9037 kJ/K																													
Absorptance	0.700000																													
Roughness	3																													
Visual Light Transmittance	0.270000																													
Solar Heat Gain Coefficient	0.290000																													
Heat Transfer Coefficient (U)	3.1292 W/(m ² ·K)																													
Analytic Construction	Double glazing domestic SC=0.																													
Thermal Resistance (R)	1.8146 (h·ft ² ·°F)/BTU																													

	Material layers	Material properties				Total OTTV _{wall} (W/m ²)																												
		U _{wall}	U _{glass}	SHGC	SC _{glass}	Thailand	Hong Kong	Singapore																										
Scenario (2) Lowering windows' U-value, SC, and SHGC																																		
G	 <p>Lightweight brick</p> <p>Analytical Properties</p> <table border="1"> <tr><td>Heat Transfer Coefficient (U)</td><td>2.5675 W/(m²·K)</td></tr> <tr><td>Thermal Resistance (R)</td><td>2.2116 (h·ft²·°F)/BTU</td></tr> <tr><td>Thermal mass</td><td>10.2214 kJ/K</td></tr> <tr><td>Absorptance</td><td>0.700000</td></tr> <tr><td>Roughness</td><td>3</td></tr> <tr><td>Thermal Conductivity</td><td>0.2700 W/(m·K)</td></tr> <tr><td>Specific Heat</td><td>840.0000 J/(kg·°C)</td></tr> <tr><td>Density</td><td>950.00 kg/m³</td></tr> </table>  <p>Double glazing SC=0.3</p> <p>Analytical Properties</p> <table border="1"> <tr><td>Visual Light Transmittance</td><td>0.270000</td></tr> <tr><td>Solar Heat Gain Coefficient</td><td>0.290000</td></tr> <tr><td>Heat Transfer Coefficient (U)</td><td>3.1292 W/(m²·K)</td></tr> <tr><td>Analytic Construction</td><td>Double glazing domestic SC=0.3</td></tr> <tr><td>Thermal Resistance (R)</td><td>1.8146 (h·ft²·°F)/BTU</td></tr> </table>	Heat Transfer Coefficient (U)	2.5675 W/(m ² ·K)	Thermal Resistance (R)	2.2116 (h·ft ² ·°F)/BTU	Thermal mass	10.2214 kJ/K	Absorptance	0.700000	Roughness	3	Thermal Conductivity	0.2700 W/(m·K)	Specific Heat	840.0000 J/(kg·°C)	Density	950.00 kg/m ³	Visual Light Transmittance	0.270000	Solar Heat Gain Coefficient	0.290000	Heat Transfer Coefficient (U)	3.1292 W/(m ² ·K)	Analytic Construction	Double glazing domestic SC=0.3	Thermal Resistance (R)	1.8146 (h·ft ² ·°F)/BTU	2.567	3.129	0.29	0.3	41.98	23.16	34.13
Heat Transfer Coefficient (U)	2.5675 W/(m ² ·K)																																	
Thermal Resistance (R)	2.2116 (h·ft ² ·°F)/BTU																																	
Thermal mass	10.2214 kJ/K																																	
Absorptance	0.700000																																	
Roughness	3																																	
Thermal Conductivity	0.2700 W/(m·K)																																	
Specific Heat	840.0000 J/(kg·°C)																																	
Density	950.00 kg/m ³																																	
Visual Light Transmittance	0.270000																																	
Solar Heat Gain Coefficient	0.290000																																	
Heat Transfer Coefficient (U)	3.1292 W/(m ² ·K)																																	
Analytic Construction	Double glazing domestic SC=0.3																																	
Thermal Resistance (R)	1.8146 (h·ft ² ·°F)/BTU																																	
H	 <p>Lightweight brick</p> <p>Analytical Properties</p> <table border="1"> <tr><td>Heat Transfer Coefficient (U)</td><td>2.5675 W/(m²·K)</td></tr> <tr><td>Thermal Resistance (R)</td><td>2.2116 (h·ft²·°F)/BTU</td></tr> <tr><td>Thermal mass</td><td>10.2214 kJ/K</td></tr> <tr><td>Absorptance</td><td>0.700000</td></tr> <tr><td>Roughness</td><td>3</td></tr> <tr><td>Thermal Conductivity</td><td>0.2700 W/(m·K)</td></tr> <tr><td>Specific Heat</td><td>840.0000 J/(kg·°C)</td></tr> <tr><td>Density</td><td>950.00 kg/m³</td></tr> </table>  <p>Low-E double glazing SC=0.3</p> <p>Analytical Properties</p> <table border="1"> <tr><td>Visual Light Transmittance</td><td>0.570000</td></tr> <tr><td>Solar Heat Gain Coefficient</td><td>0.310000</td></tr> <tr><td>Heat Transfer Coefficient (U)</td><td>2.1030 W/(m²·K)</td></tr> <tr><td>Analytic Construction</td><td>Low-E double glazing SC=0.3</td></tr> <tr><td>Thermal Resistance (R)</td><td>2.7001 (h·ft²·°F)/BTU</td></tr> </table>	Heat Transfer Coefficient (U)	2.5675 W/(m ² ·K)	Thermal Resistance (R)	2.2116 (h·ft ² ·°F)/BTU	Thermal mass	10.2214 kJ/K	Absorptance	0.700000	Roughness	3	Thermal Conductivity	0.2700 W/(m·K)	Specific Heat	840.0000 J/(kg·°C)	Density	950.00 kg/m ³	Visual Light Transmittance	0.570000	Solar Heat Gain Coefficient	0.310000	Heat Transfer Coefficient (U)	2.1030 W/(m ² ·K)	Analytic Construction	Low-E double glazing SC=0.3	Thermal Resistance (R)	2.7001 (h·ft ² ·°F)/BTU	2.567	2.103	0.31	0.3	41.02	23.29	21.52
Heat Transfer Coefficient (U)	2.5675 W/(m ² ·K)																																	
Thermal Resistance (R)	2.2116 (h·ft ² ·°F)/BTU																																	
Thermal mass	10.2214 kJ/K																																	
Absorptance	0.700000																																	
Roughness	3																																	
Thermal Conductivity	0.2700 W/(m·K)																																	
Specific Heat	840.0000 J/(kg·°C)																																	
Density	950.00 kg/m ³																																	
Visual Light Transmittance	0.570000																																	
Solar Heat Gain Coefficient	0.310000																																	
Heat Transfer Coefficient (U)	2.1030 W/(m ² ·K)																																	
Analytic Construction	Low-E double glazing SC=0.3																																	
Thermal Resistance (R)	2.7001 (h·ft ² ·°F)/BTU																																	

Material layers	Material properties	Total OTTV _{wall} (W/m ²)																															
		U _{wall}	U _{glass}	SHGC																													
Scenario (2) Lowering windows' U-value, SC, and SHGC (continue)		Thailand	Hong Kong	Singapore																													
 <div style="display: flex; justify-content: space-between;"> <div style="width: 45%;"> Lightweight brick <p>Analytical Properties</p> <table border="1"> <tr><td>Heat Transfer Coefficient (U)</td><td>2.5675 W/(m²·K)</td></tr> <tr><td>Thermal Resistance (R)</td><td>2.2116 (h·ft²·°F)/BTU</td></tr> <tr><td>Thermal mass</td><td>10.2214 kJ/K</td></tr> <tr><td>Absorptance</td><td>0.700000</td></tr> <tr><td>Roughness</td><td>3</td></tr> <tr><td>Thermal Conductivity</td><td>0.2700 W/(m·K)</td></tr> <tr><td>Specific Heat</td><td>840.0000 J/(kg·°C)</td></tr> <tr><td>Density</td><td>950.00 kg/m³</td></tr> </table> </div> <div style="width: 45%;"> Double glazing SC=0.2 <p>Analytical Properties</p> <table border="1"> <tr><td>Visual Light Transmittance</td><td>0.180000</td></tr> <tr><td>Solar Heat Gain Coefficient</td><td>0.210000</td></tr> <tr><td>Heat Transfer Coefficient (U)</td><td>3.1292 W/(m²·K)</td></tr> <tr><td>Analytic Construction</td><td>Double glazing domestic SC=0.2</td></tr> <tr><td>Thermal Resistance (R)</td><td>1.8146 (h·ft²·°F)/BTU</td></tr> </table> </div> </div>	Heat Transfer Coefficient (U)	2.5675 W/(m ² ·K)	Thermal Resistance (R)	2.2116 (h·ft ² ·°F)/BTU	Thermal mass	10.2214 kJ/K	Absorptance	0.700000	Roughness	3	Thermal Conductivity	0.2700 W/(m·K)	Specific Heat	840.0000 J/(kg·°C)	Density	950.00 kg/m ³	Visual Light Transmittance	0.180000	Solar Heat Gain Coefficient	0.210000	Heat Transfer Coefficient (U)	3.1292 W/(m ² ·K)	Analytic Construction	Double glazing domestic SC=0.2	Thermal Resistance (R)	1.8146 (h·ft ² ·°F)/BTU	2.567	3.129	0.21	0.3	35.51	19.84	16.91
Heat Transfer Coefficient (U)	2.5675 W/(m ² ·K)																																
Thermal Resistance (R)	2.2116 (h·ft ² ·°F)/BTU																																
Thermal mass	10.2214 kJ/K																																
Absorptance	0.700000																																
Roughness	3																																
Thermal Conductivity	0.2700 W/(m·K)																																
Specific Heat	840.0000 J/(kg·°C)																																
Density	950.00 kg/m ³																																
Visual Light Transmittance	0.180000																																
Solar Heat Gain Coefficient	0.210000																																
Heat Transfer Coefficient (U)	3.1292 W/(m ² ·K)																																
Analytic Construction	Double glazing domestic SC=0.2																																
Thermal Resistance (R)	1.8146 (h·ft ² ·°F)/BTU																																
Scenario (3) Reducing the gross glazing area facing South/North		Thailand	Hong Kong	Singapore																													
 <div style="display: flex; justify-content: space-between;"> <div style="width: 45%;"> Common brick <p>Analytical Properties</p> <table border="1"> <tr><td>Heat Transfer Coefficient (U)</td><td>4.8946 W/(m²·K)</td></tr> <tr><td>Thermal Resistance (R)</td><td>1.1601 (h·ft²·°F)/BTU</td></tr> <tr><td>Thermal mass</td><td>14.9037 kJ/K</td></tr> <tr><td>Absorptance</td><td>0.700000</td></tr> <tr><td>Roughness</td><td>3</td></tr> <tr><td>Thermal Conductivity</td><td>0.5400 W/(m·K)</td></tr> <tr><td>Specific Heat</td><td>840.0000 J/(kg·°C)</td></tr> <tr><td>Density</td><td>1,550.00 kg/m³</td></tr> </table> </div> <div style="width: 45%;"> Double glazing SC=0.2 <p>Analytical Properties</p> <table border="1"> <tr><td>Visual Light Transmittance</td><td>0.180000</td></tr> <tr><td>Solar Heat Gain Coefficient</td><td>0.210000</td></tr> <tr><td>Heat Transfer Coefficient (U)</td><td>3.1292 W/(m²·K)</td></tr> <tr><td>Analytic Construction</td><td>Double glazing domestic SC=0.2</td></tr> <tr><td>Thermal Resistance (R)</td><td>1.8146 (h·ft²·°F)/BTU</td></tr> </table> </div> </div>	Heat Transfer Coefficient (U)	4.8946 W/(m ² ·K)	Thermal Resistance (R)	1.1601 (h·ft ² ·°F)/BTU	Thermal mass	14.9037 kJ/K	Absorptance	0.700000	Roughness	3	Thermal Conductivity	0.5400 W/(m·K)	Specific Heat	840.0000 J/(kg·°C)	Density	1,550.00 kg/m ³	Visual Light Transmittance	0.180000	Solar Heat Gain Coefficient	0.210000	Heat Transfer Coefficient (U)	3.1292 W/(m ² ·K)	Analytic Construction	Double glazing domestic SC=0.2	Thermal Resistance (R)	1.8146 (h·ft ² ·°F)/BTU	4.894	3.129	0.21	0.2	40.45	28.92	41.78
Heat Transfer Coefficient (U)	4.8946 W/(m ² ·K)																																
Thermal Resistance (R)	1.1601 (h·ft ² ·°F)/BTU																																
Thermal mass	14.9037 kJ/K																																
Absorptance	0.700000																																
Roughness	3																																
Thermal Conductivity	0.5400 W/(m·K)																																
Specific Heat	840.0000 J/(kg·°C)																																
Density	1,550.00 kg/m ³																																
Visual Light Transmittance	0.180000																																
Solar Heat Gain Coefficient	0.210000																																
Heat Transfer Coefficient (U)	3.1292 W/(m ² ·K)																																
Analytic Construction	Double glazing domestic SC=0.2																																
Thermal Resistance (R)	1.8146 (h·ft ² ·°F)/BTU																																

Material layers	Material properties				Total OTTV _{wall} (W/m ²)		
	U _{wall}	U _{glass}	SHGC	SC _{glass}	Thailand	Hong Kong	Singapore
Scenario (3) Reducing the gross glazing area facing South/North (continue)	2.567	3.129	0.21	0.2	33.28	19.55	28.03

K

Lightweight brick

Analytical Properties

- Heat Transfer Coefficient (U) 2.5675 W/(m².K)
- Thermal Resistance (R) 2.2116 (h·ft²·°F)/BTU
- Thermal mass 10.2214 kJ/K
- Absorptance 0.700000
- Roughness 3
- Thermal Conductivity 0.2700 W/(m·K)
- Specific Heat 840.0000 J/(kg·°C)
- Density 950.00 kg/m³

Double glazing SC=0.2

Analytical Properties

- Visual Light Transmittance 0.180000
- Solar Heat Gain Coefficient 0.210000
- Heat Transfer Coefficient (U) 3.1292 W/(m².K)
- Analytic Construction Double glazing domestic SC=0.2
- Thermal Resistance (R) 1.8146 (h·ft²·°F)/BTU

View: Floor Plan, Modify, etc.

5.8 Discussion

The results of the validation scenarios provide new insights that expand the understanding of how to extract the BIM database in order to evaluate the overall thermal performance of building envelopes, especially for nonresidential buildings. The BOTTVC system enables a holistic overview of the OTTV and feedback for building envelope design through the thermal and physical properties available in the BIM database. This provides a robust system not only to measure the OTTV but also to access other variables that are involved in energy code compliance (e.g., the U-value and R-value). Compared with traditional methods of calculating OTTVs (e.g., manual calculation and Excel spreadsheets), the proposed system provides more efficient design feedback via visual programming, which calculates OTTV quickly, evaluates design options, and provides explicit decision support regarding future designs by clearly determining an appropriate combination of building materials. The calculation times for using the BOTTVC system and manual calculation were compared. The calculation time using the BOTTVC system was decreased by 80% in our case study. The OTTV manual calculation required up to approximately two hours to calculate the coefficients (e.g., the U-value, R-value, TDeq, SC, and WWR) for a single design option, whereas the BOTTVC required approximately 20 to 30 min to access and extract data from BIM and perform OTTV calculation for several design options.

The BOTTVC system was tested using a typical office building on the basis of the context of OTTV code for Thailand, Hong Kong, and Singapore. However, other types of buildings can be easily evaluated using this system. The challenge in developing the BOTTVC system is to extract of various coefficients for materials from the BIM database and to establish a novel graphical scripting for accessing thermal properties that are not available in the current BIM's visual programming in order to facilitate the calculation of some coefficients concerned with the OTTV calculation. The findings of the validation study are summarized as follows:

- Although the BOTTVC system provides an ability to simultaneously calculate the total OTTV, some constant coefficient values required for some countries (e.g., ΔT , SF, and ESR) must be manually defined to be read from a spreadsheet file. Gathering such coefficients in the BIM authoring software enables users to directly retrieve from the BIM database, thus solving this problem.
- The proposed system provides a flexible and easy approach for the calculation of an OTTV, not only for buildings with a rectangular layout but also for buildings of any complex shape.
- The visual scripting feature in BOTTVC can be modified to suit the requirements of OTTV equations in different countries.
- With the help of BIM's visual programming, automated checking and accessing the attributes of BIM objects are allowed. Therefore, assessment and comparison of the impacts of different building enclosures' thermal properties on the overall heat transfer are more effective in the process of building envelope material selection during the design stage.

- Semi-automated extraction of the BIM database is available through the combination of manual data entry by selecting target objects and automatic derivation of the required information for calculating an OTTV.
- The extraction framework provides a method to check not only the requirements of the OTTV, but also other thermal indices, such as the U-value and R-value, which are the thermal performance factors for other building codes and building standards such as ASHRAE 90.1, IECC, BR15, BBR, and EnEv (described in Section 2.6.2).
- In order to evaluate the influence of different values of density and solar absorptivity of the building envelope on the building's energy demand, simulating different types of envelope materials using building energy simulation software should be integrated into the system.
- The thermal characteristics of the building envelope were considered in calculating the overall thermal transfer value in the proposed system. However, methods to include other factors that can be directly obtained from BIM (e.g., occupancy, building form, lighting and mechanical system design), which influence the energy efficient design, should be developed.
- Although OTTV standards have been established and employed in many countries in Southeast Asia, the calculation methods for quantifying OTTVs and variables required for OTTV equations vary depending on the climate conditions and code of practice given by local governments in different countries (e.g., TDeq, ESR, and SF), which can be a major barrier in analyzing thermal transfer through building envelope in an international design community.
- Shading from surroundings (e.g., vegetation and mountains) and nearby structures (e.g., buildings) should be included in the OTTV calculation and the proposed system.

5.9 Chapter conclusions

In this chapter, a method is developed to access the thermal and physical properties of the BIM model elements in order to extract information for calculating the OTTV and reviewing building envelope designs to ensure compliance with OTTV codes during the design process. The use of a visual programming interface for BIM plays a particularly important role in accessing the rich information stored in the BIM model.

The development comprised two major phases; (1) identifying specific coefficients for OTTV calculation by referring to the standard guiding tools, and (2) developing a BOTTVC system using a BIM visual programming interface (i.e., Dynamo). The first phase was divided into two main steps as follows: (1) reviewing prescriptive criteria and requirements of the OTTV codes in various countries and (2) categorizing all relevant coefficients to determine which target coefficients of a building material can be extracted from the BIM database. The second phase is to develop the BOTTVC system and is divided into five main steps: (1) creating a BIM model; (2) developing visual scripting in order

to connect and transfer the BIM database into our proposed system; (3) extracting material coefficients from the BIM thermal properties database (e.g., the U-value, R-value, SHGC, heat capacity, and specific heat), and calculating other variables involved in the OTTV equation (e.g., WWR, skylight to roof ratio, SC, roof orientation factor, and equivalent temperature difference for opaque wall); (4) gathering all relevant coefficients in order to automatically compute the OTTV value; and (5) evaluating the performance of building envelopes.

The BOTTVC system provides a flexible approach to manipulate input data to calculate the OTTV under the various methods for different countries. The proposed method was validated in a typical office building with a rectangular plan. The validation of the BOTTVC system was performed with respect to the different OTTV calculation methods of three countries in Southeast Asia (Thailand, Hong Kong, and Singapore) that employ the OTTV as a mandatory requirement for building energy-efficiency codes. Our initial results revealed that the system can successfully acquire information from the BIM database. The BOTTVC system provides an acceptable thermal performance value for a design by comparing multiple material setups. The prototype system provides a tool for predetermining thermal properties of the construction material of building envelopes in order to help design stakeholders in making decisions regarding selecting envelope materials with respect to OTTV building regulations.

Chapter 6 Integrating BIM and VR development engines for building indoor lighting design

6.1 Introduction

This chapter investigates a new method that uses BIM, game engines, and VR to facilitate lighting designs and lighting energy performance analysis via an immersive and interactive user experience. In this chapter, a method is proposed and BLDF prototype system is developed for realistic visualization of lighting conditions and the calculation of energy consumption with a user-friendly interface using an interactive and immersive VR environment. BLDF provides qualitative and quantitative outputs related to lighting designs. The BIM database and scripting features of the game engine are used to create a robust prototype system that performs fast calculation and image rendering. The developed system utilizes an interactive and immersive VR environment to simulate daylighting and the illumination of artificial lights in buildings, and it visualizes realistic VR scenes using HMDs. BLDF allows users to interact with design objects, to change them, and to compare multiple design scenarios and it provides real-time lighting quality and energy consumption feedback. VR technology enables designers to perceive realistic lighting scenes in their designs. Tools such as Autodesk Revit, and Unreal Engine, and its scripting environment are used in our system to create an interactive environment that allows changing and visualizing lighting scenes and to facilitate the comparison of different design scenarios in our experiments.

The objectives of this chapter are: (1) to investigate a method by which to use serious game simulations for lighting design visualization and performance analysis; (2) to develop a prototype system with a user friendly interface, which integrates BIM and a game engine to support lighting designers in identifying the optimal design parameters; (3) to investigate the applicability of the system for assessing lighting design factors, such as visual comfort, energy consumption, and lighting performance; and (4) to validate the proposed method and assess the performance of the developed tool using a real-world case study.

6.2 Development of the BLDF system

Autodesk Revit (Autodesk, 2016d), 3ds Max (Autodesk, 2016a), Unreal Engine (Epic Games, 2016) with its scripting feature, and the visual programming in Dynamo (Dynamo, 2016) are used to develop the BLDF system. The built-in lighting feature in Unreal Engine 4 uses physically based shading, in which the lighting and shading algorithms approximate the physical interaction between light and materials (Walker, 2014). For example, light intensity in lumens falls off at a rate that follows the inverse square law (Bruneton et al., 2008). BLDF system uses the built-in lighting algorithm in Unreal Engine to generate lighting scenes in a virtual environment. To simulate daylighting, Unreal Engine 4 uses Bruneton sky model, which is an accurate method to simulate skylight in real-time, and considers effects of light scattering, such as Rayleigh and Mie multiple scattering (Bruneton et al., 2008). Precomputed lighting feature in Unreal Engine is available for evaluating the lighting results at runtime. Ray Traced Distance Field is the rendering technique used in Unreal Engine 4 (Ray Traced Distance Field Soft Shadows, 2017).

BIM-based lighting design feedback is a system for visualizing lighting design using VR technology. This system provides two types of game views: first-person and birds-eye views. In the first-person view, an HMD can be used. The HMD responds to the motion and rotation of the user's head and provides a lifelike lighting experience in game scenes. A first-person view is also suitable for perceiving phenomena caused by excessive luminance in the field of view (FOV), e.g., glare. A birds-eye view (or top-down view) is provided in order to clarify the overall setup of the environment and the position of the player when they are moving in the game environment. Realistic scenes and false-color scenes are two types of visualization outputs of the BLDF system. The system calculates the amount of illuminance and generates real-time false-color visualizations. Moreover, the system helps to verify the illuminance level of the design area. A mouse and a keyboard are used as input devices to help users to navigate in the first-person view, and to change parameters.

6.2.1 BLDF system user interface components and supported interactions

The prototype system supports interactivity with which users can experiment and adjust lighting design parameters in real-time. The following interactions are supported: (a) *First-person movement*: to control the movement of users' avatars as they walk in the space; (b) *User interface control*: to customize parameters such as time (to observe the dynamic of sunlight), lighting fixtures, types, orientation, intensity, and color temperature of the bulbs, as well as the location of furniture. Unreal Motion Graphics (UMG), a visual user interface in Unreal Engine, is used to create various GUI elements in the BLDF system. The GUI interface of the proposed system is shown in Figure 33. The menus of the game environment enable players to change parameters and freely navigate among game objects using input controllers. The following widgets are created, as shown in Figure 33: (a) *Plan view*: to show the layout of furniture and the position of the user. Users can switch between false-color view and realistic

views; (b) *Shading devices menu*: to change the type of shading for windows; (c) *Material types menu*: to change the materials of indoor surfaces; (d) *Time slider*: to set time for adjusting the daylight; (e, f) *Light switches*: to turn on/off individual artificial lights; (g) *Lighting intensity menu*: to change the intensity of light sources; (h) *Color temperature control*: to change the color of lights; (i) *Lighting fixture types menu*: to choose the type of lighting fixtures; (j) *Moving and rotation tools*: to move and rotate the light source, lighting fixtures, and furniture; (k) *Lighting illuminance legend*: to help measure the illuminance level (for false-color views); (l) *Total energy usage*: to display the total lighting energy consumption of the room; (m) *Compass*: to show the orientation of users when moving; (n) *Lighting occupancy sensor*: to switch lights on/off when the space is occupied and unoccupied; (o) *Task light*: to add individual light controls to each workstation.

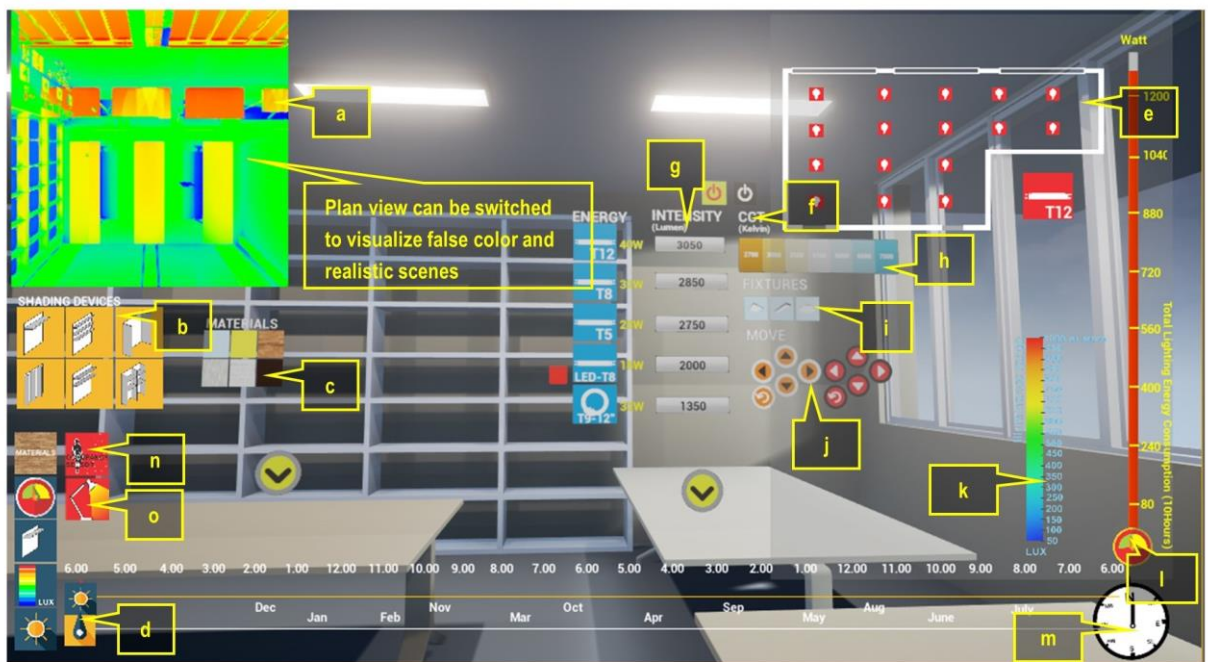


Figure 33 Screenshot of the main interface of the prototype BLDF system with all widgets visible

The global illumination algorithm in the Unreal Engine is used to automatically produce lighting illumination scenes and calculate detailed shadows at runtime. The scenes can also be visualized in false-color, which shows the illuminances at different levels in the scene. Red indicates an illuminance level that exceeds than 1000 lx, and dark blue indicates an illuminance level of less than 100 lx. The user can hide/unhide each widget on the viewport. A keyboard and mouse are used as input devices to change design parameters in the proposed system. A designer can change the light intensity (measured in lumens) and the color temperature of a light (measured in Kelvins) using associated widgets on the interface (Figures. 33g and h). Additional lighting equipment items are modeled in the BIM application and are added to the game environment as an alternative equipment repository. However, it is possible to import libraries of lighting elements from the BIM application into the game engine. After adding

items to the equipment repository, new types of lighting equipment are shown on the interface (Figure 33i). The material and texture of indoor envelopes, e.g., the floor, walls, and ceiling, can be modified using the developed widget (Figure 33c).

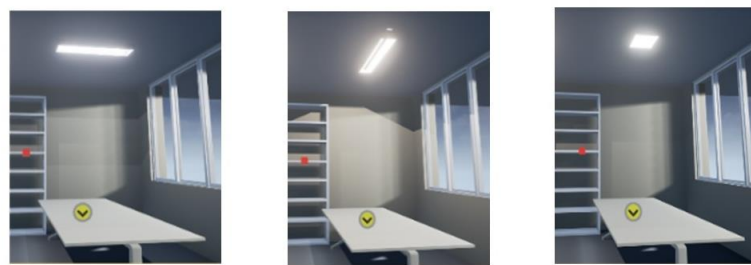
Ambient lights can be switched on/off using the light switch panel (Figure 33e). The system provides the ability to set up lighting zones when lighting control per zone is required. An additional option for lighting control is the lighting occupancy sensor, which automatically controls ambient lights and task lights (Figures. 33n and o) in the BLDF system. In order to implement occupancy sensing, the Box Trigger tool and visual scripting of Unreal Engine are used. The lights will automatically turn on when the user walks into a specific zone and automatically turn off when the specific zone is vacated.

The total energy consumption of lighting equipment is shown in the energy consumption bar. A simple lighting energy calculation formula is used to calculate lighting energy in watts (number of fixtures \times light power (W) = total consumption). The system also provides an interface to enter the time and date for adjusting the daylight duration (Figure 33d). In order to simulate sunlight, directional light is added as an actor in the game environment, and visual scripting is used to automatically control the yaw and pitch of the sun and to control the position of the sun based on the time and the season.

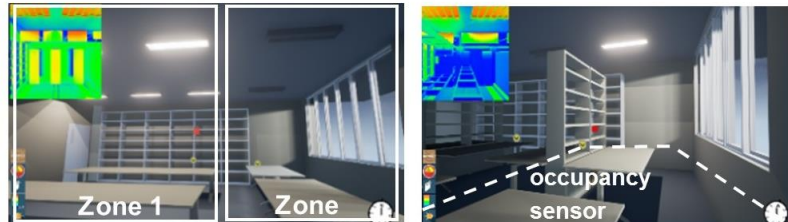
Alternatives for shading devices, e.g., horizontal panel, horizontal multiple blades, vertical fin, slanted vertical fin, and egg crate (Figure 33b), are provided in the system. Shading device models are created in BIM and are imported into the game environment as an alternative equipment repository. Users can compare the influence of shading devices on indoor lighting. The illuminance range legend (Figure 33k) is used to identify the illuminance values, and the compass (Figure 33m) helps to identify the orientation. Figure 33a shows a false-color visualization, which helps designers to preview the amount of illuminance. The sample visualizations in Figure 34 show the results of various simulations when parameters are changed using the developed widgets.



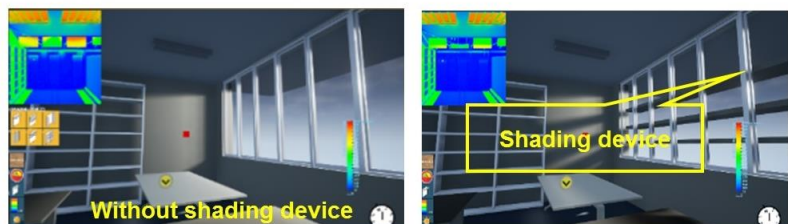
(a) Changing lighting intensity and color temperature (Figs. 33g and 33h)



(b) Changing the position and type of lighting equipment (Figs. 33i and 33j)



(c) Lighting switch panel and occupancy sensor (Figs. 33e and o)



(d) Adding shading devices (Fig. 33b)



(e) Changing material (Fig. 33c)



(f) Adding task light (Fig. 33o)

Figure 34 Sample visualizations using BLDF's GUI

6.2.2 BLDF's usage process flow

The usage process flow of the BLDF system (as shown in Figure 35) is as follows: (a) The BIM model is created in Autodesk Revit, in which the geometry and material properties of building elements are modeled; (b) A static mesh is created after exporting the FBX file from Revit to 3ds Max; (c) A 3D geometry in the game environment is automatically created after importing the FBX file of the BIM model into Unreal Engine. Due to interoperability issues between the current versions of applications, although the geometry information of the building elements and lighting equipment are successfully imported into Unreal Engine, some of their properties, such as color/textures and lighting properties, are not transferred; (d) Light bulbs and their properties (e.g., intensity and color temperature) are manually added to the game engine. In addition, the orientation, the scale of the building, and the color and textures of interior envelopes are manually configured in the game environment; (e) Lighting parameters, such as intensity, color temperature, position of lighting equipment, and interior materials, are configured using the GUI (as explained in Subsection 6.2.1); (f) The simulation is executed, which enables users to immediately view quantitative results (e.g., energy consumption) and visualizations; (g) The user analyzes the lighting design outputs; (h) If the results are satisfactory, the game parameters are saved and a text file is generated; (i) The final design information parameters, such as lighting intensities, color temperatures, and positions of fixtures and bulbs are updated in the BIM using visual programming in Dynamo (explained in Subsection 6.2.3); (j) The BIM model is saved with the updated parameters. The user can set new parameters and run simulations until a satisfactory design is achieved. Realistic scenes with walk-through capability support qualitative assessment and the false-color scenes support quantitative assessment. The system is used in design meetings to facilitate discussions between designers and clients.

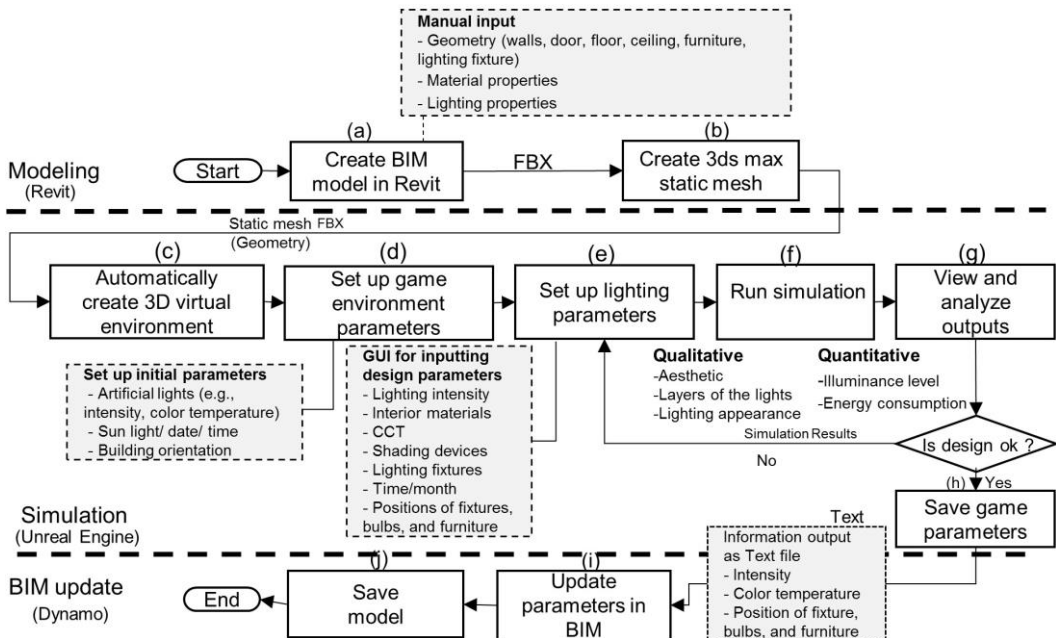


Figure 35 BLDF's usage process flow

6.2.3 Updating BIM with new design parameters

Dynamo (Autodesk, 2016b) visual programming is used to update new design parameters in the BIM application. Figure 36 shows the process flow of updating the design parameters in BIM. After finalizing parameters, such as intensity, color temperature, and fixture position for each individual light bulb, and the positions of furniture and shading devices, and the material types of interior envelopes, the new parameters are saved in a text file (Figure 36a). The developed visual script (Figure 36b) automatically updates the lighting properties in Autodesk Revit (Figure 36c) using unique IDs of model objects.

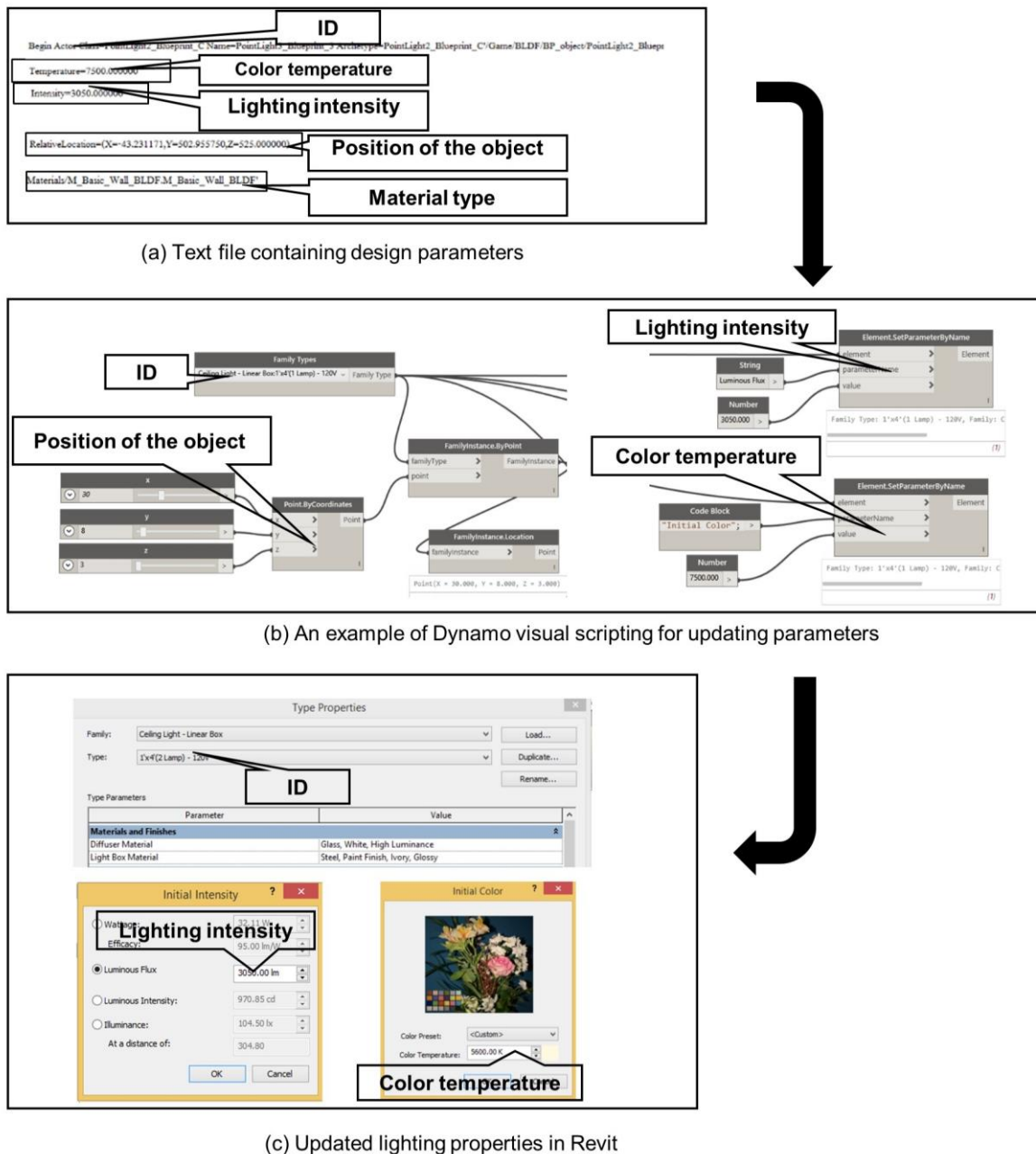


Figure 36 Updating the design parameters in BIM

6.3 System accuracy verification

An office on the fourth floor of the M3 building at Osaka University, Japan, was chosen as the area for the experiment. Figure 37 shows the actual room condition. The room has a typical rectangular shape (Figure 37a). First, a verification test was performed in order to evaluate the accuracy of the BLDF system. The verification test was performed in a section of the room shown in Figure 37b.

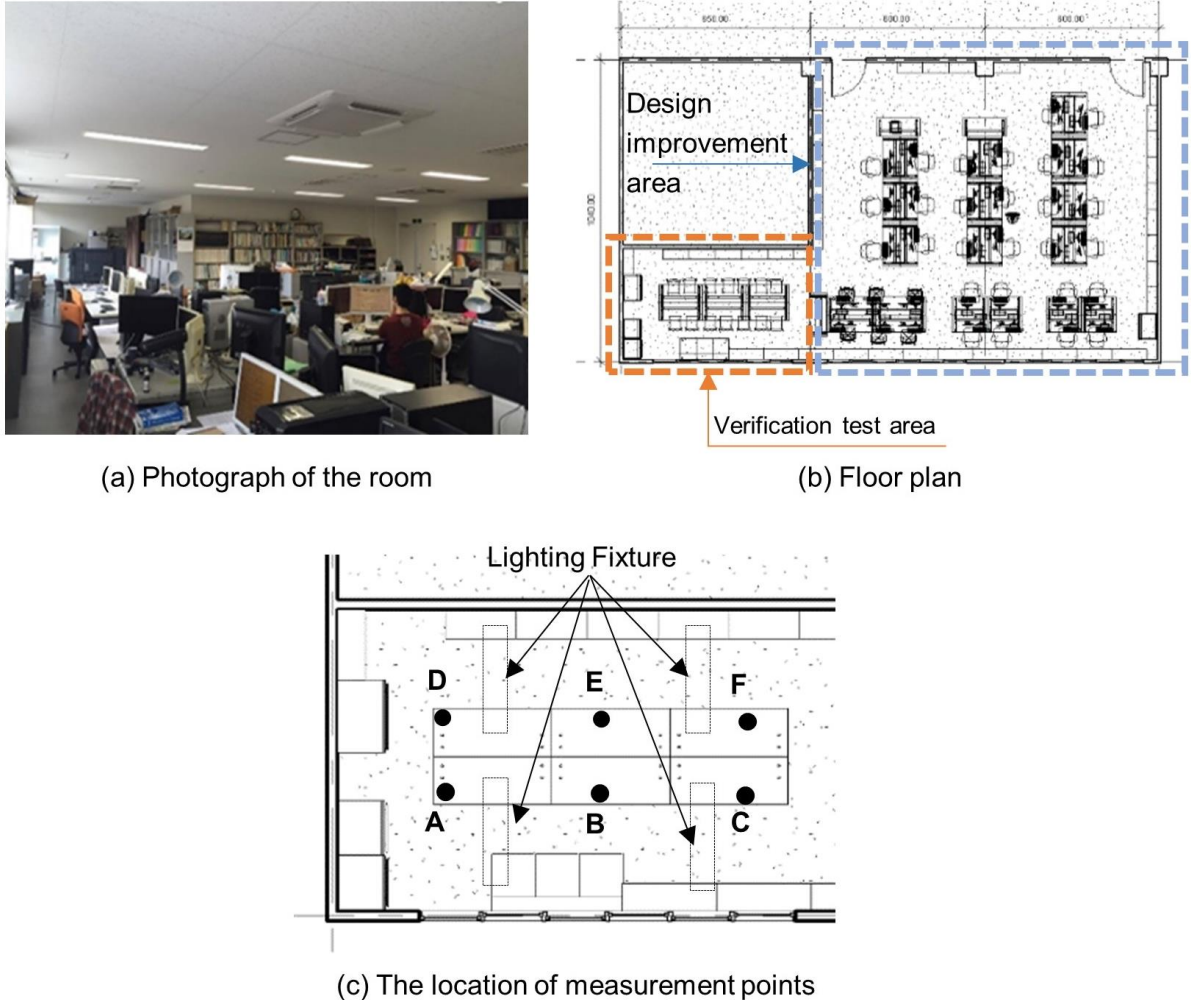


Figure 37 Actual room condition

In order to verify the accuracy of the lighting simulation outputs, lighting illumination levels calculated by the proposed system, those calculated by third-party lighting simulation software applications (i.e., Radiance and Lighting Analysis for 3ds Max) and the actual measured values using a light meter were compared. Radiance is a physically-based lighting simulation developed by Lawrence Berkeley National Laboratories in the U.S. In order to simulate lighting in Radiance, the building geometry information from Autodesk Revit is imported into Ecotect using gbXML file format to define an analysis grid, location of artificial lights, sky condition, and time. The model from Ecotect is then exported to Radiance to perform the lighting analysis. Radiance is a radiosity based lighting simulation

program and uses backward ray tracing to compute lighting values for a scene and store scene values (Ochoa et al., 2010).

In the verification test, the lighting intensity and color temperature of lamps were set based on their specifications with no obstacles between the lights and light measuring devices. The verification area (shown in Figure 37b) has four ceiling lighting fixtures with eight tubular fluorescent (T8) lamps of 32 W each (2850 lm, CCT 5000 K) (Figure 37c). The test was performed on the 23rd of August in Osaka, Japan, under a clear sky weather condition (Figure 38). The illuminance values were collected at 10:00 a.m. to evaluate the daylight (Figure 38a), at 10:10 a.m. in order to evaluate the combination of daylight and artificial lights (Figure 38b), and at 8.00 p.m. to evaluate only the artificial lights (Figure 38c).

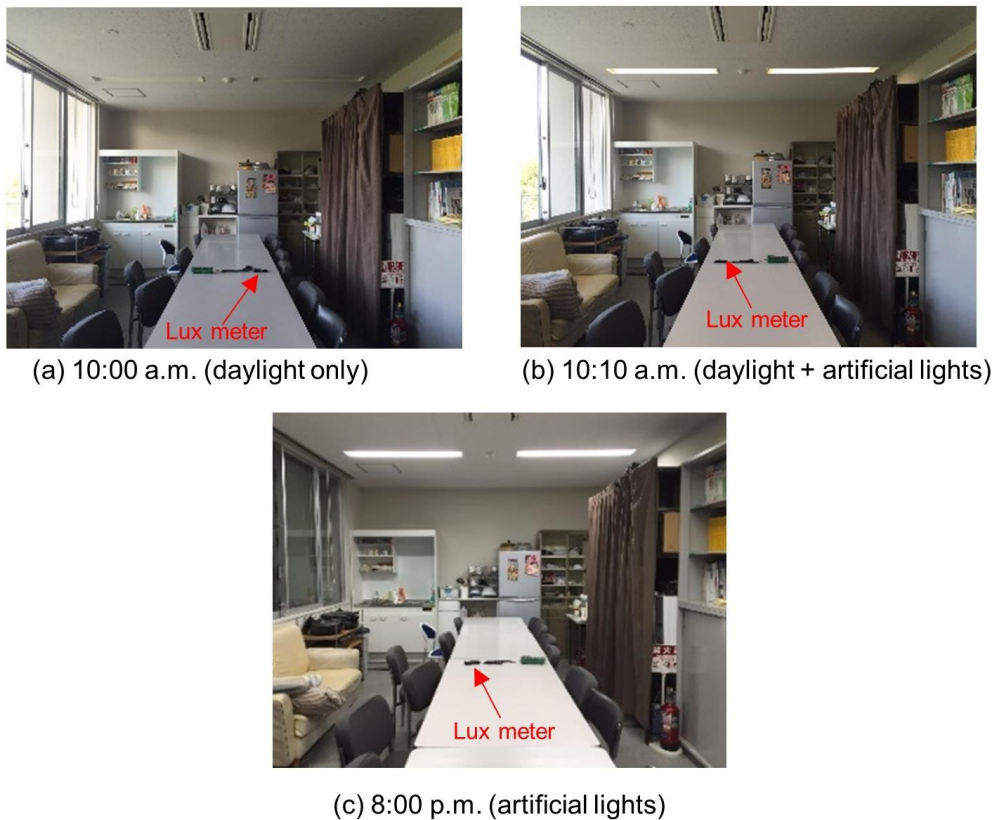


Figure 38 Conditions for the accuracy test

The illuminance values were measured at six locations on the tables shown in Figure 37c using a light meter (CEM DT-1308 light meter; accuracy: $\pm 5\%$) (Figure 38). The measurement results of the illuminance level on the table when the only lighting source is daylight are reported in Table 10(a). The results for the case of the combination of daylight and artificial lights are reported in Table 10(b), and the measured illuminance levels produced by artificial lights at night are reported in Table 10(c). The same scenarios were configured in the BLDF system, and the illuminance values were collected. Table 10 shows the data collected by light sensors, the BLDF simulation results, results of Lights Analysis

for 3ds Max, and results of Radiance. The false-color visualizations of BLDF simulation are shown in Figure 39.

Table 10 BLDF lighting simulations and results

Points	Illuminance levels (lux)		BLDF error	Illuminance levels (lux)	Radiance error	Illuminance levels (lux)	
	Sensor Reading	BLDF		Radiance		3ds Max	3ds Max error
10:00 a.m. (daylight)							
A	864	870	0.69 %	819.14	5.42%	789	8.68%
B	910	870	4.39 %	800.09	12.07%	868	4.61%
C	792	750	5.30 %	782.38	1.21%	767	3.15%
D	667	670	0.45 %	708.49	6.22%	940	40.92%
E	754	725	3.84 %	847.35	12.38%	662	12.20%
F	720	670	6.94 %	738.82	2.61%	711	1.25%
Average		3.61%		6.65%		11.80%	
10:10 a.m. (daylight + artificial lights)							
A	1203	>1000	-	1102.06	-	1064	-
B	1350	>1000	-	1175.67	-	1145	-
C	1012	950	6.12 %	982.36	2.92%	876	13.43%
D	895	900	0.55 %	952.15	6.85%	1234	37.87%
E	982	950	3.25 %	925.38	5.76%	951	3.15%
F	956	850	11.08 %	964.17	0.85%	824	13.80%
Average		5.25%		4.09%		17.06%	
(c) 8.00 p.m. (artificial lights)							
A	832	850	2.16 %	837.13	0.61%	732	12.01%
B	875	825	5.71 %	847.62	3.12%	774	11.54%
(c) 8.00 p.m. (artificial lights) (continue)							
C	768	750	2.34 %	750.20	2.31%	519	32.42%
D	822	850	3.40 %	833.16	1.35%	891	8.39%
E	844	850	0.71 %	845.58	0.18%	850	0.71%
F	722	750	3.87 %	747.89	3.58%	521	27.83%
Average		3.03%		1.85%		15.48%	

As shown in Table 10, in the case of daylighting simulation, the largest errors of the BLDF simulation, Radiance, and 3ds Max were 6.94, 12.38, and 40.92%, respectively. The average errors in the daylight simulation for the BLDF, Radiance and 3ds Max were 3.61, 6.65, and 11.80%, respectively. In the case of the combination of artificial lights and daylight, the largest absolute errors for the BLDF, Radiance and 3ds Max were 11.08, 6.85, and 37.87%, respectively. The BLDF system shows all values above 1000 lx with one color. Hence, an accurate comparison for points A and B, in this case, is not available. However, the average absolute errors for four other points (i.e., C, D, E, and F) were 5.25% for BLDF, 4.09% for Radiance, and 17.06% for 3ds Max. In addition, in the case of artificial light only, the maximum error of the BLDF system was 5.71%, whereas the maximum error of Radiance was 3.58%,

and 3ds Max was 32.42%. Furthermore, the average absolute error for artificial light was 3.03% for BLDF, 1.85% for Radiance, and 15.48% for 3ds Max. Fisher (1992) recommended an acceptable error range between measurements and simulation is 10% for average illuminance calculations and 20% for each measurement point. Therefore, the BLDF system provides a consistent level of accuracy similar to other lighting simulation systems and its accuracy similar to other lighting simulation systems and its accuracy values are within an acceptable range.

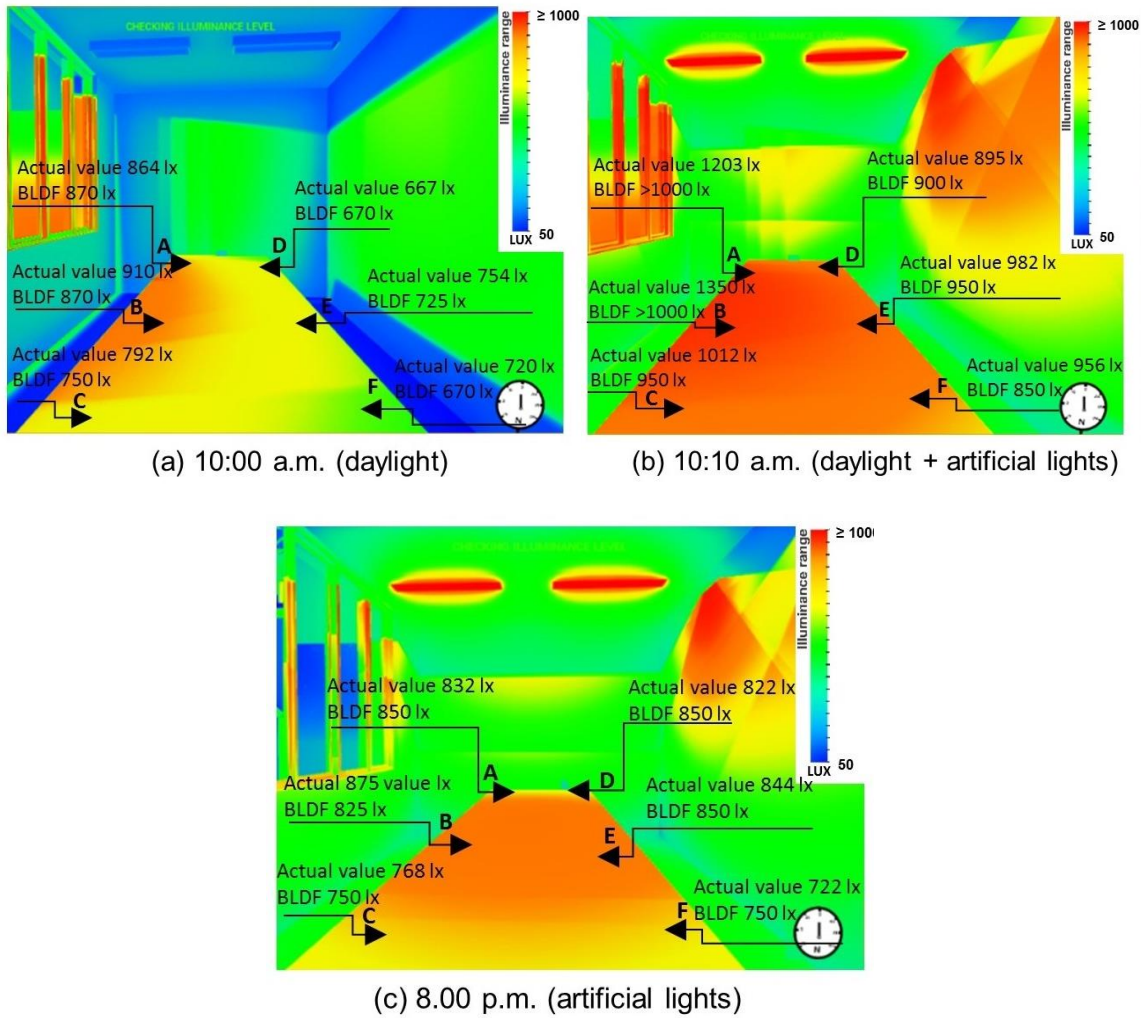


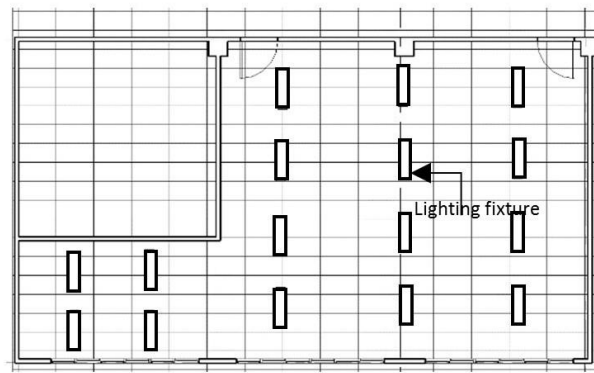
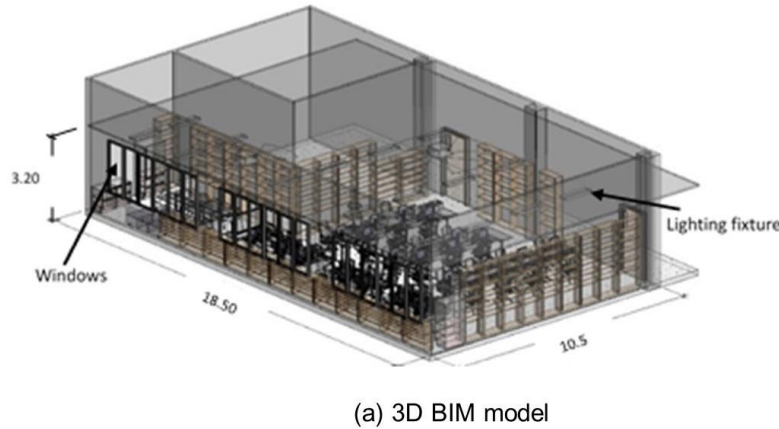
Figure 39 BLDF lighting simulations and the comparison of the results

6.4 Case study

6.4.1 BIM modeling and game engine integration

The case study was performed in an office at Osaka University, Japan. Figure 40 shows 3D BIM model and 2D plan of existing fixtures position of the case study room. The BIM model of the room was created using Autodesk Revit Architecture 2015 (Figure 40a). The BIM model contains details of the lighting system, and geometric and non-geometric information of components, e.g., building envelops and furniture. Lighting properties, such as the intensity and the color temperature, are configured based

on the specifications of the lamps. Figure 40b shows a 2D plan of existing lighting fixtures. The room has 16 lighting fixtures with 32 tubular fluorescent (T8) lamps of 32 W.



(b) Positions of lighting fixtures

Figure 40 3D BIM model and 2D plan of existing fixtures position of the case study room

The goal is to facilitate lighting design by allowing users to interact with the design and to perceive and experience the effects of the modifications simulated by the system. In order to integrate BIM with a game engine, the geometry information of building elements with their reference IDs are transferred from the BIM application (i.e., Revit) to the game engine (i.e., Unreal Engine). The BIM geometry data are transformed to a static mesh using 3ds Max. Figure 41 shows the process of transferring the model, in which the FBX file format is used to export the model from Revit into Unreal Engine. Regardless of the data export format, some important information, e.g., material textures, color temperature, and light intensity, is lost while exporting data to the game engine. The lost features must be redefined in the game environment.

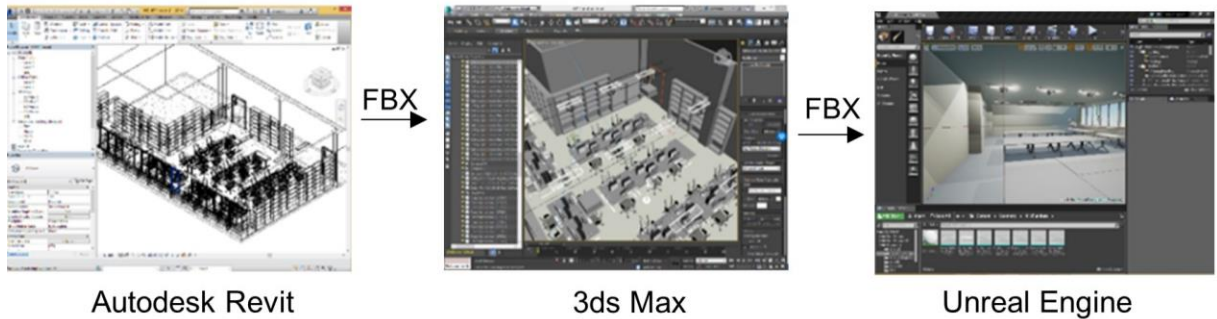


Figure 41 BIM model transfers to the game environment 3ds

6.4.2 Immersive VR for BLDF

In the experiment, users were invited to use the BLDF system with an HMD (Oculus Rift Kit 2, OLED display, 1920×1080 pixels per eye with 100° nominal field of view) to visualize the design through a first- person perspective. In the first-person perspective with an HMD, a mouse is used to interact with game objects and a keyboard is used to navigate in the virtual environment. The user can move the game objects and change the lighting design properties by clicking on the GUI buttons. The goal is to reduce the energy consumption while providing adequate illumination on desks in an aesthetically pleasant environment. In order to achieve this goal, the following six test cases were designed. The test cases are based on three fundamental aspects of lighting design of buildings: (1) evaluating the illuminance level, (2) calculating the energy consumption of the lighting system, and (3) visualizing lighting appearances.

Current design assessment

In order to evaluate the quality of artificial lights in the office zone, a simulation is performed in the daytime (8 a.m.) and at night (8 p.m.). This office zone has 12 lighting fixtures with 24 tubular fluorescent (T8) lamps of 32 W. The results revealed that the illuminance levels on desks were approximately 500 to 700 lx throughout the day. In the daytime, the illuminance levels on the desks that were close to the windows reached 800 to 900 lx. This confirmed that the current lighting condition of the office areas complied with the minimum standard of lighting design requirements (Figure 42).

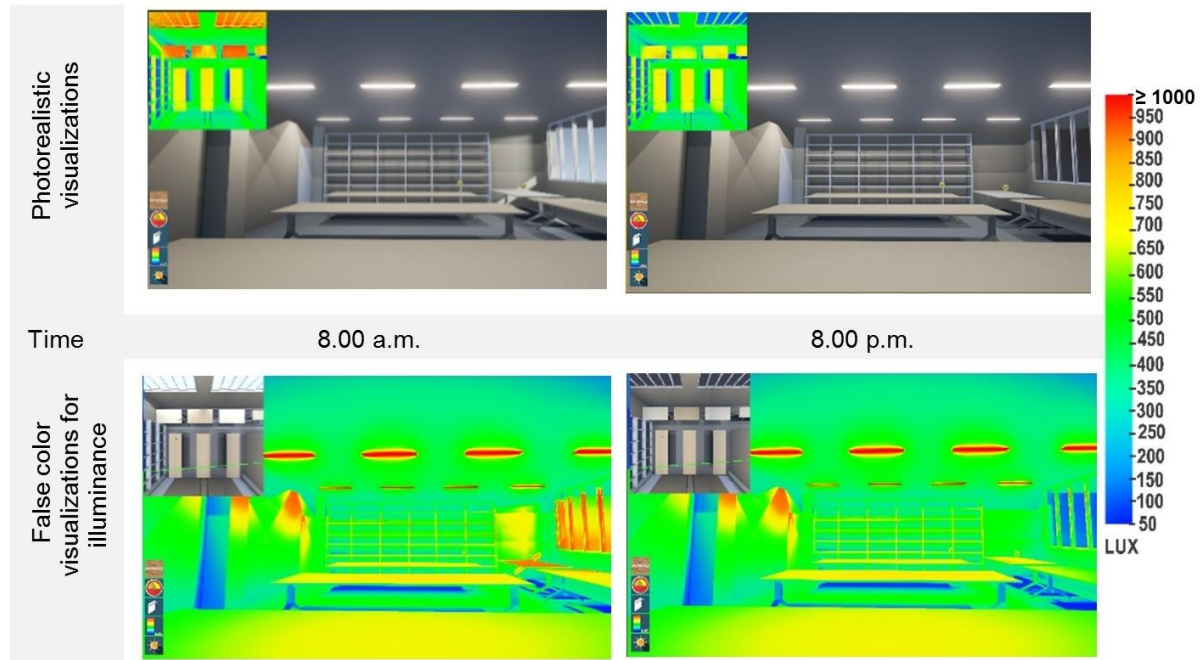


Figure 42 Lighting illumination level at daytime (left) and nighttime (right)

Daylight availability assessment

The amount of illumination on all desks from 8 a.m. to 4 p.m. for different scenarios was analyzed in the BLDF system. Figure 43 shows an example of daylighting illumination on the work desks at various times of day without using artificial lights. This shows that working desks in the windows zone still have sufficient illuminance. The working zone near the windows to a distance of approximately 4 m, can use daylight and does not require artificial light. The zone far from windows requires artificial light throughout the day.

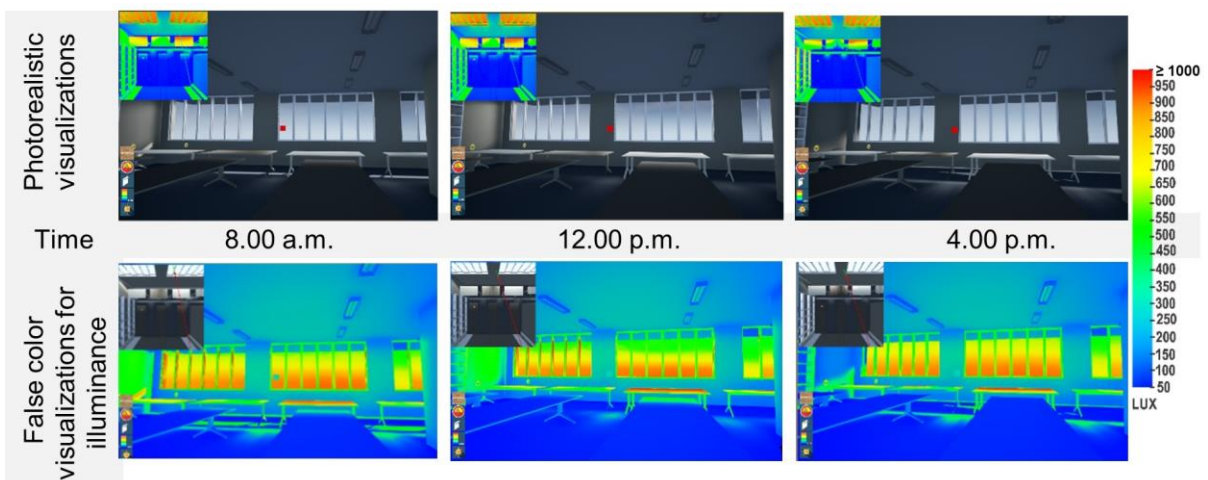


Figure 43 Examples of the illumination visualization outputs

Figure 44 shows lighting energy consumption of two setups in the daytime (8 a.m. to 4 p.m.): (1) all artificial lights are on; (2) lights close to the window are turned off. The results revealed that when all artificial lights are on, the lighting power usage is 1280 W and the energy consumption is 10.24 kWh. Moreover, the illuminance levels on the desks are approximately 700 to 800 lx. When lights for windows zone are switched off, the results revealed that the illuminance levels on the working desks in the windows zone are in the range of 450 to 650 lx, which is more than the minimum lighting requirement in the office (Shamsul, et al., 2013). In addition, the power usage of electric lights is 720 W, and the energy consumption is 5.76 kWh. In this experiment, by turning off the artificial lights in the windows zone (10 bulbs) from 8 a.m. to 4 p.m., lighting energy consumption can be reduced by 43.75%.

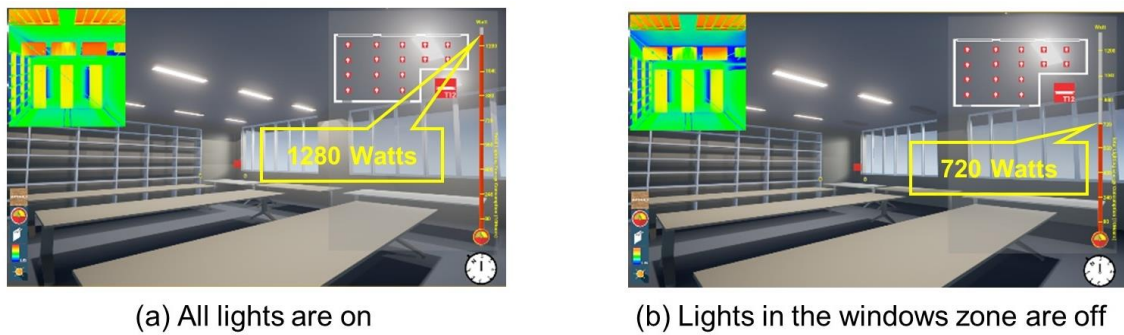


Figure 44 Lighting energy consumption for two scenarios

Lighting type design and assessment

The BLDF system shows the changes in the lighting power usage and lighting illuminance when different types of bulbs are used. In our case study, the illuminance levels and the power usage for three lamp alternatives, i.e., fluorescent T8 (32 W, 2850 lm), T5 (28 W, 2750 lm), and LED (T8) (15 W, 2000 lm) are compared when all artificial lights (32 bulbs) are turned on from 8 a.m. to 4 p.m. (Figure 45). The results show that the lighting power usages are 1024 W, 896 W, and 576 W, respectively. The total energy consumption when using T8, T5, and LED (T8) is 8.192 kWh, 7.168 kWh, and 4.536 kWh, respectively. Different illumination levels, i.e., approximately 760 lx (Figure 45a), 740 lx (Figure 45b), and 700 lx (Figure 45c), were generated at each work desk. In this experiment, LED lights provide more energy savings than T8 and T5 lights, at 35% and 25%, respectively. Adequate illuminance levels were generated by LED lights at every desk that satisfy the lighting standard for computer tasks.

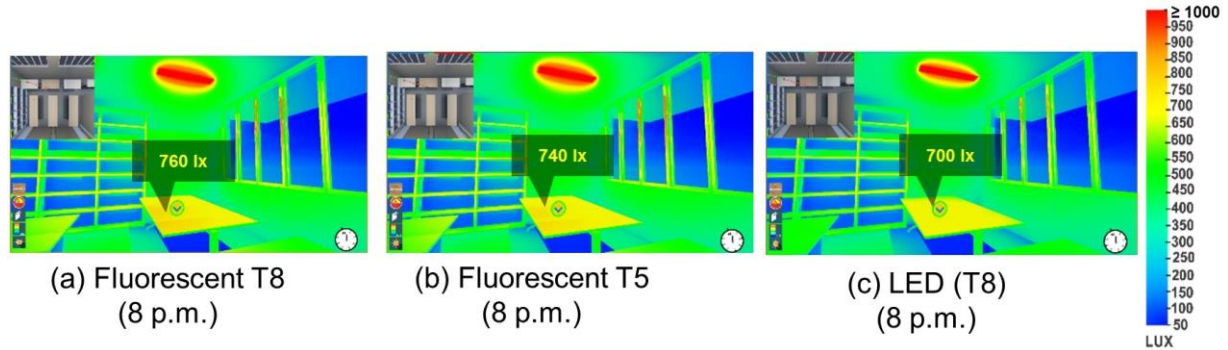


Figure 45 Illuminance levels using different bulbs

Aesthetics of lighting design assessment

As explained in Section 6.2, the BLDF system provides a holistic overview of the design atmosphere that helps designers to aesthetically assess the design and to present the outcomes of the setup to their clients. Figure 46 shows visualization examples of lighting atmospheres of different design options. For example, warm color (Figure 46a) produces orange and yellow lighting colors, which creates a relaxing atmosphere for occupants (Tomassoni et al., 2015). Cool colors or daylight colors are commonly used in office spaces (Figure 46b). Tomassoni et al. (2015) stated that colder chromatic temperatures help to stimulate greater work efficiency and productivity. For our case study, the white color temperature (7000 K) generated by fluorescent bulbs is used. The white color temperature is a mixture of cool and warm colors, which is a suitable choice for an office environment.

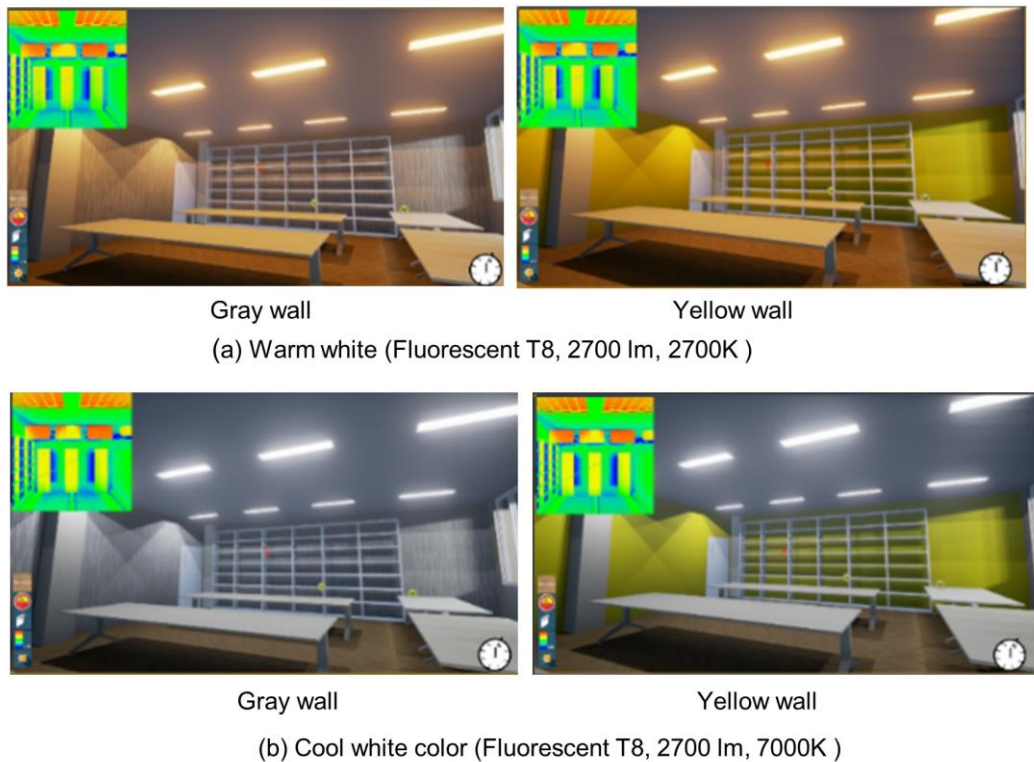


Figure 46 Lighting atmospheres

Furniture layout and illuminance level

Figure 47 shows an example of illuminance levels of different furniture layouts. Figure 47a shows the results of a simulation before placing a bookshelf. The illuminance level on the desk surface is approximately 720 lux. For the case in which a bookshelf is placed in the room, the illuminance level on the desk surface is reduced to approximately 550 lux, which is still within the acceptable lighting level required for working areas (Figure 47b).

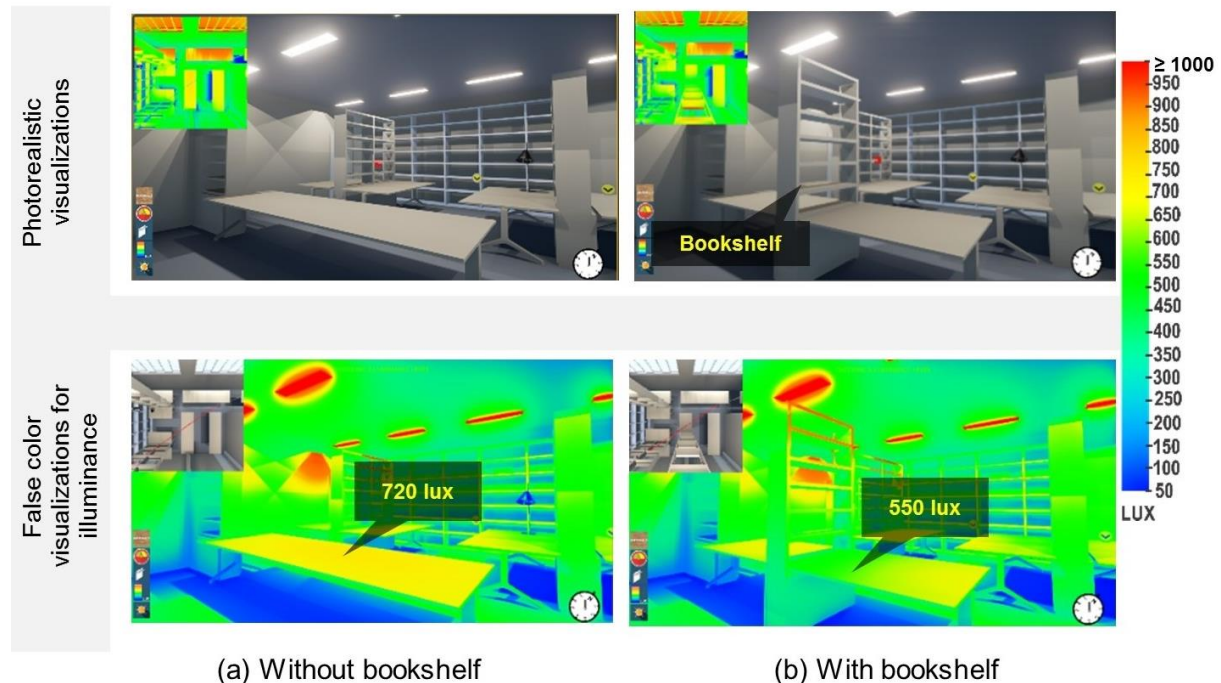


Figure 47 Illuminance levels of different furniture layouts

Integrating lighting sensor control

The occupancy sensor in the BLDF is an optional lighting control that can create an opportunity to achieve a more energy efficient design for the building (Figure 48). Ambient lights and task lights will be automatically turned on when the specified zone becomes occupied and will be automatically turned off when the specified zone is unoccupied. The user can experience the quality of lighting when occupancy sensors are added to the environment and can visually analyze the quality of the illuminance level when various lights are turned on/off in a specific work area.

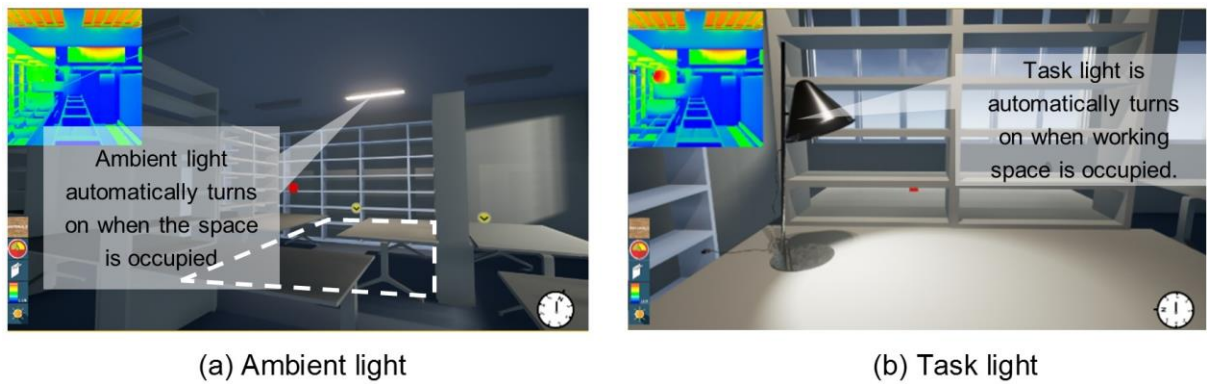


Figure 48 Adding occupancy sensors for ambient light and task light in the virtual environment Task

6.5 Results and discussion

The result of the aforementioned validation scenarios provides several new regarding the integration of a BIM and VR for indoor lighting design feedback.

Although using existing lighting simulation software packages (e.g., Ecotect, Radiance, Dialux, 3ds Max) can help improving iterative lighting design processes, such commercial software applications have limitations. For example, these applications require long processing time to calculate the illuminance level. There are also limitations in handling models with complex geometries. Additionally, operating existing software packages, such as Radiance and Dialux, usually requires specialized knowledge and technical skills. Furthermore, such applications do not provide analysis of the appearance of lighting design and quantification of the amount and the distribution of lighting in real-time. The lighting simulation outputs are mostly generated and presented as 2D photorealistic, false-color, and HDR images, which lack complementary information such as the geometry, volumetric information of the target space, and the real-life experience of the space. The conventional lighting simulations applications primarily measure the amount of light falling on surfaces (i.e., illuminance) and do not provide information about the luminance in the target area. Finally, using traditional lighting simulation applications, the human visual perception is not directly involved in the analysis process. The developed BLDF system introduced a new idea to address some of the above-mentioned drawbacks.

One of the goals of the development of the BLDF system was to provide a tool to explore and perceive luminance distribution and illuminance in a virtual environment. BLDF system provides a unique experience for realistic visualization of lighting design in an immersive environment. It allows previewing the effect of lighting in a target space and quantifying the amount of illumination with real-time visual feedback.

Currently, the BLDF system enables a holistic overview of lighting design through its visualizations. This benefits not only designers but also all parties involved in the design process (e.g., owners). Compared with non-immersive feedback (e.g., through a computer screen), the system provides more efficient feedback via immersive visualization through a first-person perspective, which helps to present and communicate ideas, and provides explicit decision support regarding future designs, by clearly indicating areas that require improvement in lighting quality. Using immersive VR display technology, BLDF delivers a semi-realistic perception of artificial and daylighting. It also generates realistic and false-color scenes at runtime. Using the GUI, material and texture of indoor envelope and several lighting parameters can be modified to suit the requirement of the designer. Performing such modifications can be very time-consuming using conventional lighting simulation applications.

The BLDF system was tested in an office building. However, other types of buildings can be easily analyzed by the system. The current BIM authoring software lack features to transfer data on light bulbs, materials and textures when exporting BIM data to VR authoring software. Although the game features worked well for our case study, a number of improvements should be considered in future research:

- The ability to visualize and compare the outcomes of different lighting setups by switching between views of alternative design settings makes the visual comparison more effective.
- In false-color scenes in VR, providing the numerical data of illuminance values for each measurement point can reduce the error of estimating the illuminance value. In our system, 1000 lx is the maximum illuminance value that can be measured and visualized in false-color scenes. Therefore, improving the system to visualize and measure illuminance values above 1000 lx is required.
- The electric power consumption in the interface only considered the total wattage. However, in order to approximate lighting energy consumption, both wattage and the duration of use per day are required. Therefore, providing an occupancy schedule that corresponds to the operating hours of artificial lights can help in calculating the total energy consumption more thoroughly.
- Although HMD provides maximum immersion in the virtual scenes, in order to accurately perceive lighting phenomena, such as glare, HMDs with high-resolution display screens are required. It is also possible to use BLDF with an LED display with a higher resolution.
- The effect of different sky conditions that influence outdoor/indoor illumination over time should be included in the BLDF.
- Using conventional input devices, such as a mouse and keyboard, is difficult while wearing an HMD. Therefore, interruptions may occur when the system is being used. The use of game controllers and motion tracking technology can solve this problem.
- The final design parameters in VR need to be updated in the BIM database both for geometry information and other properties, e.g., bulb types and light intensities. Although this can be done with the help of visual programming tools, such as Dynamo, automatic synchronization

between design parameters in VR and BIM should be developed. In addition, using visual programming requires additional time and programming experience. Hence, open source data exchange formats, such as the industry foundation classes (IFC), can be used for exchanging data between applications.

6.6 Chapter conclusions

This paper investigated a method by which to integrate BIM and a game engine for lighting design visualization and analysis. The prototype system is developed using the Unreal Engine game authoring software system with its visual scripting environment. In order to use the BLDF system, the following activities should be performed: (1) creating a BIM model; (2) exporting the BIM model into the game engine; (3) adjusting the model in the game environment and redefining the initial values of the design parameters; (4) visualizing lighting illumination, lighting atmosphere, and energy consumption using VR; (5) evaluating and analyzing the conditions of lighting designs; and 6) configuring design parameters using a Graphic User Interface (GUI) to achieve the desired lighting results. An approach to allow users to interact with design objects created in a BIM application and experience lighting design in an immersive environment was discussed. The user can define and explore design parameters, and the results can be simulated in real-time.

The developed system presents a solution for integrating lighting simulation with interactive visualization to support lighting designs. Users can perceive the influence of the design modifications on the characteristics of light in space. Using an immersive VR experience, BLDF facilitates the process of design for users. The proposed system can aid in the understanding, predicting, and assessing indoor lighting environments in real-time during the design phase, which is not possible with traditional lighting simulation tools.

The proposed method was validated in a case study in a campus building at Osaka University, Japan. The initial results revealed that the data can be successfully exchanged between the BIM database and the game engine. The BLDF system enables design parameters to be determined by comparing multiple lighting setups, and it is easy to use with its GUI, which allows design parameters to be redefined interactively. The user can easily change, move, and rotate fixtures. The quantitative and qualitative outputs of the proposed system help in analyzing the lighting design and evaluating visual comfort.

There are several limitations in our developed prototype system. Some of these limitations are related to the use of hardware and some are related to the developed tool. Although using HMDs provides a sense of immersion and realism of lighting conditions, there is a constrained Field of View (FOV) on distance perception and the pixel density of the current VR headsets. Such factors can decrease the accuracy of perceiving lighting phenomena, such as glare, brightness, and darkness. With the rapid advancement of HMD technologies, a higher level of perceptual accuracy of lighting in a future release

of HMDs is expected. Our system currently relies on the physics engine of Unreal Engine for simulating glare on the available HMD headsets; hence, accurate and realistic perception of glare is not possible. However, the simulation output of glare in the current implementation is still helpful for lighting designers.

Exchanging information between BIM and the chosen game engine is limited to only 3D geometry, and information such as the properties of light bulbs, materials, and textures cannot be transferred. Thus, the user has to manually redefine bulbs and recreate textures in the game environment. Furthermore, complex geometries contained in the BIM model (e.g., furniture models) were not transferred into the game engine. Therefore, the use of low-polygon models (level of development (LOD) 100–300) (Level of Development Specification, 2016) should be considered in the BIM modeling process.

Chapter 7 Conclusions and future works

7.1 Introduction

The work presented in this thesis aims to contribute to the integration of BIM with various technologies to optimize the prediction and evaluation of three factors influencing of the energy demand in buildings (i.e., indoor thermal comfort, building envelope and lighting design). The problem related to the lack of interoperability between environmental data and BIM to evaluate the thermal performance of building envelopes and indoor thermal comfort in the operational stage of the building is addressed in our first system of the research. The limited researches focused on integrating thermal data captured by an infrared camera and data loggers with the BIM model using the developed visual scripting. Variables to measure indoor thermal comfort are automatically derived. Visualization of the spatio-thermal data to identify patterns of inefficiency or sources of problems is provided. Our research has proposed a novel system to store surface temperature on the BIM model to be used as an input to calculate thermal comfort variables. The problem related to the complexity in the manual calculation to derive OTTVs is addressed in our second system (BOTTVC), which enables accessing the physical and thermal properties in the BIM database to facilitate a real-time thermal transfer value calculation. The problem related to the lack of interactive environment between users and the lighting design context is addressed in our third developed system (BLDF). BLDF system utilizes an interactive and immersive VR environment for a realistic visualization of lighting conditions. The simulation outputs of daylighting and artificial lights can be visualized using head-mounted-displays.

This chapter aims to summarize the findings generated in the previous chapters by considering the challenge of integrating BIM with various technologies. This allows the exchange of information on design and collaboration platforms with a centralized database to create a new way to enhance a building's performance. The three proposed systems in the research contributions, limitations, and future works to improve the proposed approaches are discussed.

7.2 Research contribution

The main research contributions to develop the systems that provide new methods to effectively use the BIM database to identify inefficiencies in the design and optimize the evaluation of building performance during operational and design phases are grouped as follows:

(1) Integrating thermal information with BIM for building envelope thermal performance analysis and thermal comfort evaluation: The proposed approach to systematically store the environmental data, such as indoor/outdoor air temperature, and surface temperature of building envelopes collected by measurement instruments and sensors in a BIM is a novel BIM-based environment data method. This method improves the analysis of thermal performance and thermal comfort level in the building by employing Grasshopper visual scripting to connect BIM geometry information with sensor data to find the correlation between time and the changes of heat distribution patterns, provide an adequate measurement technique to identify the temporal correlation between surface temperature and thermal comfort level, and facilitate the calculation of thermal comfort variables. The proposed system is different from previous BIM-based environmental data methods in term of the following: (1) enriching BIM with thermal information collected from actual locations to be used as inputs for indoor thermal comfort evaluation of buildings instead of simulating using the information from the BIM database alone; (2) using the developed visual scripting to integrate sensor data, thermographic images, and the BIM model that facilitates the process of calculating MRT considering the corresponding angle factors between a building's surface and the location of an occupant; (3) employing a BIM-based method for integrating BIM geometry data, timecoded surface temperature of the building envelope, and environment sensor data for assessing the performance of the building envelope and the indoor thermal comfort level per location; (4) introducing a new procedure for visualizing analysis the surface temperature of different area and identifying the pattern of inefficiency over time using color coding, detecting the exact location of heat sources, and monitoring the performance of building envelopes.

(2) Optimizing the evaluation of building envelope for thermal performance using a BIM-based Overall Thermal Transfer Value calculation: Based on the previous study, to directly incorporate the required data relevant to the evaluation of the performance of building envelopes from the BIM database based on OTTV standards, a seamless integration between BIM and the evaluation methods has not been fully proposed yet. The major contribution of this system is the development of a system that provides a faster and more accurate approach for calculating OTTV values as compared with manual calculation. The system reduces total calculation time by 80% in our case study. This decrease of the calculation time was achieved because the required coefficient values and variables for calculating OTTVs can be directly extracted and derived from the BIM database. There are some constant coefficients that need to be manually defined from a spreadsheet file. Using BIM's visual scripting and its API to access the physical and thermal properties of building materials in the BIM model can be easily calculated by OTTV that involves functions with various variables and coefficients.

(3) Integrating building information modeling and virtual reality for building indoor lighting design: The proposed framework to employ VR for lighting design visualization and analysis is different from

previous research in term of the following: (1) BIM-based lighting visualizations for lighting performance analysis and visual comfort evaluation have been proposed; (2) integration of game engines together with BIM geometry information as the main database is proposed for visualizing lighting illumination, lighting atmosphere, and energy consumption by allowing users to explore their designed space in a virtual environment; (3) designers can perceive realistic lighting scenes of their design through VR technology; (4) an interactive virtual environment provides users with a controller to customize design parameters, change input parameters, and freely navigate design objects with an ability to preview the lighting output in the system in real-time; (5) the developed system reduces the processing time to calculate the illumination level compared with the traditional lighting simulation tools.

7.3 Summary of research

This dissertation presented a BIM-based data model and integrated frameworks for building performance evaluation and environmental simulations. The overall concept of our proposed frameworks is to develop novel systems based on an integrated database and interoperable information of a building between the BIM database and tools to facilitate building performance evaluation with respect to ASHRAE standard regarding the measurement of indoor environments, IESNA lighting design standard regarding illumination level requirement for computer working space, and OTTV standard. Gathering knowledge on the importance of utilizing BIM for improving building energy efficiency and comfort conditions offers a major potential to realize new benefits in utilizing digital physical information of BIM technology in assessing thermal and visual comfort during the design and operational phases of a project.

The first proposed method is to visualize patterns of surface temperature changes together with sensor data values, which are all geometrically referenced within the building model using BIM-based thermal and environmental data. The adaptive method parameters for assessing indoor thermal comfort based on ASHRAE standard 55-2013 is integrated with our first system. The second method is to integrate the availability of BIM database with the developed visual scripting in measuring the average heat transfer into a building based on OTTV standard. In addition, our third method is to integrate BIM and a game engine to create a virtual interactive environment for qualitative and quantitative outputs related to lighting design. Illumination level requirement for office building from IESNA standard is used in this system. The summary of each system in this research is presented as follows:

(1) The proposed approach for enriching BIM with spatio-temporal surface and air temperature information to help analyze heat energy performance and thermal comfort level has been developed. The system development discussed the integrated thermographic images on the surface of building envelope on the BIM model for spatio-temporal analysis and thermal comfort analysis. The main advantages of the proposed approach are that the environmental data, such as indoor/outdoor air temperature, and temperature values of building envelopes collected by measurement instruments and

sensors are proposed to be systematically stored in a BIM which can be extracted as numeric temperature values with their coordinates (x,y,z). Such extracted data can be used as an input to calculate variables, such as operative temperature and MRT, considering the position of the occupant in the room for assessing the thermal comfort level. The applicability of the proposed method is validated in a real-world case study.

(2) The proposed approach for incorporating information from the BIM database with visual scripting to select an appropriate envelope material to achieve an optimum OTTV and optimize energy-efficient building design, BOTTVC was developed. This system helps access and extract the required parameters regarding the thermal properties of materials from a BIM model to evaluate the performance of envelope construction materials based on OTTV standards. In the case study, the BOTTVC system provides a flexible approach for manipulating input data to calculate the OTTV under the various methods for different countries.

(3) The proposed approach for visualizing, identifying, and examining the indoor lighting performance as well as realistic visualization of lighting conditions and the calculation of energy consumption using an interactive and immersive VR environment introduced the BLDF. The BLDF system development discusses the necessity of using immersive VR technology to enable designers to perceive realistic lighting scenes in their designs. The validation scenarios for using BLDF to compare multiple design options were performed. The proposed framework uses a digital geometry model deriving from BIM software coupling with gaming technology to create VR experience and to allow designers to visualize lighting illumination (shown with realistic scenes or false-colors), lighting atmosphere, and energy consumption feedback. The design scenarios were developed to demonstrate how the BLDF system can be used to visually analyze the quality of the illuminance level of the proposed design in a room.

As the limitation of using the current BIM described in Sections 1.1 and 1.2, using BIM is insufficient to predict indoor comfort (i.e., thermal comfort and visual comfort) of the design building, and it is insufficient to respond by providing an option to measure the thermal characteristics of envelope components in order to comply with the prescriptive criteria. To bridge the aforementioned gaps, in this research, BIM has been used as the main repository of information or database system that allows updating, managing and transferring model data across software applications to create new possibilities of using BIM database for building energy efficiency design. This can create a new way of utilizing BIM data to be more efficient in the design, operation, and maintenance process.

7.4 Limitations and future works

Although the proposed frameworks for extending the capability of using BIM to evaluate the performance of different components and systems of a building in this research provide new approaches to take advantages of BIM with the support of visual programming interface and game engine

technologies, there are some limitations in the current frameworks that need to be overcome. The potential limitations of the proposed systems are highlighted as follows:

- (1) The proposed method for integrating thermal information with BIM for building envelope thermal performance analysis and thermal comfort evaluation in a building's operational phase can be further improved by applying IFC standard that supports the exchange requirement for thermal comfort analysis. In order to automatically reconstruct a 3D thermal model, a photogrammetry technique should be employed. Moreover, the other required variables for thermal comfort measurement in an air-conditioned room, such as humidity and air velocity, should be included in the system. Finally, the BIM-based environmental data can be further enhanced to include the effect of the changes of air-temperature on indoor thermal comfort of a building. In the future, we intend to develop a method for recording environmental data and thermal information in the BIM using existing IFC resources, investigate a method by which to fully automate the construction of a thermal 3D model using photogrammetry, and extend the ability of the proposed system to evaluate indoor thermal comfort in air-conditioned buildings using the PMV and PPV methods. For the case of capturing thermal images in a semi-cloudy condition, a new technique for storing the changes of heat radiation on the surfaces of buildings should be developed.
- (2) The proposed framework for optimizing the evaluation of building envelope for thermal performance using a BIM-based overall thermal transfer value calculation can be improved by creating a plug-in extension to make it available on the BIM software application. In order to simplify the calculation of OTTVs, a GUI should be developed. Moreover, IFC resources that represent thermal and physical properties supporting the analysis of the thermal performance of building envelopes should be integrated into the system. Areas for future research include the development of a method for evaluating the performance of a building envelope based on PAL methods. We intend to investigate a method by which we can fully automate the extraction of thermal indices from the BIM database and calculate the OTTV using Revit API and Visual Studio in C#. Moreover, to provide more efficient revision guidance for assisting designers in the preliminary design stage, we intend to investigate a method to integrate our proposed system with green building rating system credits, such as the Leadership in Energy and Environmental Design, the Building Research Establishment Environmental Assessment Method, and the Comprehensive Assessment System for Built Environment Efficiency. The influence of the thermal performance of building envelopes on the demand for energy use intensity (EUI) was not considered in our prototype system. In future work, we intend to extend the ability of the proposed system to analyze the impact of different building enclosure materials on EUI.
- (3) The proposed method for integrating building information modeling and VR for building indoor lighting designs can be further improved by adding a function to analyze the impact of occupants on the lighting energy consumption. Moreover, a method to automatically synchronize the satisfied

lighting design parameters with BIM software should be investigated. Additionally, an experiment comparing the effect of weather and sky conditions on natural light in VR and actual location should be performed. Areas of future research include integrating the occupancy schedule in the system for the energy simulation, developing a method to export lighting information to the IFC format file using the proposed IFC resources, and developing a system to analyze the amount of excessive light and heat in VR. In addition, the influence of geographic locations and weather conditions was not considered in our prototype system. Therefore, in future work, we intend to study the influence of such factors on natural light in VR. Furthermore, performing glare analysis using VR technology is considered as future work in this research.

4) The proposed three systems in this thesis should be developed as an BIM's internal or external extensions, which can seamlessly connect with BIM software.

References

Abraham, M. (2017). Encyclopedia of sustainable technologies. Elsevier.

Ahn, K. U., Kim, Y. J., Park, C. S., Kim, I., & Lee, K. (2014). BIM interface for full vs. semi-automated building energy simulation. *Energy and Buildings*, 68(PART B), 671–678. <https://doi.org/10.1016/j.enbuild.2013.08.063>.

Ahuja, R., Sawhney, A., & Arif, M. (2017). Prioritizing BIM capabilities of an organization: an interpretive structural modeling analysis. *Procedia Engineering*, 196(June), 2–10. <https://doi.org/10.1016/j.proeng.2017.07.166>.

Aksamija, A., Mario, G., Rangarajan, H. P., & Meador, T. (2011). Building simulations and high-performance buildings research: use of Building Information Modeling (BIM) for integrated design and analysis. *S, Perkins+Will Research Journal*, 3(1), 32–45.

Aksamija, A., & Zaki, M. (2010). Building Performance Predictions. *Perkins+Will Research Journal*, 2, 7–32.

Almujahid, A., & Kaneesamkandi, Z. (2013). Construction of a test room for evaluating thermal performance of building wall systems under real, *Innovative Research in Science, Engineering and Technology*, 2(6), 2000–2007.

Amirkhani, M., Garcia-Hansen, V., & Isoardi, G. (2016). Reducing luminance contrast on the window wall and users' interventions in an office room. In *Proceedings of the CIE 2016 Lighting Quality and Energy Efficiency*, pp. 385–394.

Anderson, B. (2006). Conventions for U-value calculations 2006 edition. BRE Press. Wattford.

Anderson, K. (2014). Design Energy Simulation for Architects: Guide to 3D graphics, New York: Taylor & Francis.

ASHRAE. (2013). Thermal Environmental Conditions for Human Occupancy. ANSI/ASHRAE Standard 55-2010. <https://doi.org/ISSN 1041-2336>.

ASHRAE, ANSI/ASHRAE/IES Standard 90.1-2013 (2013) Energy standard for buildings except low-rise residential buildings, The American Society of Heating Refrigerating and Air Conditioning Engineers, Atlanta, GA.

Autodesk. (2016a). 3ds Max 3D modeling, animation & rendering software. <http://www.autodesk.com/products/3ds-max/overview>. (Accessed May 15, 2016).

Autodesk. (2016b). Dynamo BIM. <http://dynamobim.org>. (Accessed May 15, 2016).

Autodesk. (2016c). Improving building design project collaboration using openBIM ® Data Exchange Standards Industry Foundation Classes (IFC). <https://damassets.autodesk.net>. (Accessed February 5, 2018).

Autodesk. (2016d). Revit Family. <http://www.autodesk.com/products/revit-family/overview>. (Accessed May 16, 2016)

Babiak, J., Olesen, B. W., & Petras, D. (2007). REHVA Guidebook no. 7: Low-Temperature Heating and High-Temperature Cooling, Belgium: Federation of European Heating and Air-conditioning Associations.

Bahar, Y. N., Christian, P. (2013). Integration of thermal building simulation and VR techniques for sustainable building projects. In *Proceedings of the Conference*, pp. 1–8.

Bazjanac, V. (2009). Implementation of semi-automated energy performance simulation : building geometry. In Proceedings of the Cib W78, pp 595–602.

Benya, J., Heschong, L., McGowan, T., Miller, N., & Rubinstein, F. (2001). Advanced Lighting Guidelines (2001st ed.). USA: New Buildings Institute.

Bille, R., Smith, S. P., Maund, K., & Brewer, G. (2014). Extending building information models into game engines. In Proceedings of the 2014 Conference on Interactive Entertainment, 1–8. <https://doi.org/10.1145/2677758.2677764>.

Boeykens, S. (2012). Bridging building information modeling and parametric design. eWork and eBusiness in Architecture, Engineering and Construction. <https://doi.org/doi:10.1201/b12516-71>.

Boeykens, S., & Neuckermans, H. (2009). Visual programming in architecture: should architects be trained as programmers?. In Proceedings of the CAADFutures 2009: Joining Languages Cultures and Visions, pp 41–42.

Borrmann, D., Elseberg, J., & Nuchter, A. (2012). Thermal 3D mapping of building facades. In Proceedings of the Intelligent Autonomous Systems. <http://dx.doi.org/10.1007/978-3-642-33926-4>.

Boyce, R. P. (2003). Human Factors in Lighting, Second Edition. CRC Press.
<https://doi.org/10.1201/9780203426340>.

Brewer, R., Xu, Y., Lee, G., Katchuck, M., Moore, C., & Johnson, P. (2013). Three principles for the design of energy feedback visualizations. International Journal on Advances in Intelligent Systems, 6(3), 188–198.

Bruneton, E., & Neyret, F. (2008). Precomputed atmospheric scattering. In Proceedings of the 19th Eurographics Symposium on Rendering, pp. 1079–1086.
<https://doi.org/10.1111/j.1467-8659.2008.01245.x>.

Buildings Department, Building Energy Efficiency Regulation (B(EE)R), 2016, www.bd.gov.hk. (Accessed 10 June 2017)

BuildingSMARTalliance. (2015). National BIM Standard-United States ®. <http://www.nibs.org>. (Accessed 15 August 2016)

Center for the Built Environment (CBE). (2013). CBE thermal comfort tool, Center for the Built Environment, University of California Berkeley. <http://comfort.cbe.berkeley.edu>. (Accessed October 31, 2015)

Chan, A. L. S., & Chow, T. T. (2014). Calculation of overall thermal transfer value (OTTV) for commercial buildings constructed with naturally ventilated double skin façade in subtropical Hong Kong, Energy and Building, 69 (2014) 14–21. <https://doi.org/10.1016/j.enbuild.2013.09.049>.

Chauvel, P., Collins, J. B., Dogniaux, R., & Longmore, J. (1982). Glare from windows: current views of the problem. Lighting Research and Technology, 14, 31–46.
<https://doi.org/10.1177/096032718201400103>.

Ciribini, A. L. C., Ventura, S. M. B., & Marzia, B. (2014). Informative content validation is the key to success in a BIM-based project. Territorio Italia, 1(6), 87–111. <https://doi.org/10.14609/Ti>.

Clear, R. D. (2012). Discomfort glare: what do we actually know? Lighting Research and Technology, 45, 141–158.

Commissioner of Building Control. (2004). Guidelines on envelope thermal transfer value for buildings. <https://www.bca.gov.sg/PerformanceBased/others/ETTV.pdf>. (Accessed 10 June 2017).

Costin, A. M., & Teizer, J. (2015). Fusing passive RFID and BIM for increased accuracy in indoor localization. *Visualization in Engineering*. <https://doi.org/10.1186/s40327-015-0030-6>.

Danese, M., Demsar, U., Masini, N., & Charlton, M. (2010). Investigating material decay of historic buildings using visual analytics with multi-temporal infrared thermographic data. *Archaeometry*, 52(3), 482–501.

de Dear, R. J., Akimoto, T., Arens, E., Brager, G., Candido, C., Cheong, K. W. D., Li, B., Nishihara, N., Sekhar, S.C., Tanabe, S., Toftum, J., Zhang, H., & Zhu, Y. (2013).

Progress in thermal comfort research over the last twenty years. *Indoor Air*, 23(6), 442–461. <https://doi.org/10.1111/ina.12046>.

de Rousiers, C., & Lagarde, S. (2014). Moving to physically based rendering. In *Proceedings of the ACM SIGGRAPH 2014*, p. 119.

Decree of Ministry of the Environment on thermal insulation in a building. (2002). C3 national building code of finland - Thermal insulation in a building, https://www.edilex.fi/data/rakentamismaarakset/c3e_2003.pdf. (Accessed 15 May 2017)

Deru, M., Blair, N., & Torcellini, P. (2005). Procedure to measure indoor lighting energy performance. National Renewable Energy Laboratory. Colorado: National Renewable Energy Laboratory.

Descottes, H., & Ramos, C. E. (2011). *Architectural Lighting Designing with Lighting and Space*. (B. Casbon, Ed.). New York: Princeton Architectural Press.
<https://doi.org/10.1017/CBO9781107415324.004>.

Dutt, F., Quan, S. J., Woodworth, E., Castro-Lacouture, D., Stuart, B. J., & Yang, P. P. J. (2017). Modeling algae powered neighborhood through GIS and BIM integration. *Energy Procedia*, 105, 3830–3836. <https://doi.org/10.1016/j.egypro.2017.03.896>.

Eads, L. G., Epperly, R. A., & Jr, J. R. S. (2000). Thermography. *ASHRAE Journal*, 51–55.

Eastman, C., Teicholz, P., Rafael, S., & Liston, K. (2008). *BIM Handbook*. New Jersey: John Wiley & Sons, <https://doi.org/2007029306>.

Edwards, G., Li, H., & Wang, B. (2015). BIM-based collaborative and interactive design process using computer game engine for general end-users. *Visualization in Engineering*, 3(1).
<https://doi.org/10.1186/s40327-015-0018-2>.

Egwunatum, S., Joseph-Akwara, E., & Akaigwe, R. (2016). Optimizing energy consumption in building designs using building information model (BIM). *Slovak Journal of Civil Engineering*, 24(3), 19–28. <https://doi.org/10.1515/sjce-2016-0013>.

Einhorn, H. (1973). Discomfort glare: a formula to bridge differences. *Lighting Research and Technology*, 11(2), 90–94.

Institute for Building Environment and Energy Conservation (IBEC), Overview of the act on the improvement of energy consumption performance of buildings, 2016.
<https://www.mlit.go.jp>. (Accessed 15 May 2017)

Epic Games. (2016). What is Unreal Engine 4. <https://www.unrealengine.com/what-is-unreal-engine-4>. (Accessed May 16, 2016)

Faltýnová, M., Matoušková, E., Šedina, J., & Pavelka, K. (2016). Building facade documentation using laser scanning and photogrammetry and data implementation into BIM. In *Proceedings of the ISPRS*, pp. 215–220. <https://doi.org/10.5194/isprsarchives-XLI-B3-215-2016>.

Fang, Z., Li, N., Li, B., Luo, G., & Huang, Y. (2014). The effect of building envelope insulation on cooling energy consumption in summer. *Energy and Buildings*, 77, 197–205. <https://doi.org/10.1016/j.enbuild.2014.03.030>.

Fanger, P. (1973). Assessment of man's thermal comfort in practice. *British Journal of Industrial Medicine*, 30(4), 313–324. <https://doi.org/10.1136/oem.30.4.313>.

Fanger, P. (1970). Thermal comfort: analysis and applications in environmental engineering. New York: McGraw-Hill.

Fasi, M. A., & Budaiwi, I. M. (2015). Energy performance of windows in office buildings considering daylight integration and visual comfort in hot climates. *Energy and Buildings*, 108, 307–316. <https://doi.org/10.1016/j.enbuild.2015.09.024>.

Federal Ministry of Transport, Building and Urban Development, Federal Ministry of Economics and Technology. (2009). Energy Conservation Regulations (EnEV). *Energy*, 1, 1–66.

Fielder, W. J. (2001). *The Lit Interior*. Architectural Press.

Figueres-Munoz, A., & Merschbrock, C. (2015). Overcoming challenges in BIM and gaming integration: the case of a hospital project. *Building Information Modelling (BIM) in Design, Construction and Operations*, 149, 329–340. <https://doi.org/10.2495/BIM150281>.

Fisher, A. (1992). Tolerances in lighting design. In *Proceedings of the CIE Seminar on Computer Programs for Light and Lighting*. Vienna, Austria, pp. 102-103.

Fuchs, P. (2017). *Virtual Reality Headsets - A Theoretical and Pragmatic Approach*. CRC Press.

Fukuda, T., Mori, K., & Imaizumi, J. (2015). Integration of CFD, VR, AR and BIM for design feedback in a design process an experimental study. In *Proceedings of the 33rd eCAADe*, pp. 665–672.

Ganem, C., Barea, G., & Balter, J. (2016). Infrared thermography for quick thermal diagnostic of existing building. In *Proceedings of the PLEA 2016 (Cities, Buildings People: Toward Regenerative Environments)*.

Green Building Index, Non-residential New Construction (NRNC) - Design Reference Guide and Submission Format, 2011, www.greenbuildingindex.org. (Accessed 10 June 2017)

Giraldo Vásquez, N., Ruttakay Pereira, F. O., Olivera Pires, M., & Niero Morae, S. (2016). Investigating a method to dynamic assessment of glare using the HDR technique. In *Proceedings of the PLEA 2016 (Cities, Buildings People: Toward Regenerative Environments)*. Los Angeles.

Goedert, J., Cho, Y., Subramaniam, M., Guo, H., & Xiao, L. (2011). A framework for virtual interactive construction education (VICE). *Automation in Construction*, 20(1), 76–87. <https://doi.org/10.1016/j.autcon.2010.07.002>.

Government of Ireland, Conservation of Fuel and Energy - Dwellings - Building Regulations 2011, <http://www.housing.gov.ie/sites/default/files/publications>. (Accessed 15 May 2017)

Grinzato, E., Vavilov, V., & Kauppinen, T. (1998). Quantitative infrared thermography in buildings. *Energy and Buildings*, 29, 1–9. [https://doi.org/10.1016/S0378-7788\(97\)00039-X](https://doi.org/10.1016/S0378-7788(97)00039-X).

Gröhn, M., Mantere, M., Savioja, L., & Takala, T. (2001). 3D visualization of building services in virtual environment. In *Proceedings of the 17th Conference on Education in Computer Aided Architectural Desing in Europe*, pp. 523–528.

Gut, P., & Ackerknecht, D. (1993). *Climate Responsive Building - Appropriate Building Construction in Tropical and Subtropical Regions*. SKAT.

Guth, S. K. (1963). A method for the evaluation of discomfort glare. *Illuminating Engineering*, 58(5), 351–364. <https://doi.org/10.2150/jieij.91.63>.

Hailemariam, E., Glueck, M., Attar, R., Alex Tessier, McCrae, J., & Khan, A. (2010). Toward a unified representation system of performance-related data. In *Proceedings of the 6th eSim 2010 Conference*, Canada, pp. 117–124.

Ham, Y., & Golparvar-Fard, M. (2014). Mapping actual thermal properties to building elements in gbXML-based BIM for reliable building energy performance modeling. *Automation in Construction*, 49, 214–224. <https://doi.org/10.1016/j.autcon.2014.07.009>.

Hardin, B., & Mccool, D. (2014). *BIM and Construction Management - Proven tools, methods, and workflows*. Canada: Johnson Wiley & Sons. <https://doi.org/10.1007/s13398-014-0173-7.2>.

Hirning, M. B., Isoardi, G. L., & Cowling, I. (2014). Discomfort glare in open plan green buildings. *Energy and Buildings*, 70, 427–440. <https://doi.org/10.1016/j.enbuild.2013.11.053>.

Hitchcock, R. J., & Wong, J. (2011). Transforming IFC architectural view BIMS for energy simulation: 2011. In *Proceedings of the Building Simulation 2011: 12th Conference of International Building Performance Simulation Association*, pp. 1089–1095.

HM Government, Conservation of fuel and power, UK Building Regulation 2010 - L1A, 2013. <https://www.gov.uk/government/publications>. (Accessed 15 May 2017)

Hoegner, L., & Stilla, U. (2015). Building facade object detection from terrestrial thermal infrared image sequences combining different views. In *Proceeding of the ISPRS Annals of Photogrammetry, Remote Sensing and Spatial Information Sciences*, pp. 55–62. <https://doi.org/10.5194/isprsannals-II-3-W4-55-2015>

Hosokawa, M., Fukuda, T., Yabuki, N., Michikawa, T., & Motamedi, A. (2016). Integrating CFD and VR for indoor thermal environment design feedback. In *Proceedings of the 21st International Conference of the Association for Computer-Aided Architectural Design Research in Asia CAADRIA*, Hong Kong. pp. 1–10.

Huang, Y. C. (2008). A scalable lighting simulation tool for integrated building design. In *Proceedings of the SimBuild*, Berkery, USA. pp. 206–213.

IESNA. (2000). *The IESNA Lighting Handbook*. The Illuminating Engineering Society of North America, New York.

Inanici, M. (2007). Computational approach for determining the directionality of light: directional-to-diffuse ratio. In *Proceedings of the Building Simulation*, pp. 1182–1188.

Inanici, M., & Mehlika, N. (2003). Utilization of image technology in virtual lighting laboratory. In *Proceedings of the CIE 2003 Conference*, pp. 1–4.

Isikdag, U., Aouad, G., Underwood, J., & Wu, S. (2007). Building information models: a review on storage and exchange mechanisms. In *Proceedings of the CIB W78*, pp. 135-143.

ISO 7726. (1998). *Thermal environments-instruments for Measuring Physical Quantities*. International Standard Organization.

Jalaei, F., & Jrade, A. (2014). Integrating BIM and energy analysis tools with green building certification system to conceptually design sustainable buildings. *ITcon*, 19(11), 494–519. <https://doi.org/10.1061/9780784413517.015>.

Janda, K. B., & Busch, J. (1994). Worldwide status of energy standards for buildings. *Energy*, IV(I), 27–44.

Jones, S. a, Young Jr., N. W., & Bernstein, H. M. (2008). *Building Information Modeling (BIM): Transforming Design and Construction to Achieve Greater Industry Productivity*. McGraw Hill Construction - SmartMarket Report.

Keim, D. A., Mansmann, F., Stoffel, A., & Ziegler, H. (2009). Visual analytics. In *Proceedings of the Iwaw*, pp. 27–37.

Keim, D., Zhang, L., Krstajic, M., & Simon, S. (2012). Solving problems with visual analytics: challenges and application. In *Proceedings of the Ecml/Pkdd*, pp. 1–30.
<https://doi.org/10.1145/0000000.0000000>.

U.S Department of Commerce (1999). *STEP: The Grand Experience*. NIST Special Publication 939, 1–185. <https://doi.org/10.13140/RG.2.1.2030.2884>.

Kensek, K. M. (2014). Integration of environmental sensors with BIM: case studies using Arduino, Dynamo, and the Revit API. In *Proceedings of the Informes de La Construccion*, 66(536), <https://doi.org/10.3989/ic.13.151>.

Khan, A., & Hornbæk, K. (2011). Big data from the built environment. In *Proceedings of the 2nd International Workshop on Research in the Large*, pp. 5–8.

Kohlhammer, J., Keim, D., Pohl, M., Santucci, G., & Andrienko, G. (2011). Solving problems with visual analytics. *Procedia Computer Science*, 7, 117–120. <https://doi.org/10.1016/j.procs.2011.12.035>.

Kota, S., Haberl, J. S., Clayton, M. J., & Yan, W. (2014). Building Information Modeling (BIM)-based daylighting simulation and analysis. *Energy and Buildings*, 81, 391–403.
<https://doi.org/10.1016/j.enbuild.2014.06.043>

Kruger, A., & Seville, C. (2013). *Green Building: Principles and Practices in Residential Construction*. New York: Delmar, Cengage Learning.

Krygiel, E., & Nies, B. (2008). *Green BIM: successful sustainable design with building information modeling*. Canada: Wiley.

La Gennusa, M., Nucara, A., Rizzo, G., & Scaccianoce, G. (2005). The calculation of the mean radiant temperature of a subject exposed to the solar radiation - A generalised algorithm. *Building and Environment*, 40(3), 367–375. <https://doi.org/10.1016/j.buildenv.2004.06.019>.

Lagüela, S., Armesto, J., Arias, P., & Herráez, J. (2012). Automation in construction automation of thermographic 3D modeling through image fusion and image matching techniques. *Automation in Construction*, 27, 24–31. <https://doi.org/10.1016/j.autcon.2012.05.011>.

Lam, J. C., & Hui, S. C. M. (1996). A review of building energy standards and implications for Hong Kong. *Building Research and Information*, 24(3), 2–4.

Laustsen, J. (2008). Energy efficiency requirements in building codes, *Energy Efficiency Policies for New Buildings*. Buildings, 1–85.

Level of Development Specification. (2016). <http://bimforum.org/lod>. (Accessed May 16, 2017)

Li, H., & Malcolm, L. (2010). Measurement of thermal performance of building envelope - a comparison of some international legislation, In *Proceedings of the 2nd International Conference on Waste Engineering and Management (ICWEM)*, 2010, pp. 108–121.

Loekita, S., & Priatman, J. (2015). OTTV (SNI 03-6389-2011) and ETTV (BCA 2008) calculation for various building's shapes, orientations, envelope building materials: comparison and analysis. *Civil Engineering Dimension*, 17(2), 108–115. <https://doi.org/10.9744/ced.17.2.108-116>.

Mangkuto, R. A., Wang, S., Aries, M. B. C., van Loenen, E. J., & Hensen, J. L. M. (2014). Comparison between lighting performance of a virtual natural lighting solutions prototype and a real window based on computer simulation. *Frontiers of Architectural Research*, 3(4), 398–412. <https://doi.org/10.1016/j.foar.2014.07.001>.

Masoso, O. T., & Grobler, L. J. (2008). A new and innovative look at anti-insulation behaviour in building energy consumption. *Energy and Buildings*, 40(10), 1889–1894. <https://doi.org/10.1016/j.enbuild.2008.04.013>

Mauriello, M. L., Norooz, L., & Froehlich, J. E. (2015). Understanding the role of thermography in energy auditing : current practices and the potential for automated solutions. In *Proceedings of the 33rd Annual ACM Conference on Human Factors in Computing Systems*.

Mcneil, A., & Burrell, G. (2016). Applicability of DGP and DGI for evaluating glare in a brightly daylit space. In *Proceeding of the SimBuild*, pp. 57–64.

Menshikova, G., Bayakovski, Y., Luniakova, E., Pestun, M., & Zakharkin, D. (2012). Virtual reality technology for the visual perception study, In *Proceedings of the Transactions on Computational Science XIX*, pp. 51–54.

Miettinen, R., & Paavola, S. (2014). Beyond the BIM utopia: approaches to the development and implementation of building information modeling. *Automation in Construction*, 43, 84–91. <https://doi.org/10.1016/j.autcon.2014.03.009>.

Mihelj, M., Novak, D., & Beguš, S. (2013). *Virtual Reality Technology and Applications*. Springer Science & Business Media.

Ministry of Energy. (2009). *Ministerial Regulation: The Building Energy Conservation Promotion Act* B.E. 2009.

Motamedi, A., Wang, Z., Yabuki, N., Fukuda, T., & Michikawa, T. (2017). Signage visibility analysis and optimization system using BIM-enabled virtual reality (VR) environments. *Advanced Engineering Informatics*, 32, 248–262. <https://doi.org/10.1016/j.aei.2017.03.005>.

Murdoch, M. J., Stokkermans, M. G. M., & Lambooij, M. (2015). Towards perceptual accuracy in 3D visualizations of illuminated indoor environments. *Journal of Solid State Lighting*, 2(1), 12. <https://doi.org/10.1186/s40539-015-0029-6>.

Murthy, N. S. (1978). A decision model for the design of building enclosures. *Building and Environment*, 13, 201–216.

Nasyrov, V., Stratbucker, S., Ritter, F., Borrman, A., Hua, S., & Lindauer, M. (2014). Building information models as input for building energy performance simulation – the current state of industrial implementations. *eWork and eBusiness in Architecture, Engineering and Construction*, 479–486. <https://doi.org/10.1201/b17396-80>.

Niggli, A., Romberg, R., & Rank, E. (2004). A framework for concurrent structure analysis in building industry. In *Proceedings of the 5th European Conference on Product and Process Modeling in the Building and Construction Industry (ECPM 2004)*, pp. 233–248.

Niu, S., Pan, W., & Zhao, Y. (2015). A virtual reality supported approach to occupancy engagement in building energy design for closing the energy performance gap. *Procedia Engineering*, 118, 573–580. <https://doi.org/10.1016/j.proeng.2015.08.487>.

Noori, A., & Hwaish, A. (2015). Impact of heat exchange on building envelope in the hot climates. *International Journal of Emerging Technology and Advanced Engineering*, 5(2), 47–57.

Ochoa, C. E., Aries, M. B. C., & Hensen, J. L. M. (2010). Current perspective on lighting simulation for building science. *Building*, 1–9.

Philippine Green Building Council. (2013). Building for ecologically responsive design excellence (BERDE) for new construction: commercial buildings v1.1.0, 2013. <http://berdeonline.org>. (Accessed 10 June 2017).

Pulpitlova, J., & Detkova, P. (1993). Impact of the cultural and social background on the visual perception in living and working perception. In *Proceedings of the international symposium Design of amenity*, pp. 216–227.

Rahmani Asl, M., Zarrinmehr, S., Bergin, M., & Yan, W. (2015). BPOpt: A framework for BIM-based performance optimization. *Energy and Buildings*, 108, 401–412. <https://doi.org/10.1016/j.enbuild.2015.09.011>

Rao, D. S. P. (2008). Infrared thermography and its applications in civil engineering. *Indian Concrete Journal*, 82(5), 41–50.

Ray Traced Distance Field Soft Shadows. <https://docs.unrealengine.com/latest/INT/Engine/Rendering/LightingAndShadows/RayTracedDistanceFieldShadowing/index.html>. (Accessed 15 August 2017).

Reinhart, C., Doyle, S., Jakubiec, J. A., & Rashida, M. (2012). Glare analysis of daylit spaces: recommendations for practice. http://web.mit.edu/tito_www/Projects/Glare/GlareRecommendationsForPractice.html. (Accessed 8 August 2017).

Reinhart, C. F., & Wienold, J. (2011). The daylighting dashboard - A simulation-based design analysis for daylit spaces. *Building and Environment*, 46(2), 386–396. <https://doi.org/10.1016/j.buildenv.2010.08.001>.

Revel, G. M., Arnesano, M., Pietroni, F., & Schmidt, M., & K. O. (2014). Evaluation in a controlled environment of a low-cost IR sensor for indoor thermal comfort measurement. In *Proceedings of the International Conference QIRT 2014*, <http://dx.doi.org/10.21611/qirt.2014.133>.

Rijal, H., Humphreys, M., & Nicol, F. (2015). Adaptive thermal comfort in Japanese houses during the summer season: behavioral adaptation and the effect of humidity. *Buildings*, 5(3), 1037–1054. <https://doi.org/10.3390/buildings5031037>.

Sabol, L. (2008). Building Information Modeling & Facility Management. *Design + Construction Strategies*, 1–13.

Sadeghipour Roudsari, M., & Pak, M. (2013). Ladybug: a parametric environmental plugin for Grasshopper to help designers create an environmentally conscious design. In *Proceedings of the 13th Conference of International Building Performance Simulation Association*, pp. 3129–3135.

Sadineni, S. B., Madala, S., & Boehm, R. F. (2011). Passive building energy savings: A review of building envelope components. *Renewable and Sustainable Energy Reviews*, 15(8), 3617–3631. <https://doi.org/10.1016/j.rser.2011.07.014>.

Sampaio, A. Z., Ferreira, M. M., & Rosário, D. P. (2010). Integration of VR technology in Buildings Management The lighting system. In Proceedings of the 28th eCAADe Conference Proceedings, pp. 729–738.

Sanguinetti, P., Abdelmohsen, S., Lee, J., Lee, J., Sheward, H., & Eastman, C. (2012). General system architecture for BIM: An integrated approach for design and analysis. *Advanced Engineering Informatics*, 26(2), 317–333. <https://doi.org/10.1016/j.aei.2011.12.001>.

Santos, E. T., & Derani, L. A. (2003). An immersive virtual reality system for interior and lighting design, In Proceedings of the Computer-Aided Architectural Design Research in Asia (CAADRIA), pp. 4–6.

Scarfe, P., & Glennerster, A. (2015). Using high-fidelity virtual reality to study perception in freely moving observers. *Journal of Vision*, 15(9), 3, 1–11. <https://doi.org/10.1167/15.9.3.doi>.

Schlüter, A., & Thesseling, F. (2009). Building information model based energy/exergy performance assessment in early design stages. *Automation in Construction*, 18(2), 153–163. <https://doi.org/10.1016/j.autcon.2008.07.003>

Schreyer, A. C., & Hoque, S. (2009). Interactive three-dimensional visualization of building envelope systems using infrared thermography and SketchUp. In Proceedings of the InfraMation 2009 Proceedings, pp. 1–8.

Sedlbauer, K., Erhorn, H., Holm, A., & Sinnesbichler, H. (2015). Energy efficiency and room climate - symbiosis or contradiction. In Proceedings of the Rosenheimer Fenstertage, pp. 101–110.

Shah, A., Chovatiya, P., & Shah, N. (2017). A BIM-based lighting analysis for evaluating saving potential in lighting cost during project cycle, In Proceedings of the ICRISET2017, pp. 45–50.

Shamsul, B. M., Sia, C. C., Ng, Y., & Karmegan, K. (2013). Effects of light's colour temperatures on visual comfort level, task performances, and alertness among students. *American Journal of Public Health Research*, 1(7), 159–165. <https://doi.org/10.12691/ajphr-1-7-3>

Sherman, W. R., & Craig, A. B. (2003). *Understanding Virtual Reality Interface, Applications, and Design*. San Francisco: Morgan Kaufmann.

Shiratuddin, M. F., & Thabet, W. (2011). Utilizing a 3D game engine to develop a virtual design review system. *ITcon*, 16, 39–68.

Sik-lányi, C. (2009). Lighting in virtual reality. In Proceedings of the JAMPAPER 1, pp. 19–26.

Sorensen, K. (1987). A modern glare index method. In Proceedings of the 21st commission internationale de l'Eclairage.

Sorger, J., Ortner, T., Luksch, C., Schwärzler, M., Gröller, E., & Piringer, H. (2016). LiteVis: integrated visualization for simulation-based decision support in lighting design. *IEEE Transactions on Visualization and Computer Graphics*, 22(1), 290–299. <https://doi.org/10.1109/TVCG.2015.2468011>.

Souha, T., JJihen, A., Guillaume, M., & Philippe, W. (2005). Towards a virtual reality tool for lighting. In Proceedings of the Computer Aided Architectural Design Futures, pp. 115–124.

Stahre, B., Billger, M., & Architecture, D. (2006). Physical measurements vs visual perception, In Proceedings of the CGIV, the European Conference on Colour in Graphics, Imaging and Vision, pp. 146–151.

Stone, P., & Harker, S. D. P. (1973). Individual and group differences in discomfort glare responses. *Lighting Research & Technology*, 5(1), 41–49. <https://doi.org/10.1177/096032717300500106>.

Suk, J. Y., Schiler, M., & Kensek, K. (2017). Investigation of existing discomfort glare indices using human subject study data. *Building and Environment*, 113, 121–130.
<https://doi.org/10.1016/j.buildenv.2016.09.018>.

Szokolay, S. V. (2004). *Introduction to Architectural Science: The Basis of Sustainable Design*. Oxford: Architectural Press. <https://doi.org/10.1007/978-3-642-00716-3>

Takim, R., Harris, M., & Nawawi, A. H. (2013). Building Information Modeling (BIM): A new paradigm for quality of life within architectural, engineering and construction (AEC) industry. *Procedia - Social and Behavioral Sciences*, 101, 23–32. <https://doi.org/10.1016/j.sbspro.2013.07.175>.

Tan, Y., Fang, Y., Zhou, T., Wang, Q., & Cheng, J. C. P. (2017). Improve indoor acoustics performance by using building information modeling. In *Proceedings of the 34th International Symposium on Automation and Robotics in Construction (ISARC 2017)*.

The Danish Ministry of Economic and Business Affairs Danish Enterprise and Construction, Danish Building Regulations 2015, 2015.
http://bygningsreglementet.dk/file/591081/br15_english.pdf. (Accessed 15 May 2017).

The Energy and Resources Institute (TERI). (2004). *Sustainable Building - Design Manual: sustainable building design practices*: TERI.

The Energy Conservation Center Japan. (2010). *Energy Conservation in Modern Office Buildings*. <https://doi.org/10.2190/2L53-DUCW-J1B8-MMYW>

The Swedish National Board of Housing Building and Planning, Boverket's building regulations – mandatory provisions and general recommendations, BBR, 2016. www.boverket.se/en. (Accessed 15 May 2017).

Thomas, J. J., & Cook, K. A. (2005). Illuminating the path: the research and development agenda for visual analytics. *IEEE Computer Society*, 184. <https://doi.org/10.3389/fmicb.2011.00006>.

Thormark, C. (2006). The effect of material choice on the total energy need and recycling potential of a building. *Building and Environment*, 41(8), 1019–1026.
<https://doi.org/10.1016/j.buildenv.2005.04.026>.

Tomassoni, R., Galetta, G., & Treglia, E. (2015). Psychology of light: how light influences the health and psyche. *Psychology*, 6(10), 1216–1222. <https://doi.org/10.4236/psych.2015.610119>.

U.S. Department of Energy. (2012). Buildings energy databook.
<http://buildingsdatabook.eren.doe.gov/DataBooks.aspx>. (Accessed 15 August 2016).

US General Service Administration (GSA). (2007). *GSA BIM Guide Series 01 – Overview*. Washington, DC: US General Services Administration.

Usamentiaga, R., Venegas, P., Guerediaga, J., Vega, L., Molleda, J., & Bulnes, F. G. (2014). Infrared thermography for temperature measurement and non-destructive testing. *Sensors*, 14(7), 12305–12348. <https://doi.org/10.3390/s140712305>.

Utama, A., & Gheewala, S. H. (2009). Indonesian residential high rise buildings: A life-cycle energy assessment. *Energy and Buildings*, 41(11), 1263–1268. <https://doi.org/10.1016/j.enbuild.2009.07.025>.

Van den Berg, T. J. T. P., (René) van Rijn, L. J., Kaper-Bongers, R., Vonhoff, D. J., Völker-Dieben, H. J., Grabner, G., Coppens, J. E. (2009). Disability glare in the aging eye assessment and impact on driving. *Journal of Optometry*, 2(3), 112–118. <https://doi.org/10.3921/joptom.2009.112>.

Vidas, S., Moghadam, P., & Bosse, M. (2013). 3D thermal mapping of building interiors using an RGB-D and thermal camera. In Proceedings of the IEEE International Conference on Robotics and Automation, pp. 2311–2318. <https://doi.org/10.1109/ICRA.2013.6630890>.

Vince, J. (2004). *Introduction to Virtual Reality*. Springer Science & Business Media.

Walker, J. (2014). Physically Based Shading In UE4. <https://www.unrealengine.com/en-US/blog/physically-based-shading-in-ue4>. (Accessed 8 Aug 2017).

Wang, C., Cho, Y. K., & Gai, M. (2013). As-Is 3D Thermal modeling for existing building envelopes using a Hybrid LIDAR system. *Journal of Computing in Civil Engineering*, 27(6), 645–656. [https://doi.org/10.1061/\(ASCE\)CP.1943-5487.0000273](https://doi.org/10.1061/(ASCE)CP.1943-5487.0000273).

Wang, H., Fellow, T., Gluhak, A., Meissner, S., & Tafazolli, R. (2013). Integration of BIM and live sensing information to monitor building energy performance. In Proceedings of the 30th CIB W78 International Conference, pp. 344–352.

Wardlaw, J., Wanner, F., & Brostow, G. (2010). A new approach to thermal imaging visualization. EngD Group Project, University College London, 2010.

Warren, P. (2003). Integral Building Envelope Performance Assessment Energy Conservation in Buildings - Annex 32 Synthesis Report. UK: The International Energy Agency Energy Conversation in Building and Community Systems Programme.

WEC. (2013). World Energy Resources: 2013 survey. <http://www.worldenergy.org>. (Accessed 15 August 2016).

Weidlich, D., Cser, L., Polzin, T., Cristiano, D., & Zickner, H. (2007). Virtual reality approaches for immersive design. *CIRP Annals-Manufacturing Technology*, 56(1), 139–142. <https://doi.org/10.1016/j.cirp.2007.05.034>.

Wienold, J., & Christoffersen, J. (2006). Evaluation methods and development of a new glare prediction model for daylight environments with the use of CCD cameras. *Energy and Buildings*, 38(7), 743–757. <https://doi.org/10.1016/j.enbuild.2006.03.017>.

Wolska, A., & Sawicki, D. (2014). Evaluation of discomfort glare in the 50+ elderly: experimental study. *International Journal of Occupational Medicine And Environmental Health*, 27(3), 444–459. <https://doi.org/10.2478/s13382-014-0257-9>.

Wu, C., & Clayton, M. J. (2013). BIM-based acoustic simulation framework. In Proceedings of the CIB W78 International Conference, pp. 99–108.

Wu, W. (2015). Design for aging with BIM and game engine integration. In Proceedings of the 122nd ASEE Annual Conference and Exposition.

Yan, W., Culp, C., & Graf, R. (2011). Integrating BIM and gaming for real-time interactive architectural visualization. *Automation in Construction*, 20(4), 446–458. <https://doi.org/10.1016/j.autcon.2010.11.013>

Young S.Lee. (2012). Using building information modeling for green interior simulations and analyses. *Journal of Interior Design*, 37(1), 35–50. <https://doi.org/10.1111/j.1939-1668.2011.01069.x>.

Zhou, X., Yan, D., Hong, T., & Ren, X. (2015). Data analysis and stochastic modeling of lighting energy use in large office buildings in China. *Energy and Buildings*, 86, 275–287. <https://doi.org/10.1016/j.enbuild.2014.09.071>

Zmrhal, V., Hensen, J., & Drkal, F. (2003). Modeling and simulation of a room with a radiant cooling ceiling, In Proceedings of the IBPSA, pp. 1491–1496.

Zotkin, S. P., Ignatova, E. V., & Zotkina, I. A. (2016). The organization of Autodesk Revit software interaction with applications for structural analysis. *Procedia Engineering*, 153, 915–919. <https://doi.org/10.1016/j.proeng.2016.08.225>.

